

Indian Journal of Sustainable Building Technology

Volume No. 4

Issue No. 1

January - April 2024



ENRICHED PUBLICATIONS PVT.LTD

**JE - 18,Gupta Colony, Khirki Extn,
Malviya Nagar, New Delhi - 110017.**

E- Mail: info@enrichedpublication.com

Phone :- +91-8877340707

Indian Journal of Sustainable Building Technology

Aims and Scope

Indian Journal of Sustainable Building Technology is published quarterly by Enriched publications. An EP Journal on Architectural and Planning Research is peer reviewed journal and monitored by a team of reputed editorial board members. This journal consists of research articles, reviews, and case studies on Architecture. This journal mainly focuses on the latest and most common subjects of its domain.

Indian Journal of Sustainable Building Technology

Managing Editor
Mr. Amit Prasad

Editorial Board Member

Dr. Sumanta Deb
Department of Architecture
Indian Institute of Engineering Science
and Technology, Shibpur
sumanta04@gmail.com

Mohammad Juned
Department of Architecture
M-15, Batla House Jamia Nagar,
New Delhi-110025
ar.juned@gmail.com

Arshiya Iftekhar Ahmed
Department of Architecture
A-109, Khan Abdul Gaffar Khan Enclave,
Near Tikona Park, Jamia
Millia Islamia, Jamia Nagar, New Delhi-110025
ahmed_arshiya@yahoo.co.in

Indian Journal of Sustainable Building Technology

(Volume No. 4, Issue No. 1, January - April 2024)

Contents

Sr. No	Article/ Authors	Pg No
01	A comparative study on the use of waste brick and glass in cement mortars and their effects on strength properties <i>- Hasan DİLEK, Pınar AKPINAR</i>	1 - 16
02	A comparative study on the use of waste brick and glass in cement mortars and their effects on strength properties <i>- Hasan DİLEK, Pınar AKPINAR</i>	17 - 34
03	Mechanical, freeze-thaw, and sorptivity properties of mortars prepared with different cement types and waste marble powder <i>- Rümeyya GÜRGÖZE, Zinnur ÇELİK, Ahmet Ferhat BİNGÖL</i>	35 - 56
04	Effect of calcination on the physical, chemical, morphological, and cementitious properties of red mud <i>- Chava VENKATESH, Chereddy SONALI SRI DURGA</i>	57 - 72
05	Use of SCM in manufacturing the compressed brick for reducing embodied energy and carbon emission <i>-Tejas M. JOSHI, Hasan M. RANGWALA* , Apurv PRAJAPATI</i>	73 - 88

Thermophysical characterization of concrete reinforced with baobab trunk fibers (*Adansonia digitata* L.) for thermal insulation of buildings

Alphousseyni GHABO*1, Pape Moussa TOURÉ2, Younouss DIÉYE2, Vincent SAMBOU2

1Laboratoire des Semi-conducteurs et d'Énergie Solaire, Faculté des Sciences et Techniques, Université Cheikh Anta Diop de Dakar, Dakar, Sénégal

2Laboratoire Eau, Énergie, Environnement et Procédés Industriels, École Supérieure Polytechnique, Dakar, Sénégal

ABSTRACT

This work deals with characterizing concrete based on baobab trunk fibers for thermal insulation in buildings. The aim is to study the effect of the fiber content and the type of fiber treatment on the hygroscopic and thermo-physical properties of the concrete. Therefore, two types of treatment were carried out: an alkaline treatment and a thermo-alkaline treatment. Hygroscopic test results (34.25% to 54.92% for fiber content ranging from 14% to 28%) show that adding fibers to concrete makes them more sensitive to water. However, thermochemical treatment of the fibers reduces this water sensitivity. The thermal conductivities of concrete range from 0.202 to 0.086 W/m.K for the same fiber content. These results show that these biomaterials can be used in construction to improve building insulation.

*Cite this article as: Ghabo, A., Touré, P. M., Diéye, Y., & Sambou, V. (2023). Thermophysical characterization of concrete reinforced with baobab trunk fibers (*Adansonia digitata* L.) for thermal insulation of buildings. *J Sustain Const Mater Technol*, 8(4), 251–259.*

Key words: Baobab fibers, cement, density, thermal conductivity, water absorption

1. INTRODUCTION

The residential building sector consumes large quantities of energy for heating in cooler periods and air conditioning or ventilation in hot periods. In Senegal, the energy consumption of buildings is estimated at 49% of final national consumption [1]. This is explained by the fact that in Senegal, concrete (a conductive material) is the primary building material. With this material, air conditioning and artificial ventilation are always used to achieve minimum thermal comfort. In addition, manufacturing and recycling this material requires large amounts of energy and poses a real problem of environmental pollution and greenhouse gas emissions.

Faced with this problem, developing new alternative materials to concrete is becoming necessary. One of the solutions proposed to mitigate the environmental impact of concrete is the incorporation of vegetable fibers in the manufacture of construction materials. Vegetable fibers are local, available materials with low thermal conductivity. Thus, their use in building materials can be an alternative to reduce heat transfer. Several researchers have been interested in determining bio-composite materials

Vegetable fibers are local, available materials with low thermal conductivity. Thus, their use in building materials can be an alternative to reduce heat transfer.

Several researchers have been interested in determining bio-composite materials physical and thermal properties based on cement and plant fibers.

Benmansour et al. [2] studied the effect of fiber content on the water absorption, density, and thermal conductivity of a date palm fibers reinforced mortar. They noted a decrease in density, thermal conductivity, and an increase in water absorption as the amount of fibers in the mortar increased.

Abdullah et al. [3] studied the physical and hygroscopic behavior of a cement mortar reinforced with coconut fibers. The authors concluded that the concrete's moisture content and water absorption increase as the fiber content increases. However, the density of the concrete decreases.

Potiron et al. [4] worked on determining the thermal conductivity and density of concrete based on sugarcane bagasse. The fibers were treated with boiling and alkaline solution. The authors concluded that thermal conductivity and density decreased with increasing fiber content in the composite concrete.

Taoukil et al. [5] studied the influence of water content on the thermal properties of a cement-sand composite reinforced with wood chips. The results showed that as the percentage of wood chips increased, the concrete's thermal conductivity and thermal diffusivity decreased. However, these values increase as the moisture content of the concrete increases.

Chakraborty et al. [6] worked on the effect of adding jute fibers treated with an alkaline solution and another solution of Sika latex polymer (carboxylated Styrene Butadiene) on the density of cement mortar. The results show that treating the fibers with 5% Sika latex polymer increases the density of the composite concrete.

Panesar et al. [7] studied the influence of cork waste fiber content on a cement mortar's density and thermal conductivity. They found that the density and thermal conductivity of the mortar decreased with increasing fiber content.

Osseni et al. [8] worked on the influence of the percentage of coir fibers on the thermal properties of a mortar. The results show that the thermal diffusivity and thermal conductivity decrease by about 10% as the amount of coir fibers increases.

Ashraf et al. [9] determined concrete's thermal conductivity and density containing date palm fibers. The authors noted a decrease in the thermal conductivity and density of the concrete as the fiber content increased.

Similarly, Diaw et al. [10] manufactured and determined the thermo-physical properties of concrete incorporating typha australis aggregates. The authors concluded that these materials can be used in buildings to improve energy efficiency.

Al-Mohamadawi et al. [11] investigated the influence of increasing flax shives treated with paraffin wax on cement concrete's thermal conductivity and density. The results showed that adding raw or treated fibers decreases cement concrete's density and thermal conductivity (<0.3 W/mK). However, the density and thermal conductivity of the treated fibers concrete increased compared to that of the raw fibers concrete.

Khazma et al. [12] worked on determining the thermal conductivity and density of concrete reinforced with flax shives treated by coating with a pectin + polyethylene (pp) mixture. The

authors noted increased treated concrete's density and thermal conductivity compared to raw concrete. Abderraouf [13] studied the influence of the percentage of Diss and Doum fibers treated with a sodium hydroxide solution on the thermal conductivity of cement concretes. The results show that, for fiber content of 4% by mass, the thermal conductivity of Diss and Doum treated fibers mortars decreases by 40% and 33%, respectively, compared to the control mortar. Becchio et al. [14] studied the influence of the percentage of wood aggregates on the thermal conductivity of cement concrete. Their results showed a decrease in the thermal conductivity of composite concrete compared to control concrete.

This literature review shows that many vegetable fibers manufacture thermal insulation or filling materials in housing construction. No studies have been conducted to determine the hygroscopic and thermo-physical properties of concrete made from baobab (*Adansonia digitata* L.) trunk fibers. The baobab is a gigantic tree of the Bombacaceae family that grows in the southern, western, and southeastern regions of Senegal [15]. This tree has long been exploited for food (leaves and fruits) and traditional medicine (leaves and bark). Baobab trunk and branches are very fibrous and are used for rope making and weaving. Extracting fibers from these parts does not affect the tree's health, as these parts regenerate every six months after exploitation [16].

This work aims to develop and determine cement concrete's hygroscopic and thermo-physical properties based on baobab trunk fibers. The properties studied are water absorption, moisture content, density, and thermal conductivity. Compared to the work mentioned above, the originality of this work is the use of baobab trunk fibers in producing bio-sourced concrete to manufacture insulating cementitious concrete with low environmental impact.

2. MATERIALS AND CHARACTERIZATION METHODS

2.1. Baobab Trunk Fibers

In this study, the fibers used were extracted from the trunk of a local tree, the Baobab (*Adansonia digitata* L.). The baobab is a gigantic tree generally found in Africa's south-eastern and south-western regions, i.e., in the Sahelian and Sudano-Sahelian zones. In Senegal, the baobab is widespread in areas such as Thiès, Kaolack, Tambacounda, and in the southern regions, the Casamance. After extraction, the fibers were cleanly washed and air-dried for a week before being cut by hand into 1 cm lengths. [16, 17].

Two treatments were applied to the fibers:

- The alkaline treatment consisted of immersing the fibers for 4 hours in a sodium hydroxide (NaOH) solution of 5% concentration by mass at room temperature. They were washed thoroughly with distilled water and soaked again in a 1% sulphuric acid solution for 2 hours. Finally, the fibers were washed clean

with distilled water and dried at room temperature for 72h. This fiber is noted as F.T.NaOH.

- Thermochemical treatment involves boiling the fibers for at least four hours and rinsing them thoroughly with distilled water to remove organic substances (waxes, peptides, impurities). The exact process then treats the boiled fibers with the same sodium hydroxide solution. This fibThis fiber F.B.T.

Several studies on the characterization of bio-based composites have already shown that heat treatment and al kali treatment of plant fibers can reduce large quantities of lignin, hemicellulose, and water-soluble substances. These compounds are the primary agents responsible for the delayed setting of the cementitious matrix and poor adhesion at the fiber/cement interface [4, 18].

Table 1. The fibers hygroscopic, physical, and thermal properties [17]

Types de fibres	ω (%)	ρ (kg.m ⁻³)	λ (Wm ⁻¹ .K ⁻¹)
F.T.N _a OH	230.62	225	0.041
F.B.T.	226.08	220	0.043

Table 2. Composition chimique du ciment CEM II/ B-M 32.5 R

Composition	CaO	SiO ₂	Al ₂ O ₃	Fe ₂ O ₃	MgO	Na ₂ O	K ₂ O	SO ₃	Cl-
Weight (%)	55.8	19.7	6.2	3.9	2.2	0.33	0.70	2.6	0.07

Table 3. Mass percentages of cement and fibers

Components	CFTNaOH/C.F.B.T.					
Fibers content (%)	14	16	20	22	26	28
Cement content (%)	86	84	80	78	74	72

2.2. Sample preparation

This work uses both treated fibers (F.T.NaOH) and (F.B.T.). Their properties are listed in Table 1.

The chemical composition of the fibers was not given because no laboratory was available to carry out the chemical characterization.

The chemical composition of the cement used in this study is given in Table 2.

The concretes manufactured are composed of Portland cement CEMII/B-M 32.5 R supplied by the cement company Sococim Industries of Senegal and fibers from the baobab's trunk (*Adansonia digitata* L.). The ratio of water mass to cement mass is taken as 0.3. Table 3 shows each composite type's mass percentages of fibers and cement.

The fibers and cement were manually mixed in a 5 L capacity beater to achieve a homogeneous distribution of the fibers, and then the beater was inserted into an E095-type mixer. Mixing was maintained for 5 minutes, gradually adding the water necessary to hydrate the cement. The homogenized paste is then poured into 10 cm x 10 cm x 2 cm heat test molds. A Time-Tronic shaking machine was used to compact a total of 60 shakes. After 24 hours, the samples were removed from the molds,

placed in plastic bags to even out the distribution of water, and kept under laboratory conditions for 28 days. Before conducting the thermo-physical measurements, the samples were dried in an oven at 105 °C for 24 hours.

An example of the concrete used for hygroscopic, physical and thermal characterization is presented in Figure 1.

2.3. Characterization Methods

2.3.1. Water Absorption

First, the concretes were dried in an oven for 24 hours, and then their masses were weighed. Then, they were introduced into distilled water at room temperature.

By carrying out successive weighings, It is noted that, after 24 hours of immersion, the concretes reached their water saturation point ($\Delta m \leq 0.01$ g). Finally, the masses at saturation were weighed.



Figure 1. Baobab trunk fibers concretes.

The expression of the water absorption is:

$$\omega = \frac{m_h - m_o}{m_o} \times 100 \quad (1)$$

m_h : Mass of concrete saturated with water.

m_o : Mass of concrete in a dry state.

2.3.2. Moisture Content

The concretes were kept in the atmospheric conditions of the laboratory for 24 h before being weighed (m_a) and placed in an oven at a temperature of 105 °C. 24 hours later, the drying was stopped when the last two measurements were very similar ($\Delta m \leq 0.01$ g). The expression calculates the moisture content=

$$\frac{m_a - m_s}{m_a} \times 100 \quad (2)$$

m_s : Mass of concrete in a dry state.

m_a : Mass of the concrete in the ambient state.

2.3.3. Apparent Density and Porosity

• The bulk density is the ratio of the mass (m_a) to the bulk volume of the sample. The mass of the sample was weighed with a 0.01 g precision balance. The dimensions of the sample were measured with a caliper to calculate the apparent volume. The equation obtains the bulk density:

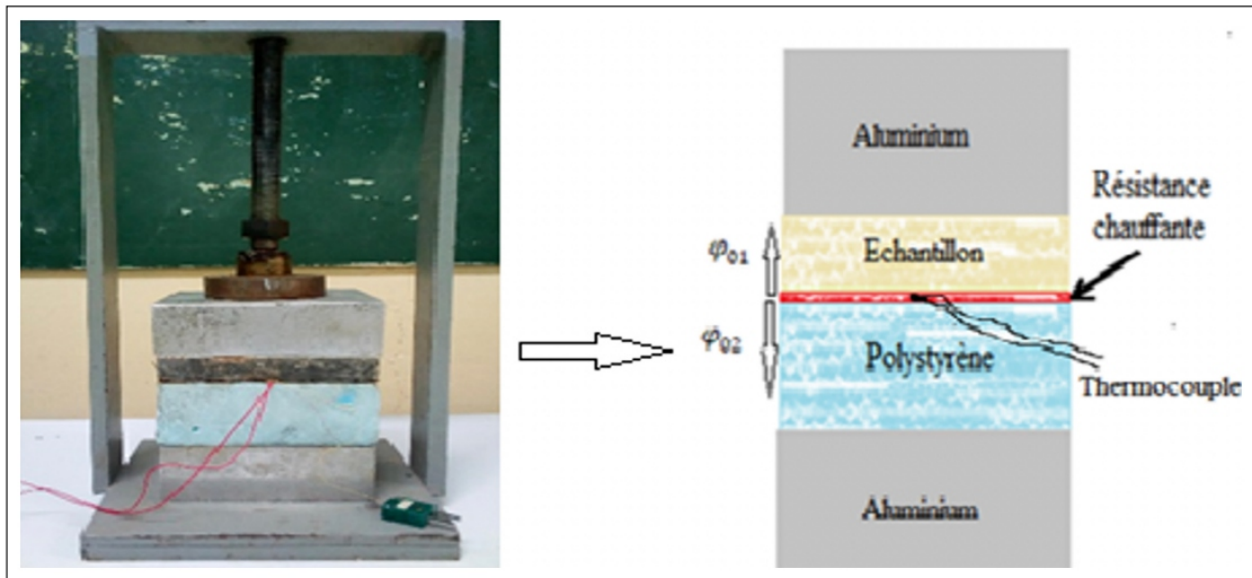


Figure 2. Asymmetrical hot-plane device.

Table 4. Thermal properties of polystyrene

e (m)	λ (Wm ⁻¹ .K ⁻¹)	E (J.K ⁻¹ .m ⁻¹ .s ^{-1/2})
0,015	0,035	43,226

$$\rho = \frac{m_0}{V} \quad (3)$$

• The water-accessible porosity is the ratio of the pore volume to the volume of the concrete. The pore volume is the difference between the mass of the water-saturated concrete (m_h) and the concrete in the dry state (m_o).

The equation gives the porosity:

$$\eta = \frac{m_h - m_o}{\rho_e V} \times 100 \quad (4)$$

η : concrete porosity

V : Volume of the sample

ρ_e : Water density

2.3.4. Thermal Characterization

The thermal characterization consisted of the simultaneous determination of thermal conductivity and thermal effusivity using the asymmetric hot plane method at a constant sample backside temperature (Fig. 2).

The principle of this method and the modeling have been described in detail by Diéye et al. [19]. System modeling is based on two hypotheses: the heat transfer at the center of the sample is unidirectional (1D), and the temperature at the back of the sample is maintained constant. During measurement, the heating element applies a constant heat flow to one side of the 10 cm x 10 cm x 2 cm sample. A thermocouple placed in the center of the heating element records the evolution of the temperature $T_s(t)$. The principle is to determine the values of the sample's thermal conductivity and thermal effusivity that minimize the squared deviation between the experimental and theoretical curves. The expression for the square deviation is:

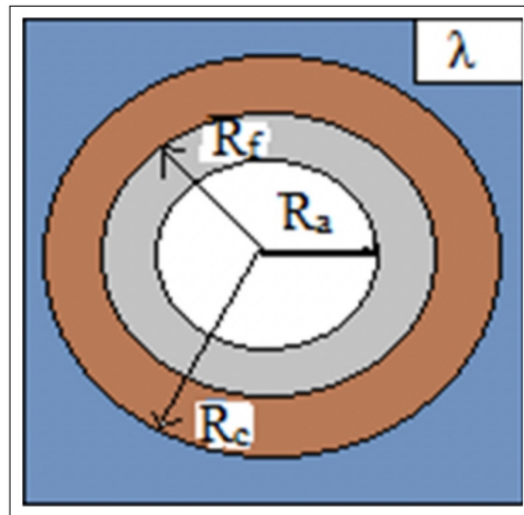


Figure 3. Three-phase homogenized medium.

$$\psi = \sum_i^n [T_{exp}(t_i) - T_{mod}(t_i)]^2$$

With:

ψ : The quadratic error between the experimental and theoretical values.

T_{exp} : Experimental temperature.

T_{mod} : Theoretical model temperature.

To test the validity of this method, an extruded polystyrene sample of known dimensions and thermal parameters was tested, and the results are presented in Table 4.

2.4. Thermal Conductivity Estimation by the Self-Consistent Method

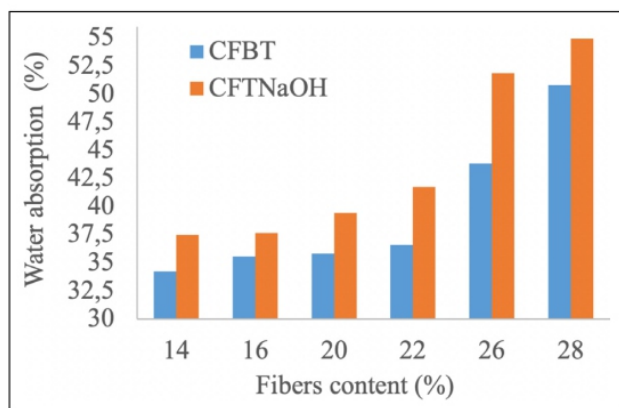
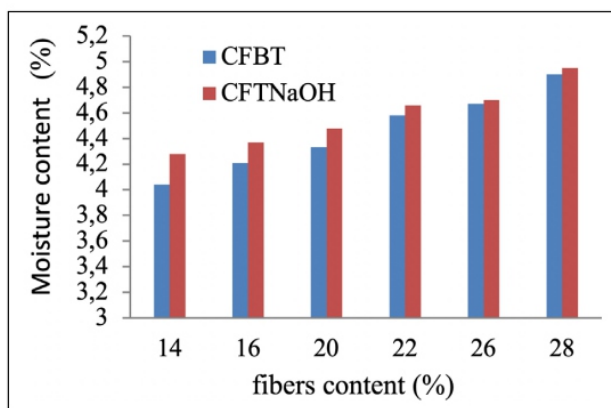
This work used the three-phase model [20, 21] to determine the homogeneous medium's equivalent thermal con

Table 5. Water absorption of composites

Fibers content (%)	14	16	20	22	26	28
Water absorption-CFBT (%)	34,25	35,56	35,82	36,57	43,84	50,79
Water absorption-CFTNaOH (%)	37,46	37,63	39,44	41,73	51,84	54,92

Table 6. Moisture content of concretes

Fibers content (%)	14	16	20	22	26	28
Moisture content - C.F.B.T. (%)	4,04	4,21	4,33	4,58	4,67	4,9
Moisture content - CFTNaOH (%)	4,28	4,37	4,48	4,66	4,7	4,95

**Figure 4.** Water absorption as a function of fiber content.**Figure 5.** Moisture content as a function of fibers content.

ductivity (λ). The principle of the method is to assimilate a heterogeneous material to a homogeneous medium whose equivalent thermal conductivity is determined. The sample has assimilated an assembly of centrally located spherical air bubbles (R_a, λ_a), covered by a concentric spherical layer of fibers particles (R_f, λ_f), and the whole is covered by a cementitious matrix (R_c, λ_c) as illustrated in Figure 3.

3. EXPERIMENTAL RESULTS AND ANALYSIS

3.1. Hygroscopic Characterization

3.1.1. Influence of Fibers Content and Treatment on

Water Absorption

The results of water absorption at saturation of the concretes are given in Table 5.

Figure 4 shows the evolution of water absorption as a function of fiber content and type of treatment. It shows that the water absorption of concrete increases as the amount of fibers increases. Baobab trunk fibers have a high water absorption coefficient [17]. Incorporating these fibers in the cementitious matrix explains the increase in water absorption of concretes when the fiber content increases. A similar behavior was observed by Xie et al. [22] on concretes based on rice straw and bamboo fibers and Benmansour et al. [2] on date palm fiber concretes. It can also be seen that the type of treatment affects the water absorption. The water absorption of C.F.B.T. concretes is slightly higher than that of

CFTNaOH concretes.

Indeed, it has been shown that the thermochemical treatment of fibers contributes better to reducing the water-soluble components responsible for the hydrophilic character of fibers [17]. This reduces the water absorption capacity of the fibers. This same behavior was observed by Abderraouf [4].

3.1.2. Influence of Fibers Content and Treatment on Moisture Content

The moisture content values of C.F.B.T. and CFTNaOH concretes are shown in Table 6.

Figure 5 shows that the concretes' moisture content increases when the fibers' mass fraction increases. This is because fibers comprise molecules with large amounts of free hydroxyl groups (-O.H.) and can bind water vapor [23]. It can be seen that the type of treatment also influences the moisture content. We noted that the C.F.B.T. concretes showed lower moisture contents than the CFTNaOH concretes (Fig. 5). This phenomenon can be explained by the fact that the thermochemical treatment leads better to the dissolution of lignin and hemicellulose. This makes the fibers less hydrophilic. This same behavior was also found by Sawsen et al. [24].

Although the water absorption and moisture content of the fibers have been reduced, it has to be recognized that the concretes studied are still highly sensitive to water. Therefore, for their use in buildings, they are either used for internal insulation in the form of panels or by applying a layer of waterproof plaster to the outside face when the concretes are used to fill the walls.

Table 7. Apparent densities and water-accessible porosity of concretes

Fibers content (%)	14	16	20	22	26	28
C.F.B.T.						
ρ (kg.m ⁻³)	1122,50	1118,15	1107,40	1018,55	945,05	861,10
Porosity (%)	38,11	38,85	39,20	39,72	41,53	45,69
CFTNaOH						
ρ (kg.m ⁻³)	1111,07	1090,50	1084,25	1027,95	920,00	859,50
Porosity (%)	39,69	40,00	41,53	42,32	46,40	47,79

Table 8. Thermal conductivity of C.F.B.T. concretes

Fibers content (%)	0	14	16	20	22	26	28
Thermal conductivity - C.F.B.T. (W/mK)	0,691	0,202	0,117	0,104	0,096	0,089	0,086
Thermal conductivity - CFTNaOH (W/mK)	0,691	0,188	0,112	0,105	0,091	0,085	0,083

3.2. Thermo-Physical Characterization

3.2.1. Influence of the Fiber Content on the Density

The values of the apparent densities and water-accessible porosity of the concrete (C.F.B.T. and CFTNaOH) are given in Table 7.

Figure 6 shows the density variation as a function of fiber content and type of fiber treatment. It is noted that the bulk density decreases as the fiber content increases. Adding plant fibers in a cementitious matrix increases the porosity of the fiber-reinforced concrete (Table 7). However, as the porosity of the concrete increases, the density decreases. This justifies the decrease in the density of concrete fibers. Potiron et al. [4] also observed the same behavior.

Figure 6 also shows that the treatment influences the bulk density of the concrete. It can be seen that the densities of C.F.B.T. concretes are slightly higher than those of CFTNaOH concretes. Some authors have shown that the treatment increases the density of the fibers Ghabo et al. [17], Asasutjarit et al. [25]. This justifies the importance of the density of C.F.B.T. concretes compared to CFTNaOH concretes.

3.2.2. Influence of Fiber Content and Treatment on Thermal Conductivity

The values of the thermal conductivities of the studied concrete are given in Table 8.

The variation in thermal conductivity as a function of fiber content and type of treatment is shown in Figure 7.

Firstly, It can be noted that the thermal conductivity of the concrete decreases as the fiber content increases. In deed, adding fibers to a cement matrix increases the porosity of the concrete. This contributes to the decrease of the thermal conductivity of the concrete when the fiber content increases. Other authors have observed similar behavior, Osseni et al. [8] and Benmansour et al. [2].

Secondly, it can be seen that the thermal conductivities of C.F.B.T. concretes are slightly higher than those of CFTNaOH concretes. The thermochemical treatment decreased the porosity of the fibers more than the chemical treatment Ghabo, et al. [17]. Thus, the incorporation of chemically

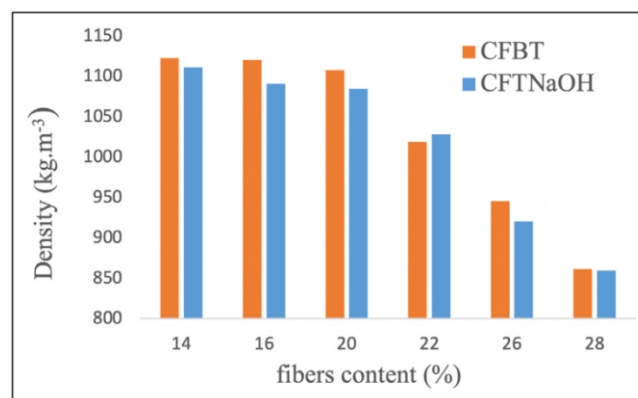


Figure 6. Density of concrete as a function of fiber content.

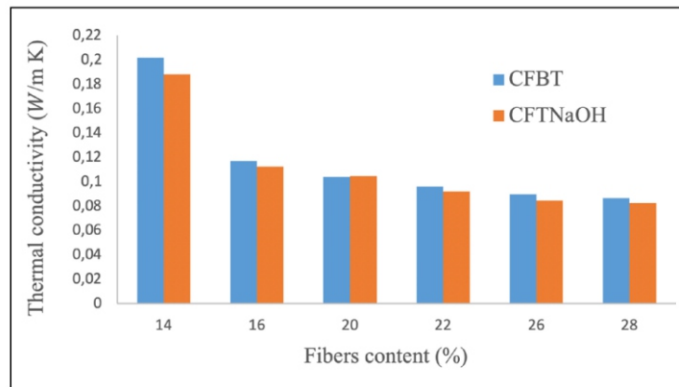


Figure 7. Thermal conductivity of C.F.B.T. and CFTNaOH as a function of fibers content type of treatment.

treated fibers reduces the thermal conductivity of the concrete more. This justifies the superior thermal conductivity of C.F.B.T. concretes. Potiron et al. [4] have observed similar behavior in concretes based on sugarcane bagasse fibers.

3.2.4. Influence of Bulk Density on Thermal Conductivity

Figure 8 and 9 show the evolution of the thermal conductivity as a function of the density of the concrete. It is noted that the thermal conductivity of concrete decreases as the density decreases. The addition of the fibers contributes,

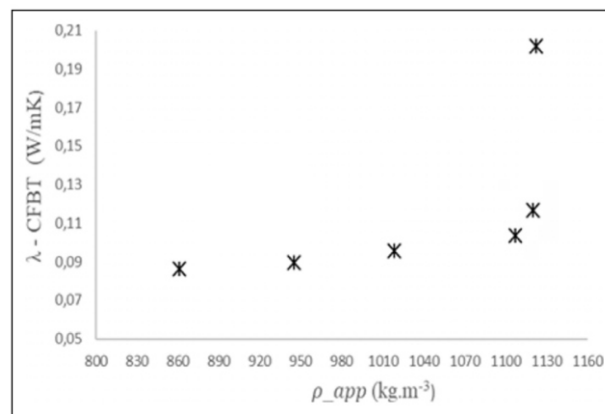


Figure 8. Thermal conductivity of CFBT concrete as a function of density.

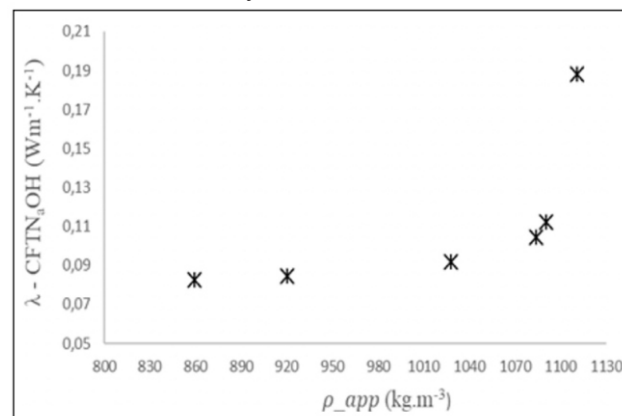


Figure 9. Thermal conductivity of CFTNaOH concrete as a function of density.

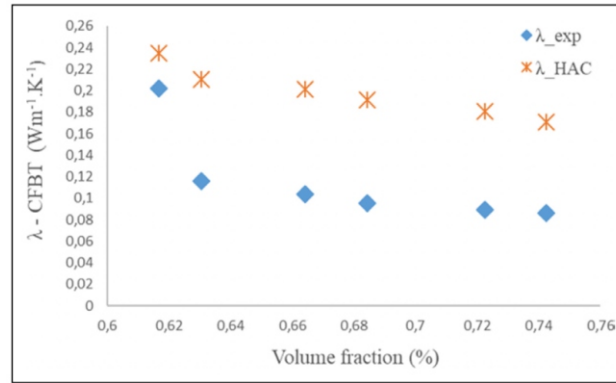


Figure 10. Thermal conductivity of C.F.B.T. concrete as a function of volume fraction.

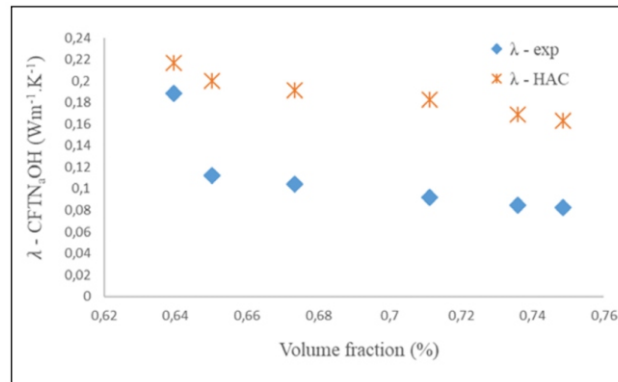


Figure 10. Thermal conductivity of CFTNaOH concretes as a function of volume fraction.

4. CONCLUSION

This work focused on the effect of incorporating bao bab trunk fibers on the thermo-physical and hygroscopic properties of concrete. The fibers were chemically and thermochemically treated to study the impact of their incorporation on the properties of concrete.

- The results obtained for the hygroscopic characterization showed that the thermo-physical treatment of the fibers contributes to reducing the moisture content and water absorption of the concretes studied.
- From a thermophysical point of view, it was noted that the incorporation of fibers resulted in a significant decrease in the thermal conductivity and density of the composites. For a fiber content of 20%, the thermal conductivity decreased by 58.64% and 58.72%, respectively, for the C.F.B.T. and C.F.T.NaOH composites compared to the control concrete.
- The theoretical results of the self-consistent method are similar to the experimental results with acceptable deviations.
- Regarding the thermal insulation of the building, both types of concrete studied showed good thermal insulation properties.
- Therefore, we propose the use of this material in construction to reduce energy consumption in the building sector.

ETHICS

There are no ethical issues with the publication of this manuscript.

DATA AVAILABILITY STATEMENT

The authors confirm that the data that supports the findings of this study are available within the article. Raw data that support the finding of this study are available from the corresponding author, upon reasonable request.

CONFLICT OF INTEREST

The authors declare that they have no conflict of interest.

FINANCIAL DISCLOSURE

The authors declared that this study has received no financial support.

PEER-REVIEW

Externally peer-reviewed.

REFERENCES

- [1] Programme national de réduction des émissions de Gaz à Effet de Serre à travers l'Efficacité Energétique dans le secteur du bâtiment au Sénégal 2013-2016. https://www.sn.undp.org/content/senegal/fr/home/operations/projects/environment_and_energy/EfficaciteEnergetique.html [CrossRef]
- [2] Agoudjil, B., Benmansour, N., Boudenne, A., Gherabli, A., & Kareche, A. (2014). Thermal and mechanical performance of natural mortar reinforced with date palm fibers for insulating materials in building. *Energy and Buildings*, 81(1), 98–108. [CrossRef]
- [3] Abdullah, A., Hussin, K., Jamaludin, S. B., & Noor, M. M. (2011). Composite cement reinforced coconut fibers: Physical and mechanical properties and fracture behavior. *Australian Journal of Basic and Applied Sciences*, 5(7): 1228–1240. <https://www.researchgate.net/publication/250310862>. [CrossRef]
- [4] Bilba, K., Delvasto, S., Passe-Coutrin, N., Potiron, C. O., & Toro, F. (2010). Sugar cane bagasse fibers reinforced cement composite: Thermal considerations. *Composites Part A: Applied Science and Manufacturing, Elsevier*, 41(4), 549–556. [CrossRef]
- [5] Ajzoul, T., El Bouardi, A., Ezbakhe, H., Mimet, A., Sick, F., & Taoukil, D. (2013). Moisture content influence on the thermal conductivity and diffusivity of wood–concrete composite. *Construction and Building Materials*, 48(1), 104–115. [CrossRef]
- [6] Adhikari, B., Chakraborty, S., Kundu, S. P., Majumder, S. B., & Roy, A. (2013). Polymer modified

-
-
- jute fibre as reinforcing agent controlling the physical and mechanical characteristics of cement mortar. *Construction and Building Materials*, 49(1), 214–222. [CrossRef]
- [7] Panesar, D. K., & Shindman, B. (2012) *The mechanical, transport and thermal properties of mortar and concrete containing waste cork*. *Cement & Concrete Composites* 34(1), 982–992. [CrossRef]
- [8] Ahouannou, C., Apovo, B. D., Jannot, E. Y., Osseni, S. O. G., & Sanya, E. A. (2016). *Caractérisation thermique des mortiers de ciment dopés en fibres de coco par la méthode du plan chaud asymétrique à une mesure de température*, *Afrique SCIENCE* 12(6), 119–129.
- [9] Al Kutti, W., Al Maziad, F. A., Ashraf, N., & Nasir, M. (2020). *Assessment of thermal and energy performance of masonry blocks prepared with date palm ash*. *Materials for Renewable and Sustainable Energy*, 9(17), 1–13. [CrossRef]
- [10] Bal, H., Diallo, O., Diaw, A., Gaye, S., Ndiaye, M., & Wade, M. (2021). *Thermophysical characterization of typha's concrete for its integration into construction*. *Journal of Building Construction and Planning Research*, 9(1), 56–65. [CrossRef]
- [11] Al-Mohamadawi, A., Benhabib, K., Dheilly, R., & Goullieux, A. (2016). *Influence of lignocellulosic aggregate coating with paraffin wax on flax shive and cement-shive composite properties*. *Construction and Building Materials*, 102(1), 94–104. [CrossRef]
- [12] Dheilly, R., Goullieux, A., Khazma, M., & Quéneudec, M. (2012). *Coating of a lignocellulosic aggregate with pectin/polyethylenimine mixtures: Effects on flax shive and cement-shive composite properties*. *Cement & Concrete Composites*, 34(1), 223–230. [CrossRef]
- [13] Abderraouf, A. (2017). *Etude des performances des mortiers renforcés de fibres naturelles: Valorisation des plantes locales*. [Doctoral Thesis, Université Aboubakr Belkaïd–Tlemcen].
- [14] Becchio, C., Corgnati, S. P., Kindinis, A., & Paglioli, S. (2009). *Improving environmental sustainability of concrete products: Investigation on M.W.C. thermal and mechanical properties*. *Energy and Buildings*, 41(1), 1127–1134. [CrossRef]
- [15] Alioune, S., Mady, C., Mama, S., Mar, D. C., & Nicolas, A. (2018). *Le baobab (Adansonia digitata L.): Taxonomie, importance socio-économique et variabilité des caractéristiques physico-chimiques*. *International Journal of Innovation and Scientific Research*, 39(1), 12–23.
- [16] Cisse, M., Diop, A. G., Dornier, M., Reynes, M. & Sakho, M. (2005). *Le baobab africain (Adansonia digitata L.): Principales caractéristiques et utilisations*. *Fruits*, 61(1), 55–69. [CrossRef]
- [17] Dièye, Y., Ghabo, A., Sambou, V., & Sarr, J. & Touré, P. M. (2020). *Physical and hygroscopic characterization of fibers extracted from the Baobab trunk for their use as reinforcement in a building material*. *International Journal of Engineering and Technical Research*, 10(1), 2454–4698.
- [18] Amziane, S., Merzoud, M., & Sellami, A. (2013). *Improvement of mechanical properties of green concrete by treatment of the vegetal fibers*. *Construction and Building Materials*, 47(1), 1117–1124. [CrossRef]
-
-

-
-
- [19] Adj, M., Azilinson, D., Dieye, Y., Faye, M., Sambou, V., & Thiam, A., (2017). Thermo-mechanical characterization of a building material based on *Typha Australis*. *Journal of Building Engineering*, 9(19), 142–146. [CrossRef]
- [20] Collet, F., & Prétot, S. (2014). Thermal conductivity of hemp concretes: Variation with formulation, density and water content. *Construction and Building Materials*, 65(1), 612–619. [CrossRef]
- [21] Cerezo, V. (2005). *Propriétés mécaniques, thermiques et acoustiques d'un matériau à base de particules végétales: Approche expérimentale et modélisation théorique*. [Thèse de doctorat, L'Institut National des Sciences Appliquées de Lyon].
- [22] Hui, D., Jiang, M., Wang, Z., Xie, X., Xu, X., & Zhou, Z. (2015). Cellulosic fibers from rice straw and bamboo used as reinforcement of cement-based composites for remarkably improving mechanical properties. *Composites Part B: Engineering*, 78(1), 153–161. [CrossRef]
- [23] Magniont, C. (2010). *Contribution à la Formulation et à la Caractérisation d'un Eco matériau de Construction à Base d'Agro Ressources*. [Thèse de doctorat, Université de Toulouse III - Paul Sabatier; Génie Civil, Laboratoire de Matériaux et Durabilité des Constructions (LMDC)].
- [24] Fouzia, K., Mohamed, B., Moussa, G., & Sawsen, C. (2014). Optimizing the formulation of flax fiber-reinforced cement composites. *Construction and Building Materials*, 54(1), 659–664. [CrossRef]
- [25] Asasutjarit, C., Charoenvai, S., Cheul, S. U., Hirunlabh, J., Khedari, J., & Zeghamati, B. (2007). Development of coconut coir-based lightweight cement board. *Construction and Building Materials*, 21(2), 277–288. [CrossRef]
- [26] Benazzouk, A., Douzane, O., Mezreb, K., Laidoudi, B., & Quéneudec, M. (2008).
- [27] Thermal conductivity of cement composites containing rubber waste particles: Experimental study and modelling. *Construction and Building Materials*, 22(4), 573–579. [CrossRef]

A comparative study on the use of waste brick and glass in cement

Hasan DİLEK¹, Pınar AKPINAR^{*2}

¹Department of Civil Engineering, European University of Lefke, Faculty of Engineering, Lefke, Turkish Republic of Northern Cyprus

²Department of Civil Engineering, Bahçeşehir Cyprus University, Faculty of Architecture and Engineering, Nicosia,

ABSTRACT

Sustainable development of the construction industry should use recycled materials to the greatest extent to reduce natural hazards due to the increased accumulation of waste and the depletion of natural resources. However, engineering applications using waste materials are always expected to perform satisfactorily. In this aspect, detailed and systematically carried out experimental studies are critical in selecting the type and the quantities of waste materials that will be recycled through their use within engineering applications. This study provides systematically produced experimental data on compressive and flexural strength performance to quantitatively compare the effects of using different percentages of waste glass and brick aggregates in cement mortars with a specified workability characteristic. Results show that mortar samples with waste glass aggregates perform better under compressive loading since only around 14% strength decrease compared to the control mix was yielded with the inclusion of waste glass. In contrast, in both cases, a 30% strength decrease was recorded with the inclusion of waste bricks for 100% replacement of natural sand in the mortars. In the case of flexural strength performance, 50% replacements of natural aggregates with waste bricks and glass yielded around 27% and 38% strength decrease, indicating that using waste brick in cement mortars could result in a better flexural strength performance in comparison, provided that its content is controlled. Replacement of natural sand in cement mortars with waste brick and glass yielded less significant flexural strength, decreasing the difference between the two types of wastes when the replacement ratio was as high as 100%. Hence, based on the presented experimental evidence, it is concluded that the decision on the type and the quantity of the waste materials to be used should be made considering the area of the use of the mortar and its expected service type.

Cite this article as: Dilek, H., & Akpınar, P. (2023). A comparative study on the use of waste brick and glass in cement mortars and their effects on strength properties. *J Sustain Const Mater Technol*, 8(4), 269–277.

Key words: Cement mortar, compressive strength, flexural strength, waste brick aggregates, waste glass aggregates, workability

1. INTRODUCTION

Concrete is undoubtedly one of the most popular construction materials used all around the globe. The fact that 75% of the volume of concrete is composed of aggregates brings two important issues. Firstly, and in the civil engineering aspect, the quality and performance of concrete constructions would be highly affected by the characteristics of the aggregates used within, considering the volume they occupy in the mix [1]. Secondly, and globally, using natural (i.e., quarried) aggregates for manufacturing bil

lions of tons of concrete would accelerate the depletion of natural sources of aggregates on planet Earth while posing threats to nature in most cases. Several aggregate quarries on the Beşparmak (Pentadaktylos) Mountains in North Cyprus that are unfortunately mismanaged are observed to cause loss of sources loss of vegetational and animal life in their surroundings, as seen in Figure 1. Another environmental hazard that has been building up simultaneously is the increased quantities of waste generation caused by the needs of modern life when societies do not adopt the concept of sustainability. Engineers and scientists have proposed using waste materials as a replacement for natural aggregates in concrete in the last decades to reduce the two aforementioned environmental hazards, and the published works in the literature yielded promising results for this approach [2–6]. Similar to concrete, cement mortars are also consumed in constructions in huge quantities, mainly for all kinds of repair and maintenance works as well as in masonry works and so forth [7]. Additionally, since the main difference between mortar and concrete is the size of the aggregates used within them, cement mortars are also widely used in civil engineering research studies due to being accepted as highly indicative of concrete's performance and behavior. Hence, the use of waste materials to replace fine aggregates in cement mortars is also of concern.

Regarding the use of waste materials as a replacement for natural (i.e., quarried) fine aggregates in cement mortars, several interesting previous works have been considered. Among these, Bektas et al. [8] propose using crushed waste brick as a replacement for natural sand in mortars and report that the highly porous nature of brick aggregates affects the properties of fabricated mortar bars. This property of brick aggregates has been reported to yield increased water absorption for the mortars. Another noteworthy observation reported by this study was that the compressive strength of the mortars containing waste bricks was not negatively affected up to a limit of 20% (by mass) replacement of natural aggregates [8]. Zhu and Zhu (2020) [9] also report that the porous nature of waste brick aggregates caused increased water absorption and reduced compressive strength of cement mortar samples when added beyond specific contents. However, the surface texture of these waste aggregates has been reported to yield higher splitting tensile strength [9].

Another interesting study was presented by Tan and Du [10], which proposes using crushed waste glass as a replacement for natural sand in cement mortars. This interesting study reports that waste glass aggregates have smooth surface texture, and this characteristic yields weaker bonds between the waste aggregate and the cement paste, eventually yielding a decrease in the tensile strength of the mortar samples. Lu and Poon [11] also reports similar finding on the use of waste glass as a replacement for natural sand in cement mortars, stating that increased contents of glass aggregates yielded decreased tensile strength of mortars due to the smooth texture of this type of waste aggregates. Another noteworthy performance information provided by this study indicates that glass aggregates have very low



Figure 1. A view of the damaged nature due to aggregate quarries on Beşparmak (Pentadaktylos) Mountains, North Cyprus.

Table 1. The mortar mixes used and their waste types and contents

Mix name	Natural aggregate (NA)	Recycled brick aggregate (RBA)	Recycled glass aggregate (RGA)
Mix 1 (control set)	100%	0	0
Mix 2a	50%	50%	0
Mix 2b	0	100%	0
Mix 3a	50%	0	50%
Mix 3b	0	0	100%

absorption characteristics. Hence, they do not negatively affect the workability of fresh cement mortar mixes [11].

These noteworthy and interesting research studies provide insights into some characteristics of mortar bars produced using mentioned waste aggregates. However, each study is observed to have an independent experimental campaign design, and hence, it becomes difficult to relate and compare their findings for engineering applications. Therefore, the related literature has detected a lack of systematical and comparable experimental information on cement mortars' fresh and hardened properties specifically made with waste glass and bricks. Therefore, the main objective of this study is to provide experimental data to investigate the performance of cement mortars having specified workability characteristics that are produced with recycled glass aggregates (RGA) and recycled brick aggregates (RBA) that were used as replacements for natural (i.e., quarried) sand. In this way, the suitability and the advantages of using waste glass and waste bricks in cement mortars could be directly compared based on the obtained experimental results, yielding potentially beneficial insights for

practical applications in the construction sector aiming to contribute to the sustainable development of societies.

2. MATERIALS AND METHODS

Five different mortar mixtures, including 0%, 50%, and 100% waste brick and glass used as replacements (by weight) for natural aggregates, were used in this study, as presented in Table 1.

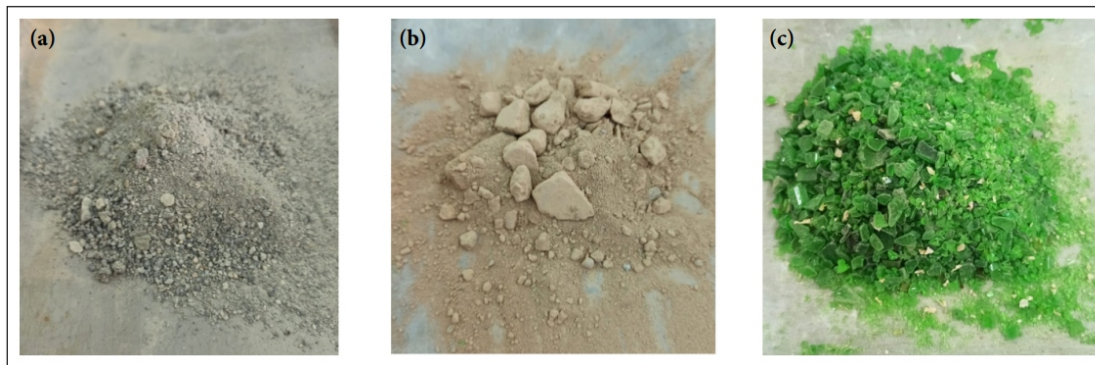


Figure 2. (a) Natural fine aggregates. (b) Crushed waste bricks. (c) Crushed waste glass.

Table 2. Quantities of materials used in the manufacture of each cement mortar mix

Aggregate particle size	Water (kg/m ³)	Cement (kg/m ³)	Natural (quarried) fine aggregates (kg/m ³)				Waste fine aggregates (waste bricks /waste glass) (kg/m ³)			
			0.15 mm	0.3 mm	0.6 mm	1.18 mm	0.15 mm	0.3 mm	0.6 mm	1.18 mm
Mix 1 (control set)	367	611	122	244	367	489	0	0	0	0
Mix 2a (50% waste brick aggregates)	530	726	47	93	142	189	47	93	142	189
Mix 2b (100% waste brick aggregates)	541	721	0	0	0	0	94	187	281	375
Mix 3a (50% waste glass aggregates)	392	603	60	121	181	241	60	121	181	241
Mix 3b (100% waste glass aggregates)	367	611	0	0	0	0	122	244	367	489

Indeed, the workability of a cement mortar mixture is one of its most essential characteristics since it directly affects the practical applications of the mortar on the construction site. A mortar that is not satisfactorily workable is generally not preferred to be used on the site. Its rather difficult application might also affect its proper placement and final strength properties if used. Results of the literature survey showed that 35 second flow duration is accepted as an efficient flow according to ASTM-C939, and it also indicates that the efflux time for pure water is 8 seconds. Consequently, the optimum efflux time for cement mortar is between 8 seconds and 35 seconds, where higher efflux time means lower flowability and workability [12]. Also, results of the previous work [13] forming the basis for this study showed that cement mortars having 35 seconds of flow according to ASTM C939 yielded a slump interval of 260–270 mm with Abrams cone according to ASTM C143 procedure [14]. Hence, this slump interval of 260–270 mm was selected as the specified workability range for all mortar mixes, and with

several trial batches, the quantity of water to be added to each mix was determined to yield this specified slump value [15].

CEM I 42,5 R cement conforming EN 197-1 [16], having a reported specific gravity value of 3.15 g/cm³ was used for all mortar mixes in this study. Natural aggregates were obtained from the active quarries in the Beşparmak (Pentadaktylos) Mountains of Cyprus, where this study was carried out. Waste bricks and glasses used in this study were wastes collected from nature from North Cyprus. The experimental results presented in this study are a fraction of a broader experimental campaign carried out within the same institution. The gravities of waste bricks and glasses obtained from varying sources used in the experimental campaign ranged between 1.95–2.25 for waste bricks and 2.40–2.53 for waste glass used in the mixes. The natural (i.e., quarried) sand used in this study had a specific gravity of 2.64, which the supplier company reported.

After being collected and cleaned from other impurities, waste bricks and glass were crushed in the laboratory and sieved following the EN 933-1 (2012) procedure [17]. For all types of aggregates, the gradation of particles was maintained between the upper and lower content limits defined for the 0.15 mm–1.18 mm size range, following the specifications described in BS 882:1992 [18]. Figure 2a–c illustrate the natural and the recycled (i.e., waste) fine aggregates used in this study.

Table 2 summarizes the exact quantities of all materials used for this study's five distinct mortar mixes. The mixing procedure for all mortar mixes was conforming EN 00196-1–2005, with all mentioned ingredient contents [19].

Once the fresh mortar is placed on the site and it sets and hardens, its performance is determined according to its behavior and response under loading. The compressive strength behavior of concrete is typically regarded as the most critical indicator of its quality [20–22], which is known to be the case for cement mortars. In addition to

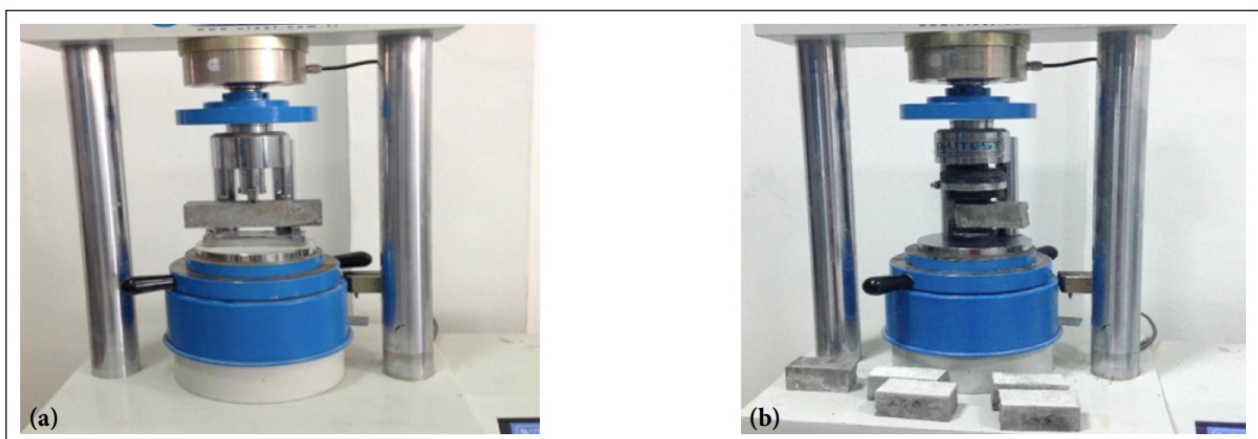


Figure 3. (a) Flexural strength testing on mortar prisms. (b) Compressive strength testing on halved prisms.

compressive strength, flexural strength behavior will also determine how the mortars would carry on with their service functions since flexural or bending actions could also act frequently on them depending on their service locations on the site. Hence, this study considers compressive and flexural strength testing to observe the efficiency of using waste glass and bricks in cement mortars concerning their hardened-state performance.

Six mortar bars having 40 mm x 40 mm x 160 mm dimensions were produced for each mortar mix. Samples were cast and compacted following the EN 196-1:2005 standard procedure and cured until the testing age [19].

Three of these six bars of each mix were tested at seven days to observe the early strength behavior of the bars, while the remaining 3 bars of each mix were tested at the age of 28 days.

Mortar bars were initially tested under flexural loading, and then, when the bar failed under flexure, the two halves obtained were tested under compressive loading, conforming EN 196-1:2005 part 1 [23]. Figure 3 a and b shows the mortar bars' Flexural and Compressive strength testing.

3. RESULTS AND DISCUSSIONS

The objective of this research study was to provide directly comparable experimental data for the strength behavior of waste brick and glass, including cement mortars that were produced to perform within the same workability range. For this purpose, trial mortar bars, including each specified waste type and content, were fabricated with different water additions, and the water/cement ratio that provided the specified slump range of 260 mm–270 mm was recorded.

Table 3 shows the determined w/c ratios for each type of mortar mix that yielded the targeted slump range.

It was observed that the use of waste glass as a replacement for natural sand in the mortar mix has not caused any significant increase in the water demand of the mix. Similar findings are also reported in the related literature, and this observed behavior was attributed to the non-porous nature of glass, which yielded deficient water absorption [11].

Table 3. Water/cement ratios yield the targeted workability range and the slump values obtained for each mortar mix

Mix	w/c ratio yielding targeted slump range	Obtained exact slump values (mm)
1	0.6	268
2a	0.73	269
2b	0.75	264
3a	0.65	266
3b	0.60	263

The control set (i.e., Mix 1) and waste glass-containing mixes (i.e., Mix 3 a & b) were observed to yield the targeted slump within a w/c ratio range of 0.6–0.65. On the other hand, the mixes made with waste bricks (i.e., Mix 2 a & b) were observed to have higher water demand; the w/c was determined to be 0.75 as the ratio needed to yield the targeted slump, which is 25% higher compared to the w/c of the control mix (i.e., Mix 1). The increase in the water demand of waste brick-containing mortar mixes observed in this study is expected to be due to the relatively porous texture of bricks compared to the texture of waste glass. A similar observation was reported by investigations of the characteristics of fresh mortars, including up to 20% brick replacement [24]. This study also showed that the presence of waste brick in mortar decreased the mix's slump, as noted in this study. Bektas et al. [8] and Zhu and Zhu [9] also report and confirm that the porous nature of the waste brick aggregates yielded adverse effects on the water demand and the workability characteristics of cement mortars.

3.1. Compressive Strength Test Results

Table 4 demonstrates the compressive strength values determined by testing each mortar mix and the strength decrease tendencies observed in each mix compared to control set samples containing no waste aggregates. Figure 4 illustrates the compressive strength development of all mortar mixes until 28 days. Errors bars are equivalent to one standard deviation.

Table 4. Compressive strength test results for each mortar mix used in this study

	w/c ratio	Compressive strength (MPa) 7 days	Compressive strength decrease compared to Mix 1 (7 days) Average	Compressive strength (MPa) 28 days	Compressive strength decrease compared to Mix 1 (28 days) Average
Mix 1	0.60	35.0	0%	42.0	0%
Mix 2a	0.75	31.0	11.43%	36.0	14.29%
Mix 2b	0.73	23.3	33.43%	29.3	30.24%
Mix 3a	0.60	29.3	16.29%	35.4	15.71%
Mix 3b	0.65	28.9	17.43%	36.2	13.81%

The control set (i.e., Mix 1, having only natural aggregates) is observed to yield the highest compressive strength at both seven days and 28 days. Hence, adding any of these waste materials as a replacement for natural sand was observed to cause a reduction in the overall compressive strength of the samples. For all mixes, the compressive strength was observed to have an increasing tendency with the increasing testing age, which is expected to be due to the ongoing hydration of cement in the mixes. Mix 2a and 2b, which are the samples containing 50% and 100% waste brick aggregates, were observed to have up to a 19% strength decrease between each other (when waste brick content was increased) and up to a 30% strength decrease when compared to the control set, at the age of 28 days. The w/c ratio required to yield the targeted slump was observed to have only a 2% difference between the two mixes having brick waste aggregates. Parallel findings are also reported in the related literature. Bektas et al. [8] and Zhu and Zhu [9] reported reduced compressive strength values for cement mortar samples when waste brick aggregates were added beyond certain contents defined their experimental campaigns, and both studies attributed this observed performance change to the porous nature of waste brick aggregates.

Further studies also reported that increasing the addition of waste brick in the mortar decreased the compressive strength of the cement mortars. It is also reported that the increasing addition of waste brick in the mortar decreased the compressive strength of the cement mortars. In their study, Aboutaleb et al. [25] presented that samples including 0% waste brick have 34 and 47 MPa compressive strength values at 7 and 28 days, but samples containing 100% waste brick have 18 and 35 MPa compressive strength values at 7 and 28 days, respectively; indicating a noticeable decrease in strength with the inclusion of wastes within the mortar. The compressive strength decreases recorded in this way with 100% brick aggregate containing mortars (compared to 0%) were 47.06% and 25.53% for 7 and 28 days, respectively. Another study also indicated that waste brick replacement of natural sand in mortar by up to 25% decreased the compressive strength values of mortars considerably. According to Shakir (2017) [26], samples including % five waste bricks yielded 15.12 and 19.12 MPa compressive strength values at 7 and 28 days. On the other hand, samples containing 25% waste brick yielded 2.4 and 8.16 MPa compressive strength

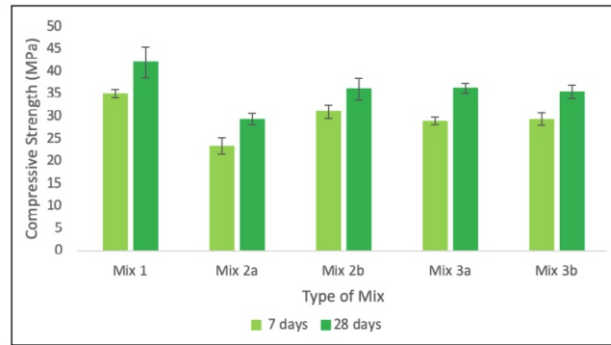


Figure 4. Compressive strength development for each mix between 7 and 28 days.

values at 7 and 28 days, respectively. These results show that the strength decrease was recorded as 84.7% and 57.3% at 7 and 28 days while comparing 5% and 25% brick-containing samples, respectively. The results are in parallel with the results presented in the research conducted. Demir et al. [27] indicate that the compressive strength of the mortar, including 50% waste brick and 50% natural sand, is approximately 31 MPa. The mortar, which included 100% waste brick, had a 7.8% lower compressive strength than the mortar containing 50% waste brick. Hence, the compressive strength of the mortar is reported to decrease with an increased percentage of waste brick inclusion in other studies as well. To illustrate, samples containing %0 waste brick have 33.5 and 42.5 MPa compressive strength values at 7 and 28 days, while samples containing %15 waste brick have 28.8 and 38 MPa compressive strength values at 7 and 28 days, respectively.

The results show that strength decreases as much as % 14.03 and % 10.59 at 7 and 28 days while comparing %0 and %15 brick content samples, respectively. On the other hand, Mix 3a and 3b, the samples having 50% and 100% waste glass aggregates, respectively, were observed to yield only a 3% strength difference at the age of 28 days, even though the waste glass aggregate content was doubled with Mix 3b. Moreover, with these mixed contents, Mix 3b, which has more waste aggregate, is observed to yield slightly higher compressive strength. When the water/cement ratios of the two mixes were compared, the reason for this slight increase could be potentially attributed to the lower w/c ratio of the mix 3b, which was sufficient to yield the targeted slump. Hence, these results indicate that the difference in the water content of the mixtures has a relatively more governing effect; even though the waste content was increased, the lower water content of the mix could positively affect the ultimate compressive strength determined at the age of 28 days. The waste glass aggregate-containing mixes (Mix 3a & 3b) were observed to yield up to a 16% strength decrease in general compared to "no waste-containing" Mix 1 samples at 28 days. This decrease of 16% with waste glass aggregates inclusion (when compared to Mix 1) could be considered as approximately half of the 30% strength decrease (compared to Mix 1) that was observed with the samples that contained waste brick aggregates (i.e., Mix 2a & 2b). Waste glass aggregate inclusion in the mortar bars was reported to yield a decrease in the compressive strength of mortars, as reported in the related literature. Similar studies also report a neg

ative effect on compressive strength upon adding waste brick aggregates. The results presented by Bhandari et al. [28] indicated that compressive strength values for mortar samples, including 20% waste glass, experienced around an 18% strength decrease compared to the case of not using waste aggregates. Additionally, Darshita and Anoop reported a 17% compressive strength decrease when 50% of the aggregates in the mortars were replaced with waste glass aggregates [29].

Mix 2b used in this study, having 100% waste brick aggregates, yielded the lowest compressive strength value, 29.3MPa at 28 days, among all mixes. Even though the type of waste aggregate is expected to be one of the causes of this strength decrease, it is also expected that the unavoidable increase in the water demand of this mix also played a considerable role in the observed reduction in strength.

Nevertheless, this increase in the water demand is attributed to the "type" of the waste aggregate since the relatively more porous texture of the brick could be observed when compared to the waste glass aggregates.

Similar to the case in concrete, compressive strength values of mortars are accepted as the main indicator of material quality.

The standard ASTM C270 [30] provides specifications for cement mortars and defines four categories, namely M, S, N, and O types of mortars for different site applications. Among these, type M mortar is defined for uses that require especially high compressive strength, and the mentioned standard defines its strength requirement as a minimum of 17.2MPa. In contrast, type N mortar, known to be used for general-purpose applications, is determined to have a compressive strength of 5.2 MPa in 28 days. As shown in Table 4, all mortar mixes used in this study are observed to yield 28-day compressive strength values that are well beyond the real application requirements defined in ASTM C270 [30]. Mix 2b (50% brick aggregate) and Mix 3b (50% glass aggregate) mortar mixtures proposed and tested within this study yielded 29.3MPa and 36.2MPa strength values, respectively, which enables them to be safely eligible to be used in the site applications according to the standards.

On the other hand, it is known that engineering applications require optimization in materials selection and quantity determination to meet criteria regarding safety and economy, which are both essential. In this study, the research priority and scope have been defined as providing systematical experimental data on the feasibility of manufacturing cement mortars including up to 100% waste aggregates, which, as a first step, considered only the safety aspect of engineering applications rather than the economy. The achieved strength results within this frame indicate the feasibility of using waste brick and glass aggregates in this preliminary step. The study's next step should focus on manufacturing more economical mortar mixes to eliminate the maximum amount of waste materials. One straightforward approach to reduce the cost is undoubtedly by reducing the cement content of the mix. As the strength values achieved are already higher than commonly expected mortar strength values (based on mortar strength performance defined in ASTM C270), reducing cement content up to a certain level is expected

to be tolerated. However, detailed studies should be employed to verify the optimum cement content to be used with maximum allowable waste content while obtaining safe and economical mortar mixes.

3.2. Flexural Strength Results

Table 5 demonstrates the flexural strength values yielded by each mortar mix and the strength decrease tendencies compared to control set samples that contained no waste aggregates, where Figure 5 illustrates the flexural strength development of all mortar mixes between the ages of 7 and 28 days, in comparison with each other. Errors bars are equivalent to one standard deviation.

As was observed within the compressive strength development of the mortar samples, Mix-1 yielded the highest flexural strength values at each testing age compared to the values obtained by other mixes containing waste aggregates. Even though the lowest flexural strength values recorded at the periods of 7 and 28 days were both yielded by 100% waste glass aggregate-containing mix 3b, it was noted that the strength values yielded by Mix 3b, 3a, and 2b were significantly close to each other. Mix 2a was observed to stand out from the rest of the waste aggregate-containing mortar mixes while yielding the second-highest strength values, following the control mix.

In another study, Abbas (2017) [31] indicates that it is also reported that the presence of %30 waste glass content in the samples generally yielded slightly negative effects on the flexural strength development of mortars. Their results demonstrated that flexural strength values for samples, including 30% waste glass, decreased to 1.37% compared to their control mixture. According to Tuaum (2018) [32], The research also investigated the flexural strength behavior of mortar specimens made with CEM I cement and reported that the lowest flexural strength value for 50% waste glass replacement was approximately 9 MPa at 28 days, which is highly by the results presented in the research. In addition, the study reports up to 11.76% flexural strength decrease at 28 days using 50% waste glass aggregates compared to their control set.

Table 5. Flexural strength test results for each mortar mix used in this study

	w/c	Flexural strength (MPa) seven days	Flexural strength decrease compared to Mix 1 (7 days) Average	Flexural strength (MPa) 28 days	Flexural strength reduce compared to Mix 1 (28 days) Average
Mix 1	0.6	8.1	–	9	–
Mix 2a	0.75	5.8	28.40%	6.6	26.67%
Mix 2b	0.73	4.9	39.51%	5.7	36.67%
Mix 3a	0.6	4.8	40.74%	5.6	37.78%
Mix 3b	0.65	4.3	46.91%	5.5	38.89%

Even though the 50% waste brick aggregate-containing Mix 2a and 50% waste glass aggregate-containing Mix 3b were observed to yield very similar compressive strength values, their flexural strength values were observed to differ; since mix 2a's flexural strength value was higher even though it contained higher water content. This behavior could be attributed to the rougher surface texture of the waste brick aggregates compared to the texture of glass aggregates, as the bonding between the aggregate and the cement paste is expected to be enhanced with the increased surface texture of the aggregates. Compressive strength testing is primarily affected by the mortar mixture's porosity. Hence, the effects of the water/cement ratio of the mortar, the general strength of the mortar, and the strength of aggregates are detectable with compressive strength testing. On the other hand, flexural strength testing is known to be more likely to reveal any strength decrease due to lack of bonding of the aggregates since the action of bending the samples would quickly cause detachment of aggregates and the paste very quickly, in case there is lack of adhesion due to aggregates' surface texture [33]. Highly parallel findings were also presented by Tan and Du (2013) [10] and Lu and Poon (2018) [11], as mentioned earlier within the literature information presented in the introduction section. These studies reported that the smooth surface texture of the glass aggregate yielded weaker bonds between the glass aggregate and the cement paste and hence yielded lower splitting tensile strength (known to be correlated with the flexural strength) of the mortar samples tested. Therefore, the difference between the surface texture of glass and brick aggregates and their influence on the mortars' performance should also be evaluated with flexural strength testing observations.

Concrete flexural strength is 10–20% of its compressive strength as a general tendency [33–35]. Mortar behavior is not directly equivalent to concrete behavior; however, a coherent behavior of cement-based materials could reasonably be expected. Within this frame, the 28-day flexural strength values observed for all mortar mixes manufactured in this study yielded a performance higher than at least 16% of their recorded compressive strength. In this case, the obtained results confirm that yielded flexural strength performance is coherent with the engineering performance expectations, especially considering that their compressive strength values are much higher than the high-strength Type M cement mortars defined in ASTM C270

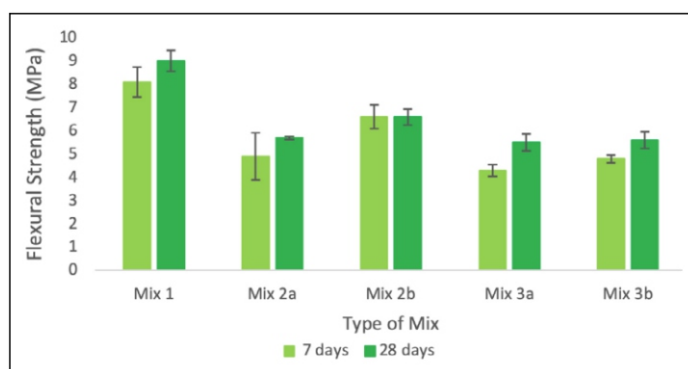


Figure 5. Flexural strength development for each mix at the ages of 7 and 28 days.

4. CONCLUSIVE REMARKS AND RECOMMENDATIONS FOR FUTURE STUDIES

This study investigates the effects of using recycled brick and glass aggregates as a replacement for natural sands used in cement mortars quantitatively and comparably. Recycling waste materials is critical for preserving nature and natural resources and is a key to sustainable development. On the other hand, waste materials within cement mortars, a very widely used construction material, would be considered feasible and acceptable only if the obtained performance could satisfy the civil engineering needs at least at a satisfactory level. The systematic experimental studies carried out on cement mortars that included waste glass and bricks separately, at 50% and 100% replacement ratios, provided the following quantitative comparisons and conclusive remarks:

I- Using recycled brick aggregates to replace natural sand in the mortar mixes caused a higher water demand to yield the specified workability characteristics when compared with the help of recycled glass aggregates. This is expected to be due to the increased absorption of brick aggregates, which are observed to be relatively more porous.

II- The necessity to increase the water content of the mortar mix with brick aggregates to obtain a satisfactorily workable mix had negative effects on the observed compressive strength behavior yielded by the mortar samples. The minimum compressive strength was obtained with the samples with 100% waste brick aggregates; these samples, on average, yielded a 30% compressive strength decrease compared to the control mix with no waste addition.

III- The mortar samples, including waste glass aggregates, were observed to yield higher compressive strength values. The decrease in compressive strength yielded by 100% waste glass aggregate inclusion into the mortars was only up to 16% compared to the control mix, which could be considered half of the strength decrease yielded when using brick aggregates. The compressive strength performance exhibited by samples with 100% waste glass is very similar to those with waste brick aggregates up to 50%.

IV- When the flexural strength testing results were considered, it was observed that the samples made with waste glass aggregates inclusion yielded much lower strength performance compared to the samples made with waste brick aggregates. The total strength decrease (compared to the control set) recorded for samples having 100% waste glass aggregates is up to almost 39%. This behavior is expected to be due to potentially reduced bonding between the paste and the glass aggregates, which have relatively smooth surface texture compared to the brick aggregates with rougher surface texture.

V- When compared with the standard specifications provided in ASTM C270 defining minimum compressive strength performance expected from cement mortars for real engineering applications on-site, all mortar mixes, including the ones with 50% waste aggregate replacements, have been observed to perform satisfactorily regarding the needs of engineering applications. Additionally, the flexural

strength performance of all mortar mixes used in this study was greater than at least 16% of each mix's compressive strength, indicating coherence with the general engineering expectations. Hence, the proposed mortar mixes with up to 50% (by mass) waste aggregate replacement have been observed to be suitable for real engineering applications.

VI-The obtained experimental results show that the type of waste aggregate for cement mortars should be selected considering the specific service location of the mortar used in the construction applications and their designed functions. If the mortar is required to perform well, specifically under compressive loads in the construction site, using waste glass aggregates in the mortar mix, even with high percentages, would yield better performance than waste brick aggregates. On the other hand, if the mortar is required to perform well, specifically under flexural actions in the construction site, the use of waste brick aggregates in the mortar mix, even with high percentages, is expected to perform better under these conditions.

In this way, eliminating higher quantities of waste (through being used in construction materials) would be possible without sacrificing the required engineering performance.

As recommendations for future studies, using further waste brick and glass aggregates with varying ages and properties is expected to yield significant insights into the effects of waste aggregates on cement mortars. Carrying out systematical experiments to determine the characteristics of waste aggregate particles, such as their specific gravity and absorption capacities, would be essential to relate their observed consequences on mortars, mainly if several samples of the same waste type (brick or glass) are employed with varying ages and conditions. Including these waste aggregates with different percentages is also recommended to provide an extended range of experimental data sets. Future studies should also consider carrying out systematical investigations on the optimum cement content that will be used in such mortars together with waste aggregates to provide both safe and economical site applications of mortars. Moreover, the segregation likelihood of the mortar mixes and effects of the characteristics of materials selected to be used should be studied as well to provide more complete data that will be beneficial, especially for the actual site applications. Finally, in addition to the fresh and hardened mortar properties such as workability and strength, complementary SEM analyses are recommended for future studies to relate further the surface texture and bonding characteristics of each waste aggregate employed to the ultimately observed mortar properties.

ETHICS

There are no ethical issues with the publication of this manuscript.

DATA AVAILABILITY STATEMENT

The authors confirm that the data that supports the findings of this study are available within the article.

Raw data that support the finding of this study are available from the corresponding author, upon reasonable request.

CONFLICT OF INTEREST

The authors declare that they have no conflict of interest.

FINANCIAL DISCLOSURE

The authors declared that this study has received no financial support.

PEER-REVIEW

Externally peer-reviewed.

REFERENCES

- [1] De Brito, J., & Saikia, N. (2012). *Recycled aggregate in concrete: use of industrial, construction, and demolition waste*. Springer Science & Business Media. [CrossRef]
- [2] Shi, C., & Zheng, K. (2007). A review on the use of waste glasses in cement and concrete production. *Resources, conservation, and recycling*, 52(2), 234–247. [CrossRef]
- [3] Du, H. & Tan, K. H. (2013). Use of waste glass as sand in mortar: Part I – Fresh, mechanical and durability properties. *Cement and Concrete Composites*, 35(1), 109–117. [CrossRef]
- [4] Aygün, B. F. (2021). An overview of the impact of using glass powder on mechanical, durability properties in self-compacting concrete. *Journal of Sustainable Construction Materials and Technologies*, 6(3), 116–123. [CrossRef]
- [5] Dilbas, H. (2022). An investigation on the effect of aggregate distribution on physical and mechanical properties of recycled aggregate concrete (RAC). *Journal of Sustainable Construction Materials and Technologies*, 7(2), 108–118. [CrossRef]
- [6] Dimaculangan, E. (2023). Current construction and demolition waste management strategies for Philippine construction sector – A systematic literature review. *Journal of Sustainable Construction Materials and Technologies*, 8(1), 47-56. [CrossRef]
- [7] Maurenbrecher, A. P. (2004). Mortars for repair of traditional masonry. *Practice Periodical On Structural Design And Construction*, 9(2), 62–65. [CrossRef]
- [8] Bektas, F., Wang, K., & Ceylan, H. (2009). Effects of crushed clay brick aggregate on mortar durability. *Construction and Building Materials*, 23(5), 1909–1914. [CrossRef]
- [9] Zhu, L., & Zhu, Z. (2020). Reuse of clay brick waste in mortar and concrete. *Advances in Materials Science and Engineering*, 2020(1), 1–11. [CrossRef]
- [10] Du, H. & Tan, K. H. (2013). Use of waste glass as sand in mortar: Part I – Fresh, mechanical and

-
-
- durability properties. Cement and Concrete Composites, 35(1), 109–117. [CrossRef]*
- [11] Lu, J. X., & Poon, C. S. (2018). *Use of waste glass in alkali activated cement mortar. Construction and Building Materials, 160(1), 399–407. [CrossRef]*
- [12] Afnan, R., Hadiyatmoko, D., Meyarto, C., Muhammad, P., Satyarno, I., & Solehudin, A. P. (2014). *Practical method for mix design of cement-based grout. Procedia Engineering, 95(2014), 356–365. [CrossRef]*
- [13] Alazzeah, A. M. A. (2018). *The Effect of Aggregate Gradation on The Performance of Fresh and Hardened Cement Grout. [Graduate Study Thesis, Faculty of Civil and Environmental Engineering, Near East University, Nicosia].*
- [14] ASTM C143 / C143M. (2020). *Standart Test Method for Slump of Hydraulic Cement Concrete (Standards Volume: 04.02).*
- [15] ASTM C 939. (2002). *Standard Test Method for Flow of Grout for Preplaced-Aggregate Concrete (Flow Cone Method) (Document No. ASTM-C939-02).*
- [16] TS EN 197-1:2012. (2012). *Cement - Section 1: Compound, properties and conformity criteria of general cements.*
- [17] EN 933-1. (2012). *Tests for geometrical properties of aggregates Part 1: Determination of particle size distribution. (Sieving method, European Norms).*
- [18] BS 882. (1992). *Specification for aggregates from natural sources for concrete. (European Norms).*
- [19] EN 196-1. (2005). *Methods of testing cement.*
- [20] Akpınar, P., & Khashman, A. (2017). *Intelligent classification system for concrete compressive strength. Procedia Computer Science, 120(1), 712–718. [CrossRef]*
- [21] Akpınar, P., & Khashman, A. (2017). *Non-Destructive Prediction of Concrete Compressive Strength Using Neural Networks. Procedia Computer Science, 108(1), 2358–2362. [CrossRef]*
- [22] Akpınar P., Al-Gburi S. N. A., & Helwan A. (2022). *Machine learning in concrete's strength prediction. Computers and Concrete, 29(6), 433–444.*
- [23] EN 196-1. (2005). *Methods of testing cement - Part 1: Determination of strength. (European Norms).*
- [24] Bhat A. A., Irfan, Z., & Shafi Z. S. (2017). *Utilization of surkhi as a partial replacement of sand in concrete. International Journal for Research in Applied Science & Engineering Technology, 8(12), 2321–9653.*
- [25] Aboutaleb, D., Belaid, A., Chahour, K., & Safi, B. (2017). *Use of refractory bricks as sand replacement in self-compacting mortar. Cogent Engineering, 4(1), 1360235. [CrossRef]*
- [26] Shakir, A. A. (2017). *The use of crushed brick waste for the internal curing in cement mortar. Muthanna Journal of Engineering and Technology, 5(1), 16–21.*
-
-

-
-
- [27] Demir, I., Simsek, O., & Yaprak, H. A. S. B. I. (2011). Performance of cement mortars replaced by ground waste brick in different aggressive conditions. *Ceramics-Silikáty*, 55(3), 268–275.
- [28] Bhandari, P. S., Dhale S. A., Ghutke V. S., & Pathan V. G. (2014). Influence of fine glass aggregate on cement mortar. *International Journal of Engineering and Computer Science*, 3(1), 3607–3610.
- [29] Anoop, P., & Darshita, T. (2014). Study of strength and workability of different grades of concrete by partial re-placement of fine aggregate by crushed brick and recycled glass powder. *International Journal of Science and Research*, 3(6), 1–5.
- [30] Astm, C. (2007). 270. Standard specification for mortar for unit masonry. *United States American Society for Testing and Materials*, 2–13.
- [31] Abbas, Z. K., Abbood, A. A., & Awad, H. K. (2017). Some properties of mortar and concrete using brick, glass and tile waste as partial replacement of cement. *International Journal of Science and Research*, 6(5), 1210–1215.
- [32] Oyawa, W., Shitote, S., & Tuum, A. (2018). Experimental Study of Self-Compacting Mortar Incorporating Recycled Glass Aggregate. *Buildings*, 8(2), 15. [CrossRef]
- [33] Neville, A. M. (1995). *Properties of Concrete*. Long man.[34] National Ready Mix Concrete Association. (2000). *Concrete in Practice; CIP 16 Flexural Strength of Concrete*. (888-84NRMC).
- [35] Lee, D. T. C., & Lee, T. S. (2017). The effect of aggregate condition during mixing on the mechanical properties of oil palm shell (OPS) concrete. In *MATEC Web of Conferences* 87(01019). [CrossRef]

Mechanical, freeze-thaw, and sorptivity properties of mortars prepared with different cement types and waste marble powder

Rümeysa GÜRGÖZE¹, Zinnur ÇELİK*², Ahmet Ferhat BİNGÖL¹

¹Department of Civil Engineering, Atatürk University Faculty of Engineering, Erzurum, Türkiye

²Pasinler Vocational School, Atatürk University, Erzurum, Türkiye*

ABSTRACT

The cement production process contributes significantly to Co₂ gas emissions and environmental pollution. To reduce this adverse effect, the substitution of waste marble powder as a cement additive was investigated. In this study, the properties of mortar specimens were analyzed by using waste marble powder as a partial substitute for three different cement types: CEM I 42.5R Ordinary Portland Cement (OPC), CEM II/B-L 42.5R White Cement (WC) and CA-40 Calcium Aluminate Cement (CAC). Waste marble powder has been replaced with cement at 5%, 10%, and 15%. The compressive and flexural strength, capillary water absorption, and sorptivity values of the prepared mixtures were determined before and after freezing and thawing. It was carried out after 28 days of water curing on 50 x 50 x 50 mm specimens for compressive strength and 160 x 40 x 40 mm specimens for flexural strength test. Freeze-thaw testing of the mixture samples was conducted according to ASTM C666 Procedure A. Test results showed that the highest compressive strength before freeze-thaw was obtained in calcium aluminate cement-based mortars containing 10% by weight waste marble powder replacement for cement. The appropriate waste marble powder ratio was determined as 10% in all cement types used in the study. Before freeze-thaw, the mechanical properties of CAC-based mixtures were higher than those of other cement types. However, as the number of freeze-thaw cycles increased, the strength losses were more significant compared to OPC and WC.

Cite this article as: Gürgöze, R., Çelik, Z., & Bingöl A. F. (2023). Mechanical, freeze-thaw, and sorptivity properties of mortars prepared with different cement types and waste marble powder. *J Sustain Const Mater Technol*, 8(4), 307–318.

Key words: Calcium aluminate cement, freeze-thaw, mechanical properties, waste marble powder

1. INTRODUCTION

Concrete is the most widely used building material worldwide due to its low price, easy accessibility of its components, ability to give the desired shape, and provide the necessary strength and durability [1, 2]. Cement, the most used binder material in concrete production, is the primary source of Co₂ emissions. Ordinary Portland Cement (OPC) production contributes about 5% to 7% of global Co₂ emissions [3, 4]. It has been determined that the concrete production in Türkiye as of 2014 is approximately 70 Million Tonnes (Mt); therefore, about 65 Mt of CO₂ has been released [5, 6].

Cement production significantly impacts Co₂ emissions and can be reduced using waste materials that

improve concrete's fresh and mechanical properties. Among these waste materials, marble powder, mainly found in Turkey, India, China, and Italy, is used as a cement substitute in concrete production. The production of marble waste is estimated to be around 3 Mt annually [5]. During the processing of natural marble, a significant amount of powder particles are released into the environment, creating waste.

Disposing waste materials from these powder particles can be complex and contribute significantly to environmental damage by contaminating natural resources [6].

Marble powder is used in concrete and mortar production due to its chemical structure and filling properties. This can reduce environmental damage and contribute to a sustainable approach in the construction industry. The filling effect of marble powder forms a denser mixture, improving the transition zone and cement matrix. This may cause an increase in the strength of the mixtures by adding low amounts of marble powder. Additionally, dolomite ($\text{CaMg}(\text{-CO}_3)_2$) found in WMP reacts with the alkalis of cement to form calcium carbonate (CaCO_3). As a result of the reaction between calcium carbonate and the C_3A component of cement, a more compact structure is formed that increases the binding capacity of the matrix [7]. Munir et al. [8] reported that calcite in WMP reacted with C_3A to form calcium carbo-aluminate, and better compressive strength was obtained in mixtures containing WMP. There are several studies in the literature on the substitution of waste marble powder (WMP) for Ordinary Portland Cement (OPC). Uysal and Yilmaz [9] determined that the properties of fresh concrete were improved by replacing the cement with marble powder at 10%, 20%, and 30% by mass. Aliabdo et al. [10] determined that the 28-day compressive strength decreased by 7%, 4%, 5%, and 14% when replacing 5%, 7.5%, 10%, and 15% marble powder with OPC compared to the control specimen. Ergün [11] reported that substituting 5% and 7.5% WMP for cement increased the compressive strength, but using 15% decreased the strength. Ashish [5] observed that adding 15% WMP to the concrete increased the compressive strength by 4.5% and 10.4% at 28 and 91 days of curing times, respectively, compared to the control specimen. Rodrigues et al. [12] determined that replacing cement with marble powder up to 10% in concrete does not adversely affect the compressive strength. Still, replacing 20% marble powder reduces the compressive strength by 25%.

Studies in the literature on the durability of concrete are attracting increasing attention. Freeze-thaw (FT) is among the main reasons for the loss of durability of concrete, especially in cold climates [13, 14]. Due to the porous structure of concrete, repetitive FT cycles cause the concrete to lose strength and crumble by exfoliating [15]. Freeze-thaw studies in the literature on waste marble powder have generally focused on substituting WMP with fine aggregate in concrete [15–18]. İnce et al. [16] reported that the FT resistance of concrete to which waste marble powder was added increased.

Another issue is that the Ordinary Portland Cement (OPC) was used in all studies based on the literature above. However, due to the large amount of CO_2 released by OPC, studies on the discovery and

application of cementing materials to ensure sustainability in cement production continue [19]. Calcium aluminate cement (CAC) releases approximately 30% less CO₂ than OPC during production. In addition, CAC is preferred in refractory material production, wastewater, and industrial floor applications due to its high early strength and resistance to harsh environmental conditions such as acid and high temperature [20, 21].

However, the use of CAC in structural system elements is prohibited due to instability in compressive strength due to the transformation of hydration products that contribute to the early high strength of CAC [22, 23].

2. RESEARCH SIGNIFICANCE

Studies on sustainability in the building sector have attracted much attention in recent decades. In most studies, WMP has been used by replacing fine aggregate. Although this situation contributes to the use of waste materials, it does not positively affect the CO₂ emission originating from the cement. In addition, most of the studies in the literature have focused on OPC. However, regarding sustainability, examining and using CAC, which causes less CO₂ emissions, is very valuable in reducing environmental problems. This study aims to investigate the freeze-thaw effect, lacking in the literature, by substituting waste marble powder in the mortar instead of cement. Another important aim is to examine the usability of CAC and white cement (WC) with WPM and compare it with OPC. The study was considered to compare CEM I cement, which is frequently used in practice, with two particular types of cement (white and calcium aluminate). The use of CAC and WMP together is important in terms of sustainability. In this context, mortar specimens were prepared by replacing 5%, 10%, and 15% WMP with three different types of cement. In addition, silica fume (SF) was used at the ratio of 10% by weight of cement in all mixtures. These specimens were subjected to compressive strength, flexural strength, and capillary permeability tests. In addition, the specimens were left to 3 different freeze-thaw cycles, and the same tests were repeated.

3. EXPERIMENTAL PROGRAMME

3.1. Materials

In this study, three different types of cement were used in the preparation of mortar mixes: OPC (CEM I 42.5 R), CAC (CA-40), and WC (CEM II/B-L 42.5R). WMP was replaced by weight with three different cement types at 5%, 10%, and 15%. In addition, since the risk of segregation was observed in the mixtures as a result of preliminary experiments, 10% of the binder amount of SF was used in all mixtures to increase the viscosity. The chemical and physical properties of OPC, CAC, WC, SF, and WMP are in Tables 1 and 2, respectively.

Table 1. Chemical characteristics of OPC, CAC, WC, SF and WMP

Compound	OPC (%)	CAC (%)	WC (%)	SF (%)	WMP (%)
SiO ₂	17.73	3.60	21.60	95.60	0.80
Al ₂ O ₃	4.56	39.80	4.05	0.40	0.60
Fe ₂ O ₃	3.07	17.10	0.26	0.80	0.80
CaO	62.81	36.20	63.70	0.40	57.20
MgO	2.07	0.65	1.30	0.60	9.60
K ₂ O	0.62		0.35	0.40	0.03
SO ₃	2.90	0.04	3.30	0.20	0.04

Table 2. Physical properties of OPC, CAC, WC, SF and WMP

Property	OPC	CAC	WC	SF	WMP
Specific gravity	3.15	3.25	3.06	2.20	2.73
Loss on ignition (%)	2.05	0.30	3.20	0.60	42.60
Insoluble residue (%)	0.66	0.16	0.18		0.91
Specific surface	3450 ^a	3000 ^a	4600 ^a	19800 ^b	
Compressive strength of cement (Mpa)					
Two days	25	60	24		
28 days	48		46		

a: Blaine method (cm²/g); b: BET method (m²/kg).

Table 3. Mix proportions of mortars (kg/m³)

Mixture codes	Cement	Silica fume	WMP	Fine agg.	Water	Superplasticizer
OPC-0	540	60		1404	252	6
OPC-5	510	60	30	1398	252	6
OPC-10	480	60	60	1396	252	6
OPC-15	450	60	90	1391	252	6
CAC-0	540	60		1416	252	6
CAC-5	510	60	30	1412	252	6
CAC-10	480	60	60	1409	252	6
CAC-15	450	60	90	1404	252	6
WC-0	540	60		1391	252	6
WC-5	510	60	30	1386	252	6
WC-10	480	60	60	1383	252	6
WC-15	450	60	90	1380	252	6

Within the scope of the experimental study, the specific gravity and water absorption ratio of the sand were determined according to EN 1097-6 [24]. River sand with a specific gravity of 2.60, water absorption value of 1.80%, and fineness modulus of 3.42 was used as fine aggregate. In addition, in this study, a new generation superplasticizer polycarboxylate-based with the pH and specific gravity of 6 and 1.065, respectively.

3.2. Mix Proportions

The mixing ratios of the mortar specimens prepared within the scope of this study are given in Table 3. In

similar studies in the literature, it has been determined that generally, between 500–600 kg/m³ of binder material is used. In EFNARC 2005 [25], the total powder content was recommended to be 400–600 kg/m³. All mixtures kept the binder amount constant at 600 kg/m³ for these reasons. In addition, 10% of the binder amount of SF was used in all the mixtures. Waste marble powder was replaced with cement at 5%, 10%, and 15% of the total binder amount. The water/binder ratio was determined as 0.42 in all mixtures. To ensure the workability of the fresh mortar, 1% of the binder amount was used as a superplasticizer. According to these parameters, 13 different mortar mixtures were prepared. Each mixture is named according to the type of cement used in the mix and the ratio of waste marble powder. For example, in a CAC-10 code, the first three letters (CAC) indicate the use of calcium aluminate cement, and the adjacent numbers (10) represent the amount of waste marble powder in the mortar mix.

3.3. Test Methods

To determine the workability of the self-compacting mortar (SCM), the mini-slump flow test was applied according to EFNARC [25]. The workability values of the SCMs were evaluated according to criteria of 240–260 mm for the slump flow diameter. The mortar specimens' compressive and flexural strength tests were carried out by ASTM C109 [26] and ASTM C348 [27] standards, respectively. It was carried out after 28 days of water curing on 50 x 50 x 50 mm specimens for compressive strength and 160 x 40 x 40 mm specimens for flexural strength test.

Also, within the scope of the experimental program, 50 × 50 × 50 mm cube specimens were tested at age 28 days according to ASTM C1585-13 [28] to calculate the capillary water absorption and sorptivity coefficients of SCM mixtures. For the capillary water absorption test, the four side surfaces of the specimens were covered with a seal using vinyl electrician tape and exposed to 1–3 mm of water from only one surface. All mixture specimens' weight and cross-sectional area were measured before the capillary water absorption test. Capillary water absorption was deter



Figure 1. SCM specimens (a) in mixture, (b) slump test, (c) in water curing pool, (d) sorptivity test, (e) flexural strength test.

mined by measuring the weights of the specimens at 5, 10, 30, 60, 120, 180, 240, 300, and 360 min time intervals. Laboratory images of experimental studies are given in Figure 1. Freeze-thaw (F-T) testing of mixed specimens was performed according to ASTM C666 [29] Procedure A. The specimens were subjected to 3 different cycles (30, 60, 90) after 28 days of curing, and then compressive strength, flexural strength, and capillary permeability tests were performed. Ambient conditions were set to have cycles of freezing at -18°C and thawing at 4°C .

4. RESULTS AND DISCUSSIONS

4.1. Workability

The slump-flow diameter test results of the mixtures are presented in Figure 2. Significant decreases were detected in the slump flow diameters of the mixtures with WMP added, and this was more evident in the mixtures using 10% and 15% WMP. This can be attributed to the fact that the specific surface area of waste marble powder is higher than cement, thus reducing workability by increasing internal friction [5]. Rashwan et al. [30] reported that waste marble powder's angular, rough shape and high fineness reduce workability. Li et al. [31] stated that drier mixtures were obtained by substituting cement paste with waste marble powder at higher rates than the control mixture. It was determined that the flow diameters of all mixtures were between 240–260 mm, specified in EFNARC, with the effect of the superplasticizer. OPC-based mixtures were obtained with slump flow diameters of 258, 257, 252, and

248 mm

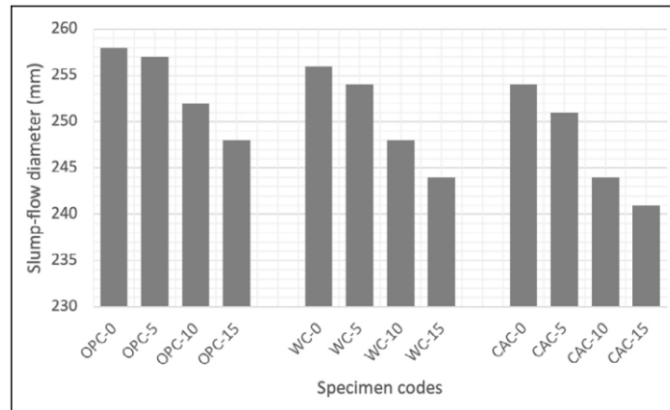


Figure 2. Slump-flow diameters of mixtures.

for OPC-0, OPC-5, OPC-10, and OPC-15, respectively. The slump-flow diameters of the WC-based mixes ranged from 24.4 to 25.6 cm. The lower flow diameter of WC-based mixtures compared to OPC can be attributed to the higher specific surface area of WC (4600 cm²/g) compared to OPC (3450 cm²/g). The most significant reduction in flow diameter was obtained in CAC-based mixtures. While the flow diameter of the CAC-0 series was 254 mm, this value was measured as 241 mm in the CAC-15 series.

4.2. Properties of Mortar Specimens Before Freeze Thaw Cycles

4.2.1. Compressive Strength

The 28-day compressive strength results of SCM specimens before freezing and thawing are given in Figure 3

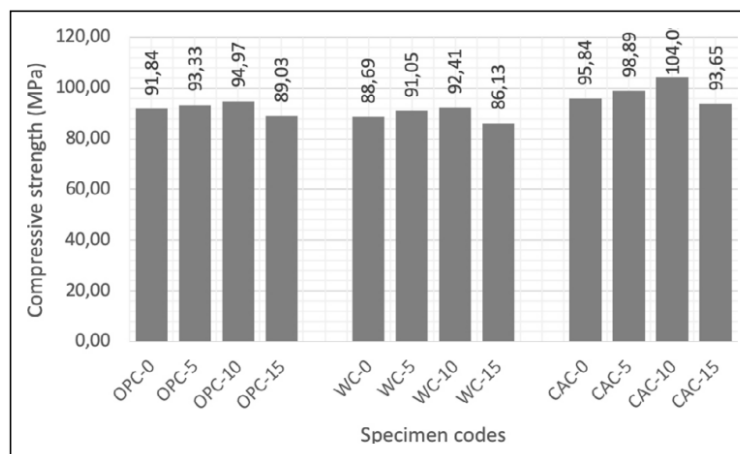


Figure 3. Compressive strength results of mixtures.

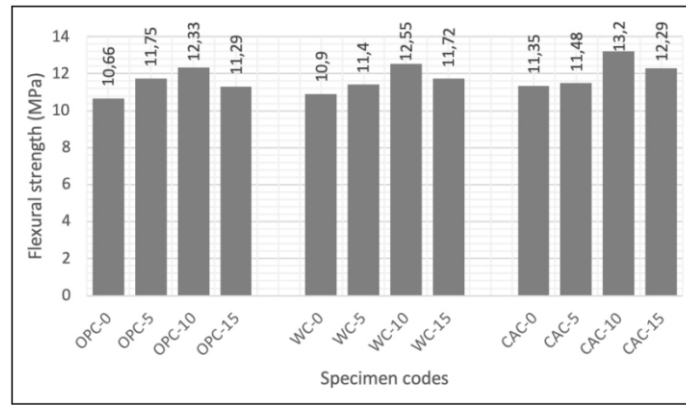


Figure 4. Flexural strength results of mixtures.

Adding WMP up to 10% in all cement series increased compressive strength. This result can be attributed to fine WMP enhancing the properties of the transition zone surrounding the aggregate through its pore-filling effect [10]. As a result of the replacement of cement with 5% WMP at 28-day curing ages, an increase of 1.62%, 2.66%, and 3.18%, respectively, in the compressive strength of the OPC, WC, and CAC series was observed. When replacing 10% WMP with cement, it was determined that the compressive strength of OPC, WC, and CAC series increased by 3.41%, 4.19%, and 8.60%, respectively. Ashish [5] found that adding 10% marble powder instead of cement increased the compressive strength by 8.44% compared to the control specimen. Aliabdo et al. [10] detected that using 5% and 10% WMP caused an increase in compressive strength of 1% and 12%, respectively. It is observed that the strength of the mortar slightly decreased at the 15% level of WMP used as a cement substitute. This is due to reduced cementing materials such as C3S, C2S, and C3A. While 15% WMP substitution reduced the strength by 3.06% in the OPC mixtures, it decreased it by 2.88% and 2.29%, respectively, in the WC and CAC mixtures.

Ergün [11] observed that substituting 5% and 7.5% of cement with WMP increases the compressive strength and decreases the strength by 15%. The optimum WMP ratio was determined as 10% for all cement types. In their research, Vardhan et al. [32] reported that the substitution of 10% WMP is optimum for cement in terms of workability and compressive strength.

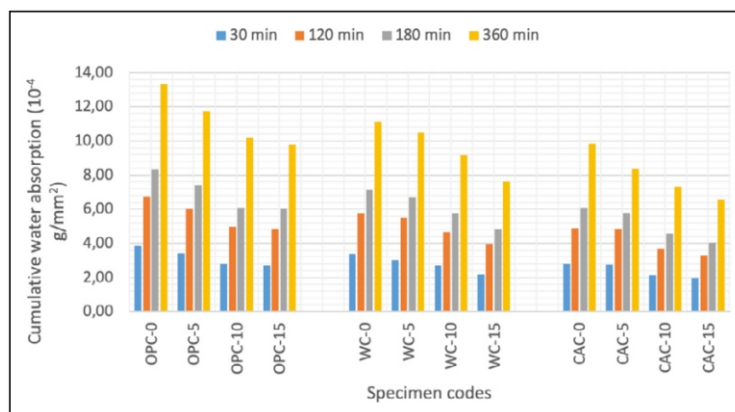
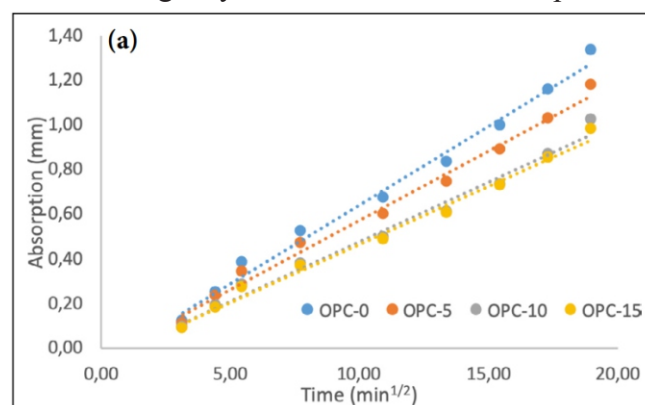


Figure 5. Cumulative capillary water absorption results of mixtures.

As a result of examining the compressive strength in cement types, the highest compressive strength value in all WMP replacement ratios was obtained in the mixtures using CAC. The highest compressive strength value of 104.09 MPa was found in CAC using 10% WMP in all mixes. Although WMP is not pozzolanic, it is not entirely inert because it can react with the alumina phases of cement [9]. If there is an excess of C₃A in the cement, carbo aluminate will be produced from the reaction between CaCO₃ and C₃A in WMP [33, 34]. This reaction, which increases compressive strength, increases with the C₃A content in the cement (OPC and WC). In the series without WMP, the highest compressive strength value was obtained from the CAC-0 series, while this value was 8.06% and 4.35% higher compared to the WC-0 and OPC-0 series. In the series using 5%, 10%, and 15% WMP, the compressive strength of CAC-based mixtures was 5.96%, 9.60%, and 5.19% higher, respectively, than OPC. Idrees et al. [35] investigated the properties of CAC and OPC at different curing temperatures using various mineral additives. As a result of the study, they observed that the 28 and 90-day strength values of the CAC-based mixtures were higher than the mixtures with OPC at low curing temperatures (200C). The high early strength of CAC compared to OPC was attributed to the formation of CAH₁₀ and C₂Ah₈, which are the dominant hydration products of CAC at low curing temperatures. The compressive strength values of WC-based mixtures using 0%, 5%, 10%, and 15% WMP were approximately 3.43%, 2.44%, 2.70% and 3.26% lower than OPC-based mixtures, respectively. The higher surface area of WP compared to OPC resulted in a decrease in its workability. This may cause small voids in SCMs that self-compact under their weight without requiring additional processing. As a result, this phenomenon may be why the compressive strength of OPC-based mixtures is slightly higher than that of WP-based mixtures.

4.2.2. Flexural Strength

The flexural strength results of the mixtures are given in Figure 4. The highest flexural strength was obtained from the CAC-10 series with 13.20 MPa. Similar to the compressive strength results, flexural strength increased in all cement types up to 10% WMP use. Substitution of 5% and 10% WMP in OPC-based blends increased flexural strength by 10.23% and 15.67% compared to the OPC-0 blend. Ergün



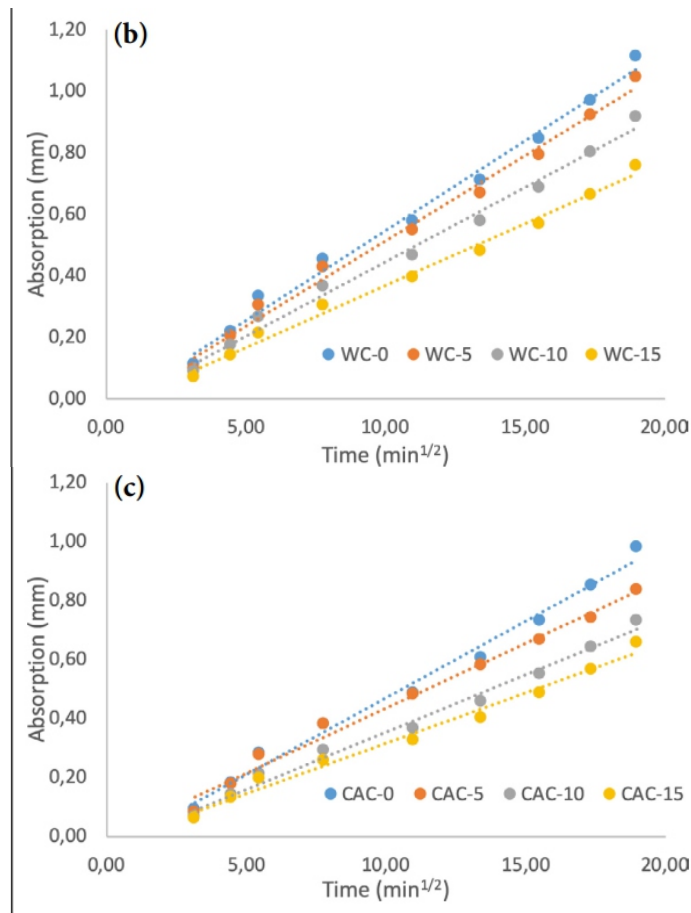


Figure 6. SCM specimens absorption (mm) (a) OPC-based mixtures, (b) WC-based mixtures, (c) CAC-based mixtures.

[11] observed that using WMP did not cause a significant change in the relative flexural strength of the mixture samples. As a result of the study, a 5% increase in the 90-day flexural strength of mixtures containing 5% WMP was reported compared to the reference sample. Kumar et al. [36] stated that 5% WMP replacement increased the flexural strength of the mixtures by 3% and 7% in 7 and 28 days, respectively. It was observed that 5% WMP substitution increased the flexural strength of WC and CAC-based mixtures by 4.59% and 1.15% compared to WC-0 and CAC-0 mixtures. 10% WMP substitution improved flexural strength by 15.14% and 16.30% compared to WC and CAC-based reference specimens. This can be attributed to the positive effect of WMP substitution at low rates, as WMP reduces the porosity of mortar samples. In addition, 5% WMP did not significantly affect WC and OPC-based mixtures, while using 10% WMP significantly improved the strength.

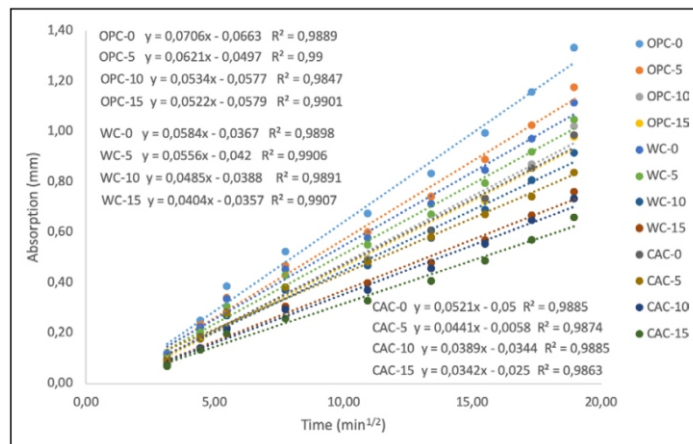


Figure 7. Sorptivity coefficient results of mixtures.

Although adding 15% WMP in all cement types decreased the flexural strength, it was higher than the reference specimens. The flexural strength of the OPC-15, WC 15, and CAC-15 series was 5.91%, 7.52%, and 8.28% higher than the control specimens.

4.2.3. Capillary Water Absorption and Sorptivity Coefficients

Capillary water absorption values of the mixtures are presented in Figure 5. Capillary water absorption values decreased with increased WMP ratio in all cement types. This can be attributed to the reduction of porosity in mortar specimens due to the filling effect of WMP use. Topçu [37] reported that adding WMP fills the voids in self-compacting concrete (SCC) and reduces capillary voids due to high workability. Aliabdo et al. [10] reported that the porosity of concrete decreased with the increase of WMP in the case of partial substitution of cement with WMP for different w/b ratios. Increasing the WMP ratio from 0 to 15 in OPC-based mixtures decreased the 6-hour surface water absorption value by 26.7%. Increasing the WMP ratio from 0% to 15% in WC and CAC-based mixtures decreased the capillary water absorption value by 31.65% and 33.30%, respectively. The least capillary water absorption was obtained from CAC-based mixtures among the different cement types. Ashish et al. [38] observed that substituting WMP instead of cement in concrete reduced the water absorption rates of concrete mixtures. Gupta et al. [39] stated that substituting up to 10% WMP reduced water absorption. This result is attributed to the pore-filling effect decreasing the void percentage due to the fineness of the WMP. Khodabakhshian et al. [40] and Zhang et al. [41] determined that the substitution of 5% SF along with 5–20% WMP reduces water absorption due to additional C-S-H gel filling the pores and improving the microstructure. The absorption and time relationship of OPC, WC, and CAC based mixtures are presented in Figure 6a–c, respectively.

To calculate the sorptivity coefficient, the amount of water adsorbed (mm³) per the cross-section of the specimen in contact with water (cm²) (Q/A) was plotted against the square root of time (t), then k was determined from the slope of the linear relationship between Q/A and t. The sorptivity and correlation

coefficients of all mixtures are given in Figure 7. As can be seen from Figure 7, the sorptivity coefficient decreased as the WMP ratio increased for all cement types. Due to the small particle size of WMP, the pores at the interfaces between the paste or aggregate and the cement paste are filled with WMP, resulting in smaller capillary pores. The lowest sorptivity coefficient in OPC-based mixtures was obtained from the mixture series using 15% WMP with $0.0522 \text{ mm/min}^{1/2}$. This value was 26.06% lower than the OPC-0 series without WMP. Adding 5%, 10%, and 15% WMP in WC-based mixtures decreased the sorptivity coefficient by 4.79%, 16.95% and 30.82%, respectively. The lower sorptivity values of WC-based mixtures compared to OPC-based mixtures can be attributed to the reduction of capillary pores due to the finer particle size of WC compared to OPC. The lowest sorptivity value among all mixes was calculated with $0.0342 \text{ mm/min}^{1/2}$ in the CAC-15 series. This value was 34.36% lower compared to the CAC-0 series. In addition, the sorptivity value of the CAC series using 15% WMP was 34.48% and 15.34% lower, respectively, compared to the OPC-15 and WC-15 series. The lower sorptivity coefficient of CAC-based mixtures compared to OPC and WC can be explained by the denser structure of CAC's metastable phases (CAH10 and C2Ah8) compared to the C-S-H phases in OPC. Moffatt [42] reported that CAC samples had a lower chloride diffusion coefficient than OPC samples and attributed this to the denser structure of CAC.

4.3. Properties of Mortar Specimens After Freeze Thaw Cycles

4.3.1. Residual Compressive Strength

All mixture specimens were subjected to freeze-thaw cycles after a 28-day curing period. The number of cycles was determined as 30, 60, and 90. After the process counts, no significant deterioration occurred in the specimens, which can be attributed to the high amount of binder. Residual compressive strength results of the mixtures after 30, 60, and 90 cycles are presented in Figure 8. The reduction in compressive strength of OPC-based mixtures after 30 cycles varies between 3.1% and 5.3%. While the least strength drop was obtained in the OPC-5 series, the highest decrease was calculated in the OPC-15 series. Similar to the compressive strength results before the freeze-thaw cycles, the residual compressive strengths of the mixtures using 5% and 10% WMP were higher than the OPC-0 series.

After 60 freeze-thaw cycles of the OPC-based mixtures, the residual compressive strengths of the OPC-0, OPC-5, and OPC-10 series were obtained as 86.39 MPa, 87.95 MPa, and 89.26 MPa, respectively. However, despite being high in compressive strength, the relative residual compressive strength (the ratio of residual compressive strength after freeze-thaw to initial compressive strength) was determined as 0.941, 0.942 and 0.940 at 0%, 5%, and 10% WMP change, respectively. A similar situation was observed after 90 cycles. Although the residual compressive strength of the OPC-5 and OPC-10 mixture series was higher than the OPC-0 series, the relative residual compressive strength was determined as 0.893, 0.892, and 0.891 for the OPC-0, OPC5 and OPC-10 mixtures, respectively. As a result, the addi

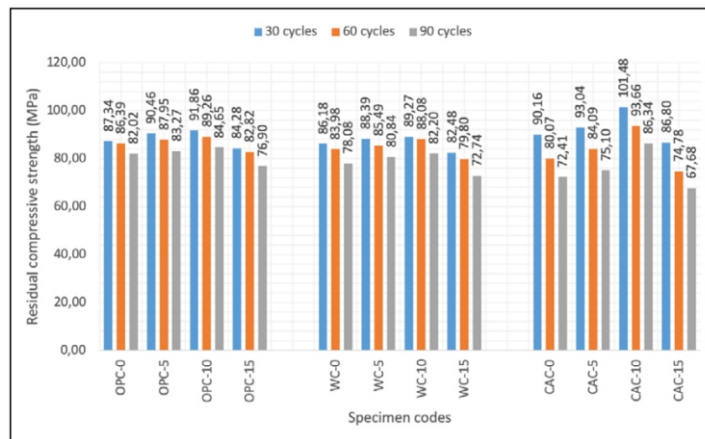


Figure 8. Residual compressive strengths after freeze-thaw.

tion of 5% and 10% WMP did not cause a significant effect on the strength of the mixtures after 60 and 90 freeze-thaw cycles. This can be attributed to the fact that the C-S-H gel content decreased due to WMP without pozzolanic activity, but the low range (5% and 10%) of WMP compensated for the decrease in strength due to the filling effect. Ince et al. [16] reported that concrete samples containing silica fume and waste marble powder suffered less strength loss after freeze-thaw cycles than the reference sample. Gencil et al. [43] stated that using waste marble powder instead of aggregate in concrete paving blocks increases the freeze-thaw resistance. With an increased WMP ratio of 15%, the freeze-thaw resistance of OPC-based mixtures decreased. After 60 and 90 cycles, the relative residual compressive strength of the OPC-15 series was obtained as 0.930 and 0.864. Increases in the amount (%15) of WMP cause a further reduction of hydration products, creating a loose structure that will increase free water and expansion stress during freeze-thaw cycles, resulting in more strength loss.

When the compressive strengths of WC-based mixtures after freeze-thaw cycles are examined in Figure 8, it is observed that the strength loss after 30 cycles varies between 2.8% and 4.2%. When the cycle number increased to 60 in WC-based mixtures, 5.3%, 7.1%, and 4.7% loss occurred in the compressive strength of the mixtures containing 0%, 5%, and 10% WMP, respectively. Similar to the compressive forces before exposure to freeze-thaw, the residual compressive strengths of 5% and 10% WMP were higher compared to the WC-0 series. After 90 freeze-thaw cycles, 0%, 5%, and 10% WMP substitution to WC-based mixes reduced the relative residual compressive strength to 0.880, 0.888, and 0.890, respectively. Similar to OPC based mixtures, using WMP in low proportions showed a filling effect, making the mortar structure denser and preventing a further decrease in strength despite the decrease in C-S-H structure. In the case of 15% WMP addition, the reduction in strength after 60 and 90 cycles was obtained as 7.3% and 15.5%, respectively. The freezing and thawing resistance of concrete or mortar highly depends on the amount of hydration products and pores. Due to the absence of significant differences in the chemical composition of OPC and WC, the strength drops after cycles are also significantly similar.

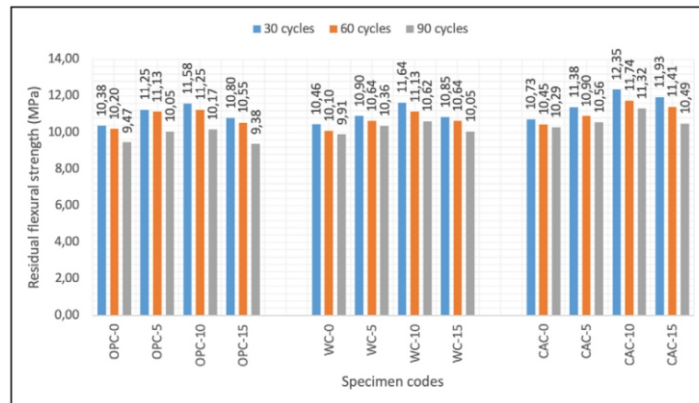


Figure 9. Residual flexural strengths after freeze-thaw

When the results of CAC-based mixtures are examined, the reductions in strength after 30 cycles range from 2.5% to 7.3%. The least strength loss was calculated from the CAC-10 series, and the maximum strength reduction was calculated from the CAC-15 series. Significant strength losses occurred in CAC-based mixtures when the number of cycles increased to 60. After 60 freeze-thaw cycles, strength loss happened in the CAC-0, CAC-5, CAC-10, and CAC-15 series at 16.5%, 15%, 10% and 20.1%, respectively. Although there was a decrease in strength loss with an increase in WMP ratio to 10%, the addition of 15% WMP increased the strength loss. After 90 freeze-thaw cycles, the compressive strength loss in CAC-based mixtures using 0%, 5%, 10%, and 15% WMP was obtained as 24.4%, 24.1%, 17.1%, and 27.7%, respectively. Although the compressive strength losses are higher than other cement types, the highest compressive strength was determined in the CAC-10 series in all cycle numbers.

The lower freeze-thaw resistance of CAC-based mixtures compared to other cement types can be explained by the transformation of the metastable phases (CAH10 and C2A_h8), which are the hydration products of CAC, into stable C3A_h6. With this phase transformation, the porosity of the concrete increases, and its compressive strength decreases [44]. This conversion reaction accelerates at high temperatures and moisture content [45]. As a result, moisture changes in the specimens during the freeze-thaw cycles may cause a decrease in strength by accelerating phase transformations.

4.3.2. Flexural Strength

The flexural strength results of the mixture specimens after freezing and thawing are given in Figure 9. After 30 cycles, the flexural strength of the OPC-based mixtures decreased between 2.6% and 6.1%. When the number of cycles increased to 60, a decrease in bending strength of 4.3%, 5.3%, 8.8%, and 6.6% were detected in the OPC-0, OPC-5, OPC-10, and OPC-15 series, respectively. Relative residual flexural strength values of the mixtures using 0%, 5%, 10%, and 15% WMP after 90 cycles were determined as 0.888, 0.855, 0.825, and 0.831, respectively. Although the strength losses increased with the addition of WMP, the residual flexural strengths were higher than the OPC-0 series without WMP. The highest residual flexural strength of OPC-based mixtures in all cycles was obtained in the OPC-10

series. Flexural strength loss in WC-0, WC-5, WC-10, and WC-15 mixture series after 30 cycles in WC-based mixtures was determined as 4%, 4.4%, 7.3% and 7.4%, respectively. After 30 cycles, the highest flexural strength was obtained from the WC-10 series. The flexural strength reduction after 60 cycles was determined as 6.7% to 11.3% in WC-based mixtures. After 90 cycles, the strength drops became more pronounced. The relative residual flexural strengths of the WC-0, WC-5, WC-10, and WC-15 mixture series were obtained as 0.909, 0.909, 0.846, and 0.858, respectively. After all cycles, the residual flexural strengths of WMP-added mixtures were higher than those without WMP. As seen in Figure 8, the residual compressive strengths of the WMP-added CAC-based mixtures were higher than the non-WMP mixture after freeze-thaw cycles. Similar to OPC and WC-based mixtures, the highest residual flexural strength after all cycles was determined in the CAC-10 series. Using 0.5%, 10%, and 15% WMP in CAC-based mixtures after 30 cycles decreased compressive strength of 5.5%, 0.9%, 6.4%, and 2.9%, respectively. The lowest decrease in strength after 60 cycles was obtained in the CAC-5 series with 5.1%. Strength losses in the CAC-10 and CAC-15 series were 11.1% and 7.2%, respectively. After 90 cycles, the relative residual flexural strengths of the CAC-0, CAC-5, CAC-10, and CAC-15 series were determined as 0.907, 0.920, 0.858, and 0.854. Although using WMP in all three cement types increased overall freeze-thaw flexural strength reductions, the residual flexural strengths were still higher than in non-WMP mixtures. This can be attributed to improving the flexural strength of WMP before the freeze-thaw cycles of the mixtures using WMP. In all cement types, the highest residual flexural strength after 30, 60, and 90 cycles was observed in the series with 10% WMP replacement.

4.3.3. Capillary Water Absorption and Sorptivity Coefficient

The capillary water absorption and sorptivity values of all cement types after 30 freeze-thaw cycles are given in Figures 10 and 11. After the freeze-thaw cycle, capillary water absorption values increased in all mixtures. As the WMP content in the mixtures increased, a decrease was observed in the capillary water absorption values. After 30 cycles, the 6-hour water absorption value of the OPC-0, OPC-5, OPC-10, and OPC-15 series increased by approximately 17.42%, 23.47%,

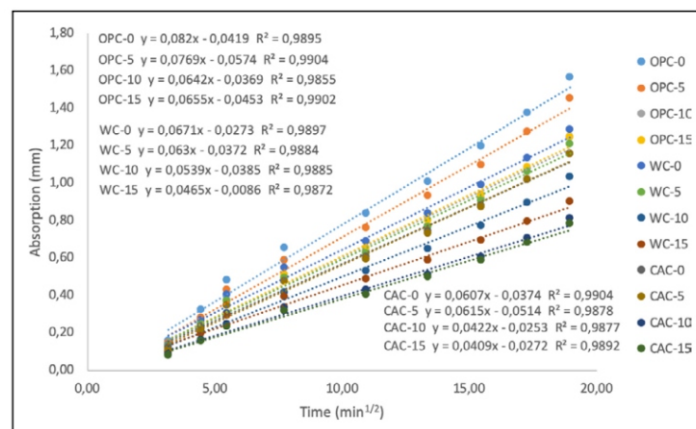


Figure 11. Sorptivity coefficient results after 30 freeze-thaw cycles.

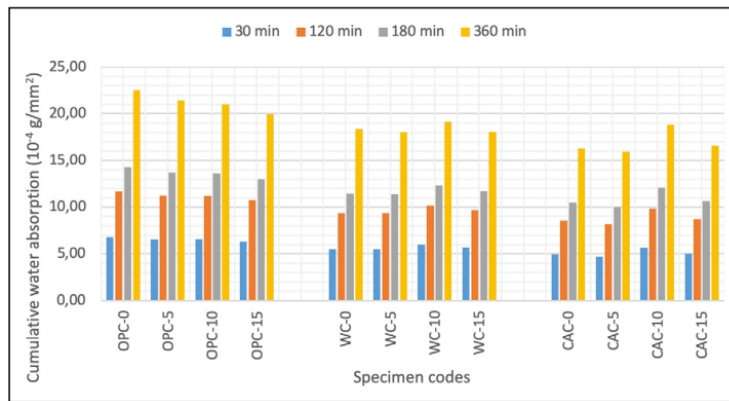


Figure 12. Cumulative capillary water absorption results after 60 freeze-thaw cycles.

21.96%, and 27.05%, respectively, compared to before exposure to freeze-thaw. This was obtained as 15.47%, 15.27%, 12.23%, and 18.42% for the WC-0, WC-5, WC-10, and WC-15 series, respectively. The capillary water absorption of CAC 10, which has the highest strength after 30 freeze-thaws, was obtained as the lowest value at 10.38%. It was determined that the capillary water absorption values of 0%, 5%, and 15% WMP substituted mixtures before freezing and thawing increased by 17.07%, 19.62%, and 18.90%, respectively.

As the WMP ratio in the mixtures increased, the sorptivity values decreased. This can be attributed to the filling effect of WMP. The lowest sorptivity value after 30 freeze-thaw was obtained from the CAC-15 series with 0.0409 mm/min^{1/2}. The sorptivity values of OPC-based mixtures vary between 0.0655 and 0.082 mm/min^{1/2}. The sorptivity values of the WC-based mixtures were lower compared to the OPC-based mixtures. This can be attributed to WC's smaller average grain size than OPC. The lowest sorptivity values in all cement types occurred in CAC-based mixtures. In CAC based mixtures, the sorptivity value decreased from 0.0607 mm/min^{1/2} to 0.0409 mm/min^{1/2} as the WMP ratio increased. Capillary water absorption and sorptivity values after 60 freeze-thaw cycles are presented in Figures 12 and 13. After 60 freeze-thaw cycles, the highest capillary water absorption value in OPC-based mixtures was obtained from the OPC0 series with 22.52x10⁻⁴ g/mm². Capillary water absorption values decreased as the WMP ratio increased in OPC-based mixes. As the WMP ratio increased in WC and CAC-based

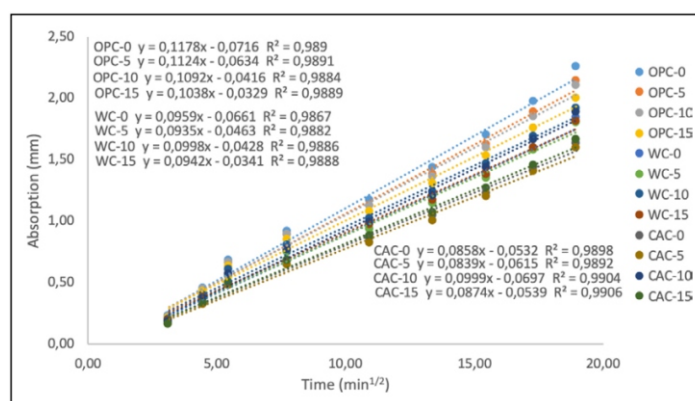


Figure 13. Sorptivity coefficient results after 60 freeze-thaw cycles.

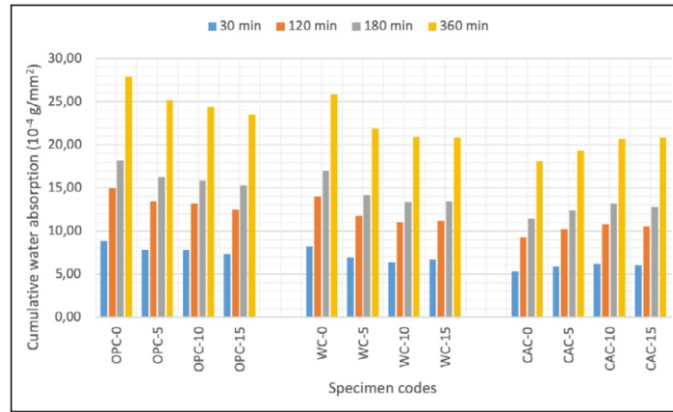


Figure 14. Cumulative capillary water absorption results after 60 freeze-thaw cycles.

mixtures, the capillary water absorption values, except for the CAC-10 series, approached. This shows that the degradation of hydration products is more important than the effect of WMP as the number of cycles increases.

After 60 cycles, the sorptivity of the OPC-based mixtures ranged from 0.1038 mm/min^{1/2} to 0.1178 mm/min^{1/2}. Similar to capillary water absorption values, the increase in WMP decreased the sorptivity in OPC-based mixtures. After 60 cycles, the OPC-0, OPC-5, OPC-10, and OPC-15 series showed an increase in sorptivity of approximately 66%, 80%, 104%, and 98%, respectively, compared to the before freeze thaw cycles. The lowest sorptivity value of 0.0935 mm/min^{1/2} in WC-based mixtures was determined in the WC-5 series. After 60 cycles, the sorptivity values of the WC-based mixtures increased in the range of approximately 64% to 133% compared to the initial sorptivity values. The lowest sorptivity values were obtained from CAC-based mixtures. However, the increase ratio compared to the initial sorptivity values is higher than other cement types. The increase in porosity can explain this situation as a result of the transformation of metastable phases in CAC into stable phases. In the CAC-0, CAC-5, CAC-10 and CAC-15 series, these values were 64%, 90%, 156% and 155%, respectively. This may be the reason for significant reductions in compressive strength compared to other cement types.

Capillary water absorption and sorptivity values after 90 freeze-thaw cycles are presented in Figures 14 and 15. Capillary water absorption values decreased as the WMP

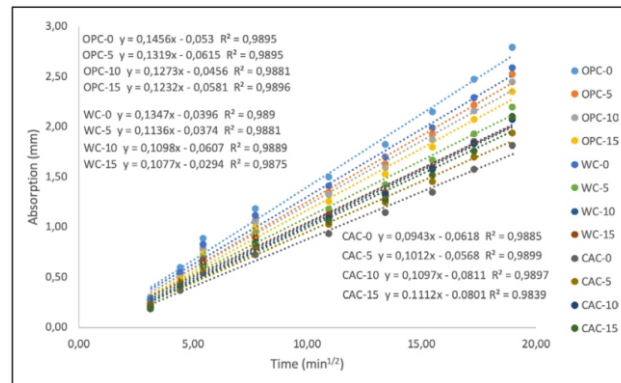


Figure 15. Sorptivity coefficient results after 90 freeze-thaw cycles.

ratio increased in OPC and WC-based mixtures. However, the opposite situation is seen in CAC-based mixtures, and capillary water absorption increased with increased WMP. When the sorptivity values after 90 cycles were examined, the lowest sorptivity in OPC-based mixtures was obtained in the OPC-15 series. The sorptivity of OPC-based mixtures ranges from 0.1232 mm/min^{1/2} to 0.1456 mm/min^{1/2}. In addition, 106%, 112%, 138%, and 136% increases were detected in the OPC-0, OPC-5, OPC-10, and OPC-15 series, respectively, according to the sorptivity before exposure to freeze-thaw cycles. In WC-based mixtures, the sorptivity values decreased as WMP increased. Sorptivity values vary between 0.1077 mm/min^{1/2} and 0.1347 mm/min^{1/2}. Contrary to OPC and WC, the increase in WMP ratio increased the sorptivity value in CAC-based mixtures. In contrast to OPC and WC, it was observed that CAC and WMP reacted to increase the strength before exposure to freeze-thaw. The sorptivity values of the CAC-0, CAC-5, CAC-10, and CAC-15 series were determined as 0.0943, 0.1012, 0.1097, and 0.1112 mm/min^{1/2}, respectively. These values were approximately 81%, 129%, 182%, and 222% higher than the baseline values. When this situation is examined, it can be thought that the capillary void ratio increases significantly compared to other cement types. As a result, it causes significant decreases in compressive strength.

5. CONCLUSIONS

- While adding 5% WMP did not affect the slump-flow diameter much, the flow diameter decreased as the use of WMP increased. However, the slump-flow diameter of all mixtures was in the range of 24 to 26 cm. The greatest loss of workability was observed in CAC-based blends.
- The highest compressive strength values before freeze-thaw cycles were obtained from CAC-based mixtures. The compressive strengths of CAC-based mixtures with 5% and 10% WMP replacement were obtained as 98.89 MPa and 104.09 MPa, respectively. The compressive strengths of the OPC and WC-based mixtures were not significantly different.
- The highest flexural strength was obtained from the CAC-10 series with 13.20 MPa. The flexural strength of the OPC-15, WC-15, and CAC-15 series was 5.91%,

7.52%, and 8.28% higher than the control specimens.

- The most appropriate WMP ratio was 10% in mechanical properties before the freeze-thaw cycles. Decreases in the strength of CAC-based mixtures after 30 cycles vary between 2.5% and 7.3%. This was calculated between 3.1%–5.3% and 2.8%–4.2% in OPC and WCbased mixtures, respectively.
- The mixtures with the lowest sorptivity values before the freeze-thaw cycles were CAC-based, and this situation was similar to the strength results.
- Significant strength reductions occurred in CAC-based mixtures, especially at 60 and 90 cycle numbers, in mixtures exposed to freeze-thaw.

ETHICS

There are no ethical issues with the publication of this manuscript.

DATA AVAILABILITY STATEMENT

The authors confirm that the data that supports the findings of this study are available within the article. Raw data that support the finding of this study are available from the corresponding author, upon reasonable request.

CONFLICT OF INTEREST

The authors declare that they have no conflict of interest.

FINANCIAL DISCLOSURE

The authors declared that this study has received no financial support.

PEER-REVIEW

Externally peer-reviewed.

REFERENCES

- [1] Zareei, S. A., Ameri, F., Bahrami, N., Shoaee, P., Moosaei, H. R., & Salemi, N. (2019). Performance of sustainable high-strength concrete with basic oxygen steel-making (BOS) slag and nano-silica. *J Build Eng*, 25, 100791. [CrossRef]
- [2] Shaikh, F. U. A. (2016). Mechanical and durability properties of fly ash geopolymer concrete containing recycled coarse aggregates. *Int J Sustain Built Environ*, 5(2), 277–287. [CrossRef]
- [3] Çelik, Z. (2023). Investigation of the use of ground raw vermiculite as a supplementary cement material in self-compacting mortars: Comparison with class C fly ash. *J Build Eng*, 65, 105745. [CrossRef]

-
-
- [4] Huntzinger, D. N., & Eatmon, T. D. (2009). *A life-cycle assessment of Portland cement manufacturing: Comparing the traditional process with alternative technologies*. *J Clean Prod*, 17(7), 668–675. [CrossRef]
- [5] Ashish, D. K. (2018). *Feasibility of waste marble powder in concrete as partial substitution of cement and sand amalgam for sustainable growth*. *J Build Eng*, 15, 236–242. [CrossRef]
- [6] Bostanci, S. C. (2020). *Use of waste marble dust and recycled glass for sustainable concrete production*. *J Clean Prod*, 251, 119785. [CrossRef]
- [7] Vardhan, K., Siddique, R., & Goyal, S. (2019). *Strength, permeation, and micro-structural characteristics of concrete incorporating waste marble*. *Constr Build Mater*, 203, 45–55. [CrossRef]
- [8] Munir, M. J., Kazmi, S. M. S., & Wu, Y. F. (2017). *Efficiency of waste marble powder in controlling alkali-silica reaction of concrete: A sustainable approach*. *Constr Build Mater*, 154, 590–599. [CrossRef]
- [9] Uysal, M., & Yilmaz, K. (2011). *Effect of mineral admixtures on properties of self-compacting concrete*. *Cem Concr Compos*, 33(7), 771–776. [CrossRef]
- [10] Aliabdo, A. A., Abd Elmoaty, M., & Auda, E. M. (2014). *Re-use of waste marble dust in the production of cement and concrete*. *Constr Build Mater*, 50, 28–41. [CrossRef]
- [11] Ergün, A. (2011). *Effects of the usage of diatomite and waste marble powder as partial replacement of cement on the mechanical properties of concrete*. *Constr Build Mater*, 25(2), 806–812. [CrossRef]
- [12] Rodrigues, R., De Brito, J., & Sardinha, M. (2015). *Mechanical properties of structural concrete containing very fine aggregates from marble cutting sludge*. *Constr Build Mater*, 77, 349–356. [CrossRef]
- [13] Zhao, J., Cai, G., Gao, D., & Zhao, S. (2014). *Influences of freeze-thaw cycle and curing time on chloride ion penetration resistance of sulphoaluminate cement concrete*. *Constr Build Mater*, 53, 305–311. [CrossRef]
- [14] Wang, R., Zhang, Q., & Li, Y. (2022). *Deterioration of concrete under the coupling effects of freeze-thaw cycles and other actions: A review*. *Constr Build Mater*, 319, 126045. [CrossRef]
- [15] Keleştemur, O., Yıldız, S., Gökçer, B., & Arıcı, E. (2014). *Statistical analysis for freeze-thaw resistance of cement mortars containing marble dust and glass fiber*. *Materials & Design*, 60, 548–555. [CrossRef]
- [16] Ince, C., Hamza, A., Derogar, S., & Ball, R. J. (2020). *Utilisation of waste marble dust for improved durability and cost efficiency of pozzolanic concrete*. *J Clean Prod*, 270, 122213. [CrossRef]
- [17] Karakurt, C., & Dumangöz, M. (2022). *Rheological and Durability Properties of Self-Compacting Concrete Produced Using Marble Dust and Blast Furnace Slag*. *Materials*, 15(5), 1795. [CrossRef]
- [18] Gencel, O., Benli, A., Bayraktar, O. Y., Kaplan, G., Sutcu, M., & Elabade, W. A. T. (2021). *Effect of waste marble powder and rice husk ash on the microstructural, physico-mechanical and transport*
-
-

properties of foam concretes exposed to high temperatures and freeze–thaw cycles. Constr Build Mater, 291, 123374. [CrossRef]

[19] Burris, L., Kurtis, K., & Morton, T. (2015). *Novel alternative cementitious materials for development of the next generation of sustainable transportation infrastructure [Tech Brief]. United States. Federal Highway Administration.*

[20] Scrivener, K. L., Cabiron, J. L., & Letourneux, R. (1999). *High-performance concretes from calcium aluminate cements. Cem Concr Res, 29(8), 1215–1223. [CrossRef]*

[21] Li, G., Zhang, A., Song, Z., Shi, C., Wang, Y., & Zhang, J. (2017). *Study on the resistance to seawater corrosion of the cementitious systems containing ordinary Portland cement or/and calcium aluminate cement. Constr Build Mater, 157, 852–859. [CrossRef]*

[22] Son, H. M., Park, S., Kim, H. Y., Seo, J. H., & Lee, H. K. (2019). *Effect of CaSO₄ on hydration and phase conversion of calcium aluminate cement. Constr Build Mater, 224, 40–47. [CrossRef]*

[23] Eren, F., Keskinates, M., Felekoğlu, B., & Felekoğlu, K. T. (2023). *Effects of mineral additive substitution on the fresh state and time-dependent hardened state properties of calcium alumina cement mortars [Article in Turkish]. Turkish J Civ Eng, 34(3), 139–162. [CrossRef]*

[24] TS EN 1097–6 (2013). *Tests for mechanical and physical properties of aggregates - part 6: determination of particle density and water absorption. Turkish Standards. Ankara, Turkiye.*

[25] EFNARC (2002). *Specifications and guidelines for self-compacting concrete. EFNARC.*

[26] ASTM C109 (2007). *Standard test method for compressive strength of hydraulic cement mortars (Using 2-in. or [50-mm] Cube specimens). Annual Book of ASTM Standards.*

[27] ASTM C348-02. *Standard test method for flexural strength of hydraulic-cement mortars. ASTM C348. Annual Book of ASTM Standards.*

[28] ASTM C1585-04. *Standard test method for measurement of rate of absorption of water by hydraulic-cement concretes.*

[29] ASTM C 666 (2003). *Standard test method for resistance of concrete to rapid freezing and thawing.*

[30] Rashwan, M. A., Al-Basiony, T. M., Mashaly, A. O., & Khalil, M. M. (2020). *Behaviour of fresh and hardened concrete incorporating marble and granite sludge as cement replacement. J Build Eng, 32, 101697. [CrossRef]*

[31] Li, L. G., Huang, Z. H., Tan, Y. P., Kwan, A. K. H., & Liu, F. (2018). *Use of marble dust as paste replacement for recycling waste and improving durability and dimensional stability of mortar. Constr Build Mater, 166, 423–432. [CrossRef]*

[32] Vardhan, K., Goyal, S., Siddique, R., & Singh, M. (2015). *Mechanical properties and microstructural analysis of cement mortar incorporating marble powder as partial replacement of cement. Constr Build Mater, 96, 615–621. [CrossRef]*

[33] Bonavetti, V. L., Rahhal, V. F., & Irassar, E. F. (2001). *Studies on the carboaluminate formation in*

-
-
- limestone filler-blended cements. Cem Concr Res, 31(6), 853–859. [CrossRef]*
- [34] Péra, J., Husson, S., & Guilhot, B. (1999). Influence of finely ground limestone on cement hydration. *Cem Concr Compos, 21(2), 99–105. [CrossRef]*
- [35] Idrees, M., Ekincioglu, O., & Sonyal, M. S. (2021). Hydration behavior of calcium aluminate cement mortars with mineral admixtures at different curing temperatures. *Constr Build Mater, 285, 122839. [CrossRef]*
- [36] Kumar, V., Singla, S., & Garg, R. (2021). Strength and microstructure correlation of binary cement blends in presence of waste marble powder. *Mater Today Proceedings, 43, 857–862. [CrossRef]*
- [37] Topcu, I. B., Bilir, T., & Uygunoğlu, T. (2009). Effect of waste marble dust content as filler on properties of self-compacting concrete. *Constr Build Mater, 23(5), 1947–1953. [CrossRef]*
- [38] Ashish, D. K., Verma, S. K., Kumar, R., & Sharma, N. (2016). Properties of concrete incorporating sand and cement with waste marble powder. *Adv Concr Constr, 4(2), 145. [CrossRef]*
- [39] Gupta, R., Choudhary, R., Jain, A., Yadav, R., & Nagar, R. (2021). Performance assessment of high strength concrete comprising marble cutting waste and fly ash. *Mater Today Proceedings, 42, 572–577. [CrossRef]*
- [40] Khodabakhshian, A., De Brito, J., Ghalehnovi, M., & Shamsabadi, E. A. (2018). Mechanical, environmental and economic performance of structural concrete containing silica fume and marble industry waste powder. *Constr Build Mater, 169, 237–251. [CrossRef]*
- [41] Zhang, S., Cao, K., Wang, C., Wang, X., Wang, J., & Sun, B. (2020). Effect of silica fume and waste marble powder on the mechanical and durability properties of cellular concrete. *Constr Build Mater, 241, 117980. [CrossRef]*
- [42] Moffatt, E. (2016). *Durability of rapid-set (ettringite-based) binders [Dissertation]. University New Brunswick.*
- [43] Gencel, O., Ozel, C., Koksal, F., Erdogmus, E., Martínez-Barrera, G., & Brostow, W. (2012). Properties of concrete paving blocks made with waste marble. *J Clean Prod, 21(1), 62–70. [CrossRef]*
- [44] Ahmed, A. A., Shakouri, M., Trejo, D., & Vaddey, N. P. (2022). Effect of curing temperature and water-to-cement ratio on corrosion of steel in calcium aluminate cement concrete. *Constr Build Mater, 350, 128875. [CrossRef]*
- [45] Matusinović, T., Šipušić, J., & Vrbos, N. (2003). Porosity–strength relation in calcium aluminate cement pastes. *Cem Concr Res, 33(11), 1801–1806. [CrossRef]*

Effect of calcination on the physical, chemical, morphological, and cementitious properties of red mud

Chava VENKATESH* , Cheretty SONALI SRI DURGA

Department of Civil Engineering, CVR College of Engineering, Vastunagar,
Mangalpalli, Ibrahimpatnam-501510, Ranga Reddy, Telangana, India

ABSTRACT

Red mud (RM), a by-product of aluminum production, poses environmental concerns with its disposal. This study explored calcining RM at 600 °C for 0–6 hours to utilize it as a cement substitute. Calcination up to 2 hours decreased particle size and increased surface area due to moisture loss, while further calcination reversed these effects. XRF analysis showed high Fe₂O₃, Al₂O₃, SiO₂ contents. XRD revealed goethite transformed to hematite and gibbsite to alumina. SEM images displayed a loose then denser structure over time. 10% calcined RM incorporated into cement showed 2-hour calcined RM exhibited optimal properties, including high strength (46.27 MPa) and strength activity index (117.24%). SEM confirmed improved C-S-H gel formation with 2-hour calcined RM. In summary, calcining RM optimally at 600 °C for 2 hours allows its effective use as a sustainable cementitious material, providing environmental and technical benefits of RM utilization in cement composites.

Cite this article as: Venkatesh, C., & Sonali Sri Durga, C. (2023). Effect of calcination on the physical, chemical, morphological, and cementitious properties of red mud. *J Sustain Const Mater Technol*, 8(4), 297–306.

Key words: Compressive strength, particle analyzer, red mud, strength activity index, x-ray diffraction analysis

1. INTRODUCTION

In recent years, there has been a growing emphasis on the development of novel technologies to transform waste into value-added products, particularly within industrial and mining sectors. This is due to the increased recognition that reducing waste is a significant environmental concern. By recycling these industrial products, it is possible to mitigate potential environmental and health-related complications, as well as enhance sustainability [1–3]. The present study is mainly focused on utilizing alumina industrial residue (i.e., red mud) as a cementing material. Red mud is a semi-solid residue produced during the extraction of alumina from bauxite, known as the Bayer process, in alumina production. Specifically, for every tonne of alumina extracted, 1.5 tonnes of red mud is generated as a residue [4, 5]. According to the Alam [6] & Mymrin [7], 4 billion tonnes of red mud is accumulated on open lands. Additionally, more than 140 million tonnes of red mud is added to this accumulation from throughout the world every year. Disposal of this large amount of red mud is very difficult due to its alkaline nature and is uneconomical as it requires much land [8]. Moreover, this disposal creates several environmental

problems, such as air, water, and land pollution. Recycling of red mud is limited due to its fineness and high alkalinity, which may create an environmental imbalance [9, 10]. Besides, as a waste product, RM does not incur any additional production costs nor does it increase emissions; rather, it decreases emissions from cement production. Utilizing RM as a substitute for cement not only addresses storage concerns but also has the potential to enhance concrete properties, provided that it is used in appropriate quantities [11].

There are mixed opinions regarding the potential of red mud as a cementing material in cement/concrete composites, based on its strength and durability properties. Nikbin [12] reported that red mud has low cementing activity and shows a negative impact on compressive strength. Therefore, the usage of red mud is limited to the construction of non-structural elements. Su & Li [13] study revealed that incorporating 10% RM resulted in a minor reduction in the compressive strength of concrete, whereas incorporating more than 10% led to a significant decrease. A study by Yang [14] examined cement mortars that were based on red mud. The researchers replaced red mud in varying amounts, ranging from 0% to 9%. The results showed that the addition of red mud increased the mortar's density and improved its compressive strength. According to Ghaleh novi [15], the use of red mud in self-compacting concrete (SCC) resulted in a decrease of 10% and 20% in compressive strength when the red mud content was 7.5% and 10%, respectively. Similarly, Venkatesh [16] reported a 19% decrease in the compressive strength of concrete with the addition of 15% red mud. However, another study found that as the amount of red mud used in concrete increased, the concrete's strength decreased [17]. The decrease in strength can be attributed to the fact that replacing cement with red mud, which has low reactivity, reduces the amount of hydration products per unit volume. Contrarily, W. C. Tang et al. [18] replaced fly ash with red mud in concrete. The study found that as the replacement percentage of red mud increased, the compressive strength improved. Specifically, when 50% of the fly ash was replaced with red mud, higher compressive strength was observed along with good improvement in Interfacial Transition Zone (ITZ). Furthermore, XRD analysis showed the presence of hatrurite and larnite. For instance, many investigations have started using red mud as a secondary or tertiary cementitious material in both normal and geopolymer concretes. In their studies, researchers have blended red mud with various cementing materials, including Slag [19], Metakaolin [20, 21], Fly ash [22], GGBFS [23], Phosphogypsum [24], Granite powder, and marble powder [25], and silica fume [26]. When red mud blend with other cementing materials has shown the considerable improvement in their strength and durability than its individual usage.

Although using red mud to prepare cement and concrete has promising application prospects, the presence of sodium in red mud can be detrimental to the strength and durability of cement and concrete. As a result, the amount of red mud utilized must be carefully controlled, or alternatively, the red mud must undergo a process of dealkalization, which ultimately restricts its application in cement and

concrete. As a result, the amount of red mud utilized must be carefully controlled, or alternatively, the red mud must undergo a process of dealkalization, which ultimately restricts its application in cement and concrete production [27]. The conventional methods of dealkalization, such as acid neutralization, water leaching, and wet carbonation, are efficient. However, they also reduce the reactivity of red mud and have a negative impact on the performance of concrete. High-temperature treatment is an efficient method for enhancing the reactivity of red mud, as it can decompose some of its inert phases, such as cancrinite, gibbsite, and aragonite, into reactive ones that can easily dissolve in the pore solution [28]. According to Luo [29], the ideal temperature for calcination to completely decompose cancrinite and birnessite in red mud is 1000 °C for one hour, while Danner [30] indicated that calcination at 800 °C for 15 minutes significantly enhanced the reactivity of red mud while decreasing the solubility of sodium. Manfroi [31] performed a calcium hydroxide consumption test and found that calcination at temperature of 600 °C for one hour was the optimal temperature for activating the pozzolanic reactivity of red mud. Liu et al. [32] stated that red mud demonstrated its highest pozzolanic activity when it was calcined for 3 hours at a temperature of 600 °C, which was attributed to the development of poorly-crystallized Ca₂SO₄. Therefore, the general consensus is that calcination is a necessary precondition for red mud to exhibit reactivity. Without calcination, red mud would remain chemically unreactive in Portland cement blends, potentially resulting in weakened strength.

Research significance: Between 2010 and 2023, a total of 6,350 research articles were published on red mud as a cementing material, but less than 50 articles focused on the effect of calcination on red mud (The data was collected from Google Scholar using the following search limitations: a custom range in years from 2010 to 2023, article type set to research articles, and the keyword 'red mud as cementing material'.) There are varying opinions on the ideal calcination temperature for red mud, as its chemical composition differs from one location to another. The red mud produced by Indian aluminium industries, in particular, has limited usage in cement and concrete production due to a lack of literature on its cementing properties. Addressing this research gap, the present study conducted a comprehensive investigation into the physical and chemical properties of red mud, as well as its cementing activity when calcined at temperatures ranging from 600 °C for 1 hour to 6 hours.

2. MATERIALS AND METHODS

2.1. Materials

The present study obtained red mud from the NALCO in Orissa, India, which was in the semi-solid form with 30–40% moisture content during collection. It was dried in a laboratory (approximately 30 °C) for 3 days and then ground in ball mills. OPC-53 Grade cement was used for compressive strength and strength activity index tests, and all properties were within the limits of ASTM C150 [33]. Specifically,

the specific surface area was 300 m²/kg, and the specific gravity was 3.12. Table 1 illustrates the Non-calcined red mud (NC-RM) and cement chemical compositions. The fine aggregates were used in accordance with IS: 383–2016 [34] and Table 2 shows its physical properties.

2.2. Calcination Process

In this study, a high-temperature muffle furnace was used for the calcination of red mud (RM), and a heating rate of 10 °C/min was maintained throughout the calcination process. The RM was calcined at a temperature of 600 °C for 1–6 hours and it is cooled at ambient air temperature for 5 hours in the laboratory after which it was ground in ball mills.

Table 1. Chemical composition (weight %)

	SiO ₂	Fe ₂ O ₃	Al ₂ O ₃	CaO	MgO	Na ₂ O	TiO ₂	K ₂ O	LOI
OPC	21.26	4.81	4.99	63.71	1.32	0.36	–	0.38	3.17
NC-RM	13.98	21.37	20.97	4.49	0.39	8.12	11.87	3.6	15.21

Table 2. Physical properties of aggregates

	Specific gravity	% of water absorption	Fineness modulus	Bulk density
Fine aggregates	2.69	1.10	2.56	1.46

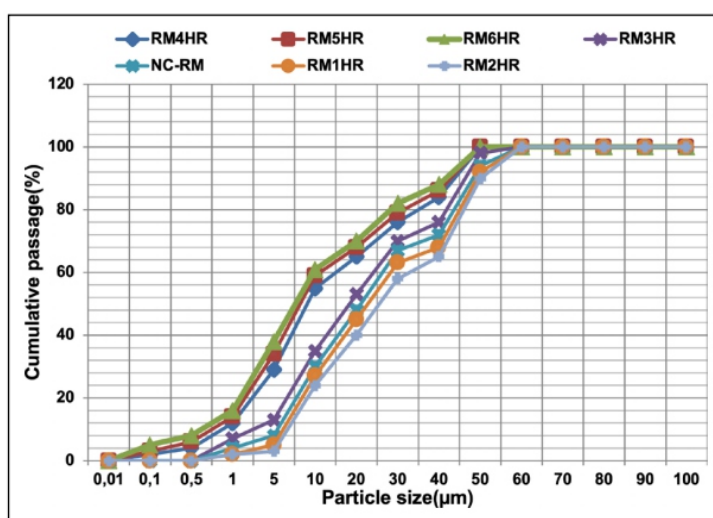


Figure 1. Particle size distribution of various calcined red muds.

2.3. Characterization Methods

In this study, the specific surface area of both calcined and non-calcined red mud samples was determined using the Micromeritics Gemini 237 and Gemini V instruments. Similarly, the particle size of the red mud samples was measured using the SZ-100Z nanoparticle analyzer from Horiba Ltd., Japan. The STA72000 thermal analyzer was used in this study to perform TG-DTA. Nitrogen (N₂) was used as a stripping gas, and all red mud samples were heated at a temperature range of 20 °C to 600 °C

with a heating rate of 10 as per Wu [35]. The Rigaku MiniFlex 600 with the following parameters was used to identify XRD patterns/phases: 40 kV voltage and 15 mA current, step scan of 0.0200°, scan range from 10° to 70° (2 θ), a scan speed of 100.00 deg/min, and CuK α /1.541862 Å wavelength. VEGA 3 SBH, TESCAN Bmo. S.R.O., CZECH REPUBLIC, was used for identifying the surface morphology of calcined and non-calcined red mud samples. In the present study, the X'pert HighScore software tool has been used to analyze the XRD results, and it is supported by the new ICDD PDF-4+/Web licenses.

2.4. Mix Proportions

According to ASTM C109/C109M [36], the mix proportions of cement mortar samples are calculated, and the proportional ratios are as follows: 1:3:0.52 (i.e., binder: fine aggregates: water-to-cement ratio). In this study, 10% of various calcined red mud has been replaced with cement in all the mixes. A total of 48 mortar samples (with a size of 50 mm on each side of the cube) are prepared and cured for 7 and 28 days in portable water, following ASTM C31/C31M [37].

2.5. Strength Activity Index

The compressive strength and strength activity index (SAI) tests are evaluated on the red mud-induced cement mortar samples according to the ASTM C109/C109M [36] and ASTM C311/C311M [38] standards. Equation 1 is used to evaluate the strength activity index of red mud-induced cement mortar samples.

$$SAI(\%) = \frac{\text{Compressive strength of red mud induced cement mortar samples}}{\text{Compressive strength of normal cement mortar samples}} \times 100 \quad \text{Eq.1}$$

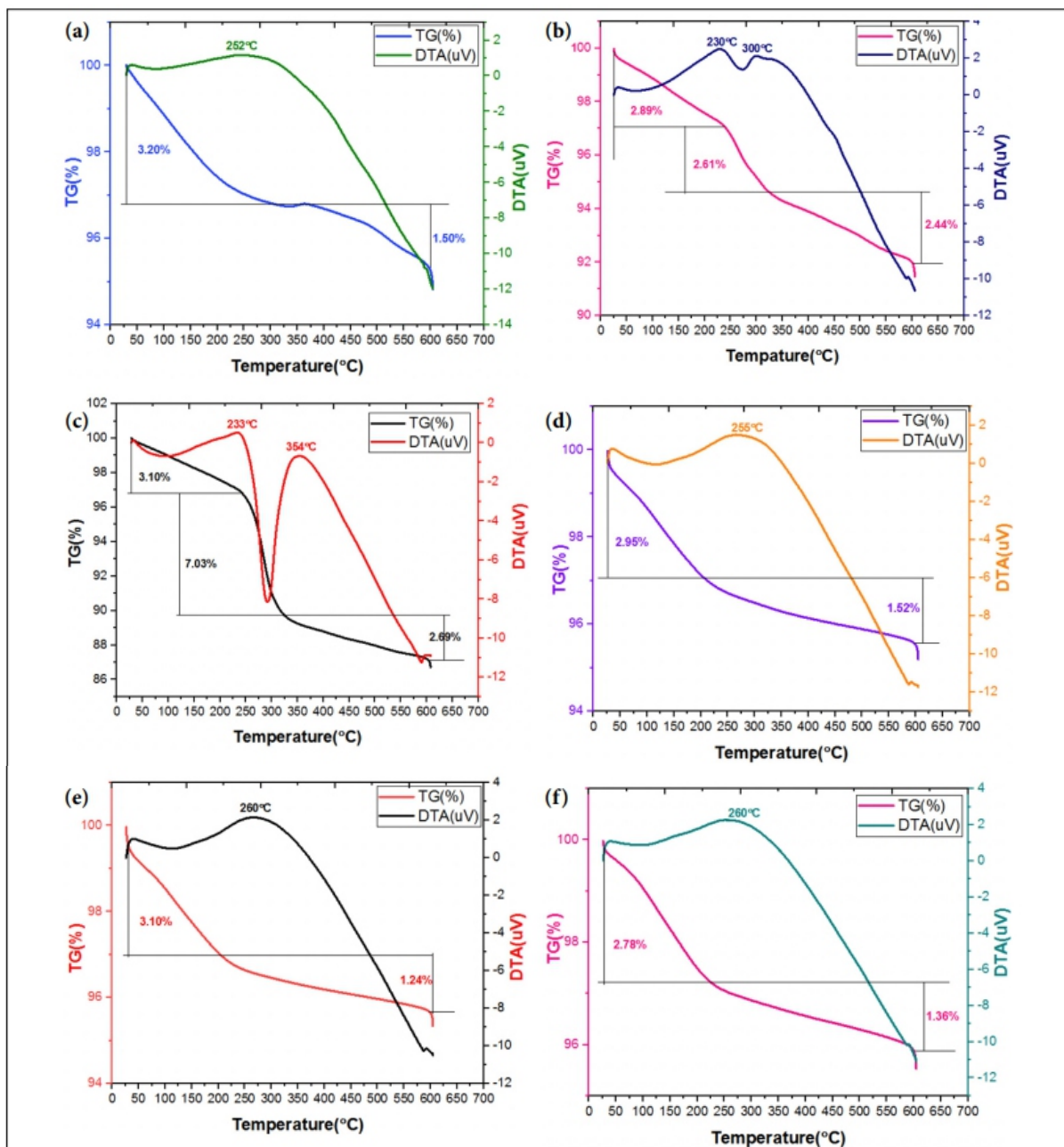
3. RESULTS AND DISCUSSION

3.1. Calcination Effect on Physical Properties of Red Mud

In this study, particle size analysis was conducted on the calcined red mud particles, as shown in Figure 1. The results show that all the red mud particles fall within the range of 1–50 μm , with an average particle size of 8 μm . The specific surface areas were measured using the BET apparatus and are illustrated in Table 2. Non-calcined red mud has a specific surface area of 1.86 m^2/g , which increases to 2.2 m^2/g after 2 hours of calcination. This increase is attributed to the loss of moisture in the particles and the destruction of alumina silicates present in the red mud particles, as mentioned by Liu [32]. They also state that specific surface area values decrease to 1.95 m^2/g after 6 hours due to particle aggregation. According to Wu [35], the crystallinity of red mud particles increased with the enlargement of red mud particle size and the reduction in specific surface area resulting from calcination. Nath [39] have made similar conclusions, stating that particle size is enriched up to 200 °C of heating due to

improved crystallinity. However, particle collision observed at a temperature of 500 °C leads to a reduction in particle size.

In this study, the specific gravity of red mud was measured according to IS 4031 Part-11 (1988) [40]. Table 3 illustrates the variations in the specific gravity of red mud when calcined at a temperature of 600 °C for 1 to 6 hours, and it is compared with non-calcined red mud. The specific gravity of red mud decreased by about 1.65% during 2 hours of calcination compared to non-calcined red mud, attributable to moisture loss in the particles. However, after 2 hours of calcination, the specific gravity values increased from 0.4% (at 3 hours) to 3.25% (at 6 hours). This effect can be attributed to agglomeration between the red



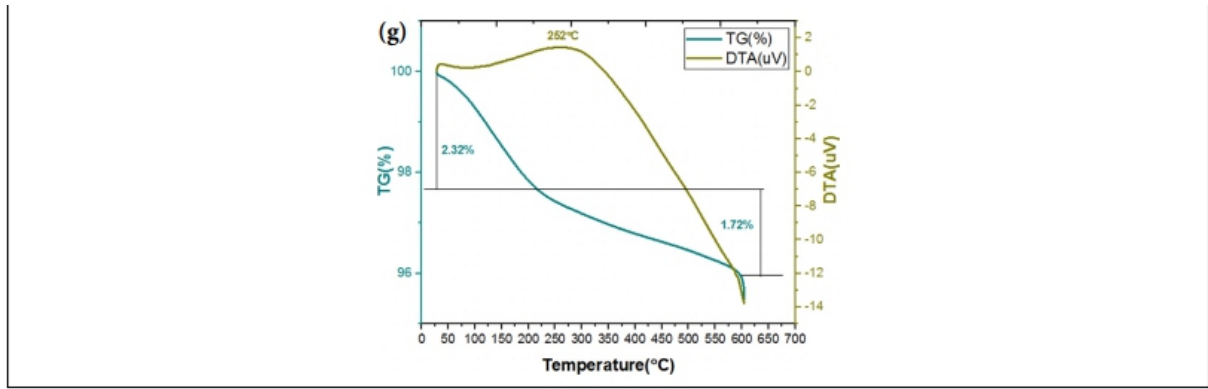


Figure 2. TG-DTA analysis of calcined red muds (a) NC-RM, (b) RM1HR, (c) RM2HR, (d) RM3HR, (e) RM4HR, (f)RM5HR and (g) RM6HR.

Table 3. Physical properties of red mud after calcination

	NC-RM	RM1HR	RM2HR	RM3HR	RM4HR	RM5HR	RM6HR
SSA (m ² /g)	1.86	1.95	2.2	2.16	2.1	2.05	1.95
Mass loss (%)	4.7	7.94	12.82	4.47	4.34	4.14	4.04
Specific gravity	2.46	2.44	2.42	2.47	2.5	2.51	2.54

Table 4. Chemical composition of calcined red mud (weight %)

Temp/time	CaO	Al ₂ O ₃	Fe ₂ O ₃	SiO ₂	Na ₂ O	K ₂ O	TiO ₂	MgO	LOI
NC-RM	4.49	20.97	21.37	13.98	8.12	3.6	11.87	0.39	15.21
RM1HR	7.53	26.15	22.54	17.6	5.44	3.03	7.92	0.84	8.95
RM2HR	10.84	22.62	21.79	21.92	3.87	1.89	5.5	0.65	10.92
RM3HR	9.66	24.63	22.47	19.82	5.03	2.48	6.72	0.92	8.27
RM4HR	8.44	21.08	24.01	19.46	5.81	2.19	7.01	1.26	10.74
RM5HR	8.54	22.54	24.06	18.47	8.24	2.27	7.19	0.41	8.28
RM6HR	12.3	20.2	21.46	16.89	10.35	2.22	8.17	0.33	8.08

mud particles Zhang [41] and Wang [42] reported that specific gravity values significantly varied when red mud was thermally activated.

In this study, thermogravimetry analysis was conducted on all calcined red mud particles to measure the mass loss, as shown in Table 3. Figure 2 depict the TG-DTA curves of all calcined red mud particles. The mass of the red mud particles varied with different calcination durations: 4.7% for non-calcined, 7.94% for 1 hour at 600 °C, 12.82% for 2 hours at 600 °C, 4.47% for 3 hours at 600 °C, 4.34% for 4 hours at 600 °C, 4.14% for 5 hours at 600 °C, and 4.04% for 6 hours at 600 °C. However, the reason for the mass loss observed up to 2 hours of calcination was attributed to dissipation of physical and chemically bound water.

Based on the obtained results, it was observed that all the physical properties, namely specific gravity, particle size, specific surface area, and mass loss, exhibited similar behavior. The calcination of red mud significantly influenced its physical properties. However, moisture loss was observed in the red mud for

up to 2 hours of calcination. Subsequently, the physical properties were enhanced, which can be attributed to particle agglomeration.

3.2 Calcination Effect on Chemical Properties of Red Mud

Table 4 displays the chemical composition of red mud under different calcination durations at a temperature of 600 °C. Alumina, silica, and iron oxides were found to be the major components in all calcined red mud samples. Among them, the red mud subjected to a 2-hour calcination at 600 °C exhibited higher levels of silica and calcium oxide compared to the other calcined red mud samples. This increase in silica and calcium oxide content contributes to the enhanced cementitious activity of the red mud particles.

In this study, X-ray diffraction analysis was conducted to evaluate the phase transformations in red mud during calcination at a temperature of 600 °C for dif

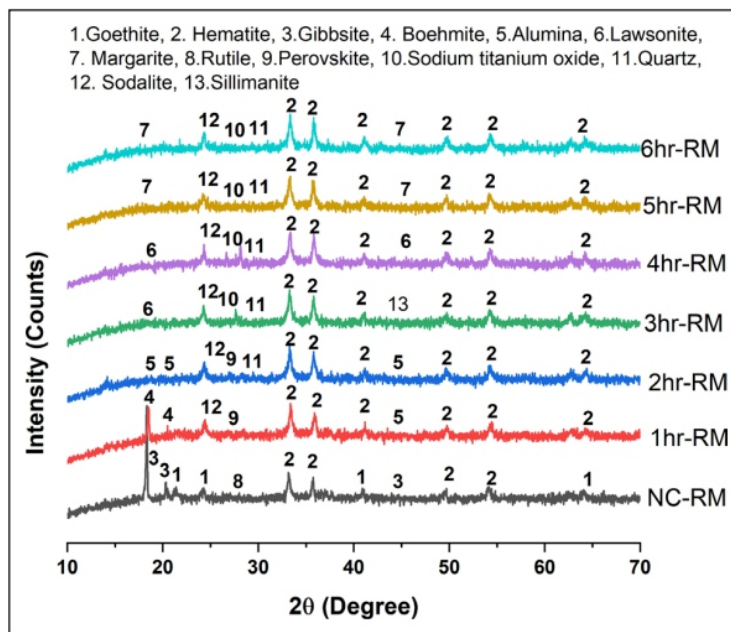


Figure 3. X-ray diffractogram of calcined red muds.

ferent durations (1 to 6 hours), as shown in Figure 3. The following mineralogical phases/compounds were identified: 1. Goethite ($\text{FeO}(\text{OH})$), 2. Hematite (Fe_2O_3), 3. Gibbsite $\text{Al}(\text{OH})_3$, 4. Boehmite ($\text{AlO}(\text{OH})$), 5. Alumina- (Al_2O_3), 6. Lawsonite- ($\text{CaAl}_2\text{Si}_2\text{O}(\text{OH})_2(\text{H}_2\text{O})$), 7. Margarite- ($\text{CaAl}_2(\text{Si}_2\text{Al}_2\text{O}_{10})(\text{H}_2\text{O})$), 8. Rutile- (TiO_2), 9. Perovskite (CaTiO_3), 10. Sodium titanium oxide (Na_2TiO_3), 11. Quartz- (SiO_2), 12. Sodalite- ($\text{Na}_{7.89}(\text{AlSiO}_4)_6(\text{NO}_3)_{1.92}$), 13. Sillimanite- ($\text{Al}_2(\text{SiO}_4)\text{O}$).

Gibbsite was observed at $2\theta=14.47$ with a d-spacing of 6.1215 in non-calcined red mud. However, after 1 hour of calcination at 600 °C, it transformed into boehmite due to moisture loss in the particles. Subsequently, boehmite further converted into alumina after 2 hours of calcination at 600 °C. Hematite showed no significant phase changes throughout all the calcined durations, with traced positions at $2\theta=33.20, 35.68$ and d-spacing of 2.6982, 2.5164. According to Nath [39], hematite remains stable up

to 1200 °C.

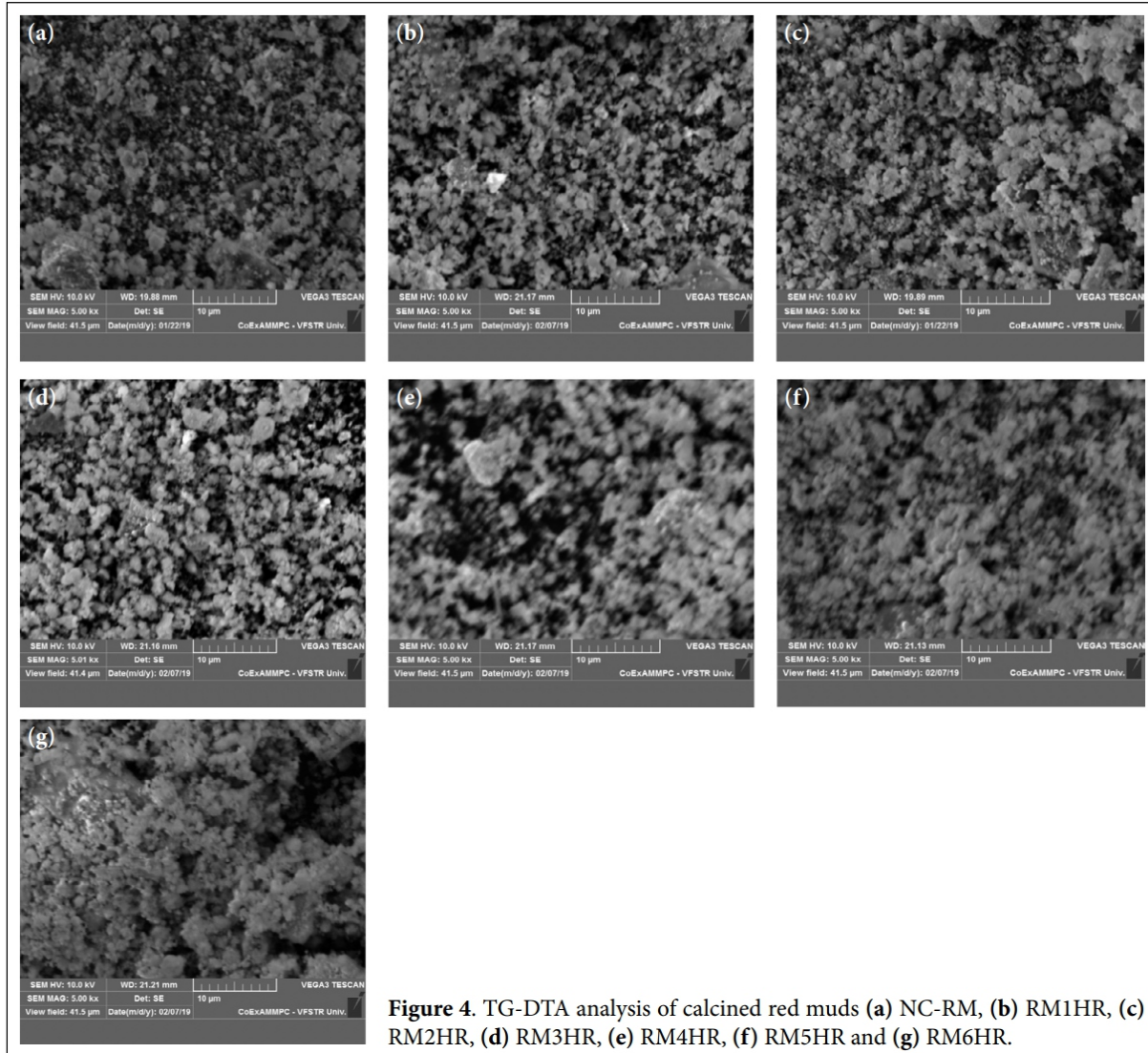


Figure 4. TG-DTA analysis of calcined red muds (a) NC-RM, (b) RM1HR, (c) RM2HR, (d) RM3HR, (e) RM4HR, (f) RM5HR and (g) RM6HR.

Table 5. Elemental composition of calcined red mud replaced mixes (weight %)

Mixes	28 days						Total
	O	Ca	Si	Al	Fe	Ca/Si	
NC-RM	56.51	22.69	16.91	3.19	0.7	1.34	100
RM1H	56.45	21.42	18.17	3.1	0.86	1.18	100
RM2H	58.71	18.2	19.19	3.09	0.81	0.95	100
RM3H	57.89	18.91	19.1	3.05	1.05	0.99	100
RM4H	61.01	21.05	15.25	2.24	0.45	1.38	100
RM5H	55.52	25.59	15	3.19	0.7	1.71	100
RM6H	55.52	24.42	16.1	3.1	0.86	1.52	100

Lawsonite transformed into sodalite, which explains the separation of calcium oxide during the calcination process. Rutile, initially present in the non-calcined red mud, changed to perovskite after 1 hour of calcination at 600 °C, and further calcination resulted in the complete transformation to sodium titanium oxide. S.N. Meher [43] also observed similar phase transformations, from rutile to perovskite.

This phase change suggests that the calcium oxide present in the red mud may react with titanium oxide and form perovskite (CaTiO₃).

Quartz was detected between 2 θ values of 25 to 30 in the 2-hour calcined red mud, and it continued to be present in further calcined red mud samples as well. The chemical

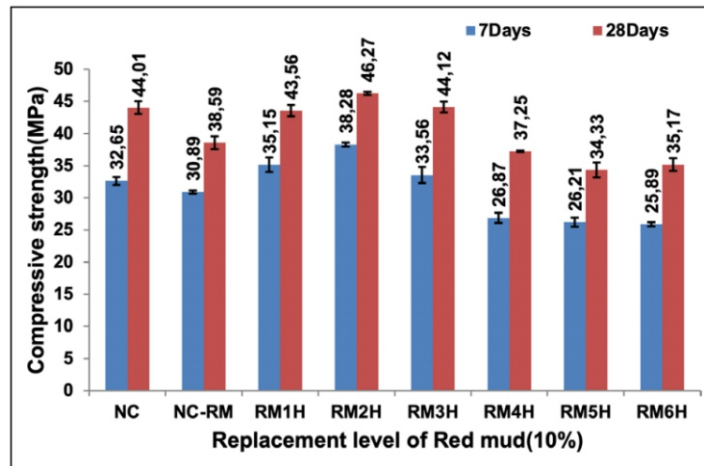


Figure 5. Compressive strength.

composition results (mentioned in Table 3) also indicated the presence of stable or higher levels of silica (SiO₂) after 2 hours of calcination.

Scanning electron microscopy (SEM) analysis was conducted to examine the surface morphology of red mud particles during various calcination processes. Figure 4 illustrates the SEM images of different calcined red mud particles. Microscopic observations revealed that the red mud particles exhibit an irregular shape. However, up to 2 hours of heating at 600 °C, the red mud particles maintain a loose structure. In particular, Figure 4c shows a more poorly crystalline structure compared to others, which may indicate higher reactivity and better cementitious activity. A similar conclusion was made by Liu [32], stating that red mud forms a poorly crystalline structure when thermally activated, providing ideal cementitious activity. Subsequently, a dense structure is observed from 2 hours to 6 hours of heating at 600 °C as the particles undergo agglomeration, resulting in their combination with surrounding particles. Similar observations regarding the physical properties of red mud were made in this study.

3.4. Calcination Effect on Cementitious Properties of Red Mud

The present study conducted the strength activity index test according to ASTM C311/C311M [38] to investigate the cementitious properties of red mud particles. In this regard, the cement mortar mixes were prepared by replacing the 10% of cement by calcined red mud (Calcined at a temperature of 600 °C during 1 to 6 hours). The results showed that the cement mortar samples containing 600 °C@2hr (i.e., RM2HR) calcined red mud exhibited high strength, specifically 46.27 MPa, as shown in Figure 5. This effect can be attributed to the higher percentage of silica and the increased specific surface area of the red mud particles, which enhance the hydration process of the cementitious matrix.

Figure 6 illustrates the strength activity index percentages of calcined red mud induced cement mortar mixes; 107.65% for RM1HR, 117.24% for RM2HR, 102.78% for RM3HR, 82.29% for RM4HR, 80.27% for RM5HR, and 79.29% for RM6HR. According to the ASTM C311/C311M [38], Wang et al. [44] and [45, 46] If the strength activity index values exceed 75%, the material exhibits good cementi

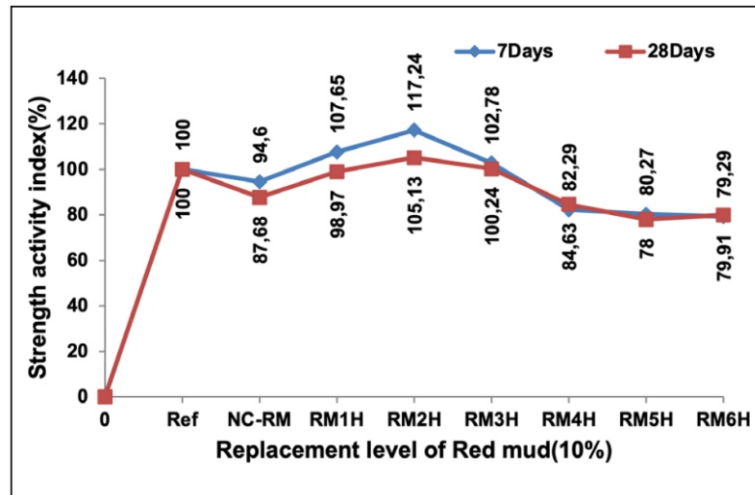


Figure 6. SAI Vs. Compressive strength.

tious properties and is suitable for use as a cementitious material in concrete/mortar. Microstructure analysis revealed that red mud possesses significant cementitious properties as like cement. SEM images in Figure 7 indicate the formation of C-S-H (calcium silicate hydrate) and CH (calcium hydroxide). Notably, the cement mortar mixes with 2hr calcined red mud replacement exhibited better C-S-H gel formation than other mixes, as observed through the Ca/Si ratios in the elemental composition of red mud replaced mixes, as shown in Table 5. The RM2HR calcined red mud containing mortar mix has low Ca/Si of 0.95 this is the reason for achievement of high strength (i.e., 46.27 MPa) and strength activity index values (i.e., 117.24%). According to Rossignolo [47] and MSR chand [48], the presence of C-S-H can be justified by the Ca/Si ratio of the EDXA (Energy-Dispersive X-ray Analysis) elemental weight percentages. A Ca/Si ratio ranging from 0.8 to 2.5 confirms the presence of C-S-H gel, while a lower Ca/Si ratio indicates a stronger or higher C-S-H gel formation Venkatesh [49].

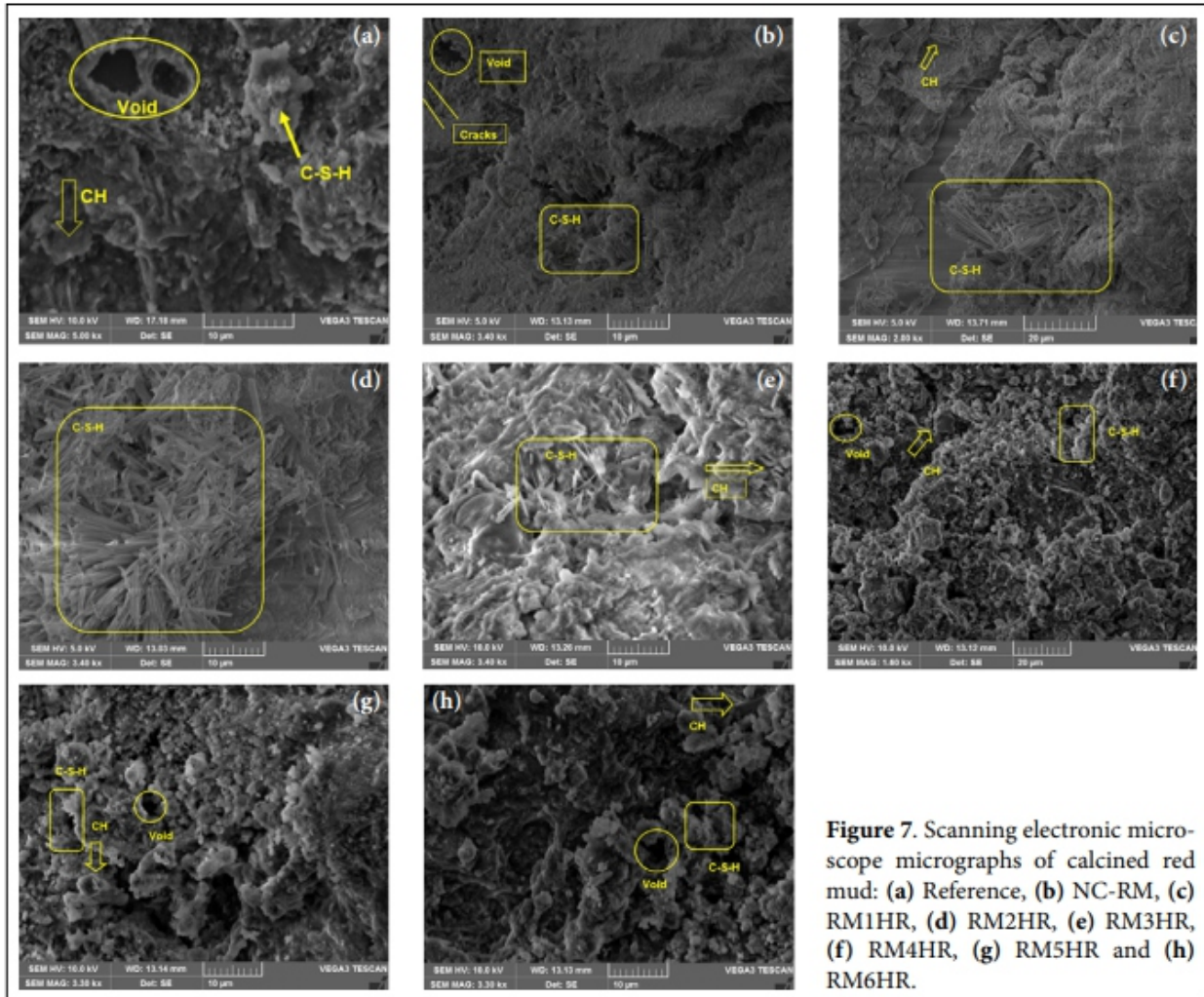
4. CONCLUSIONS

In this study, red mud, a by-product of the Indian alumina industry (specifically NALCO), was calcined at a temperature of 600 °C for 1 to 6 hours to evaluate its potential usage as a cementing material in cement/concrete production. The following conclusions were drawn after comprehensive assessments of its physical, chemical, morphological, and cementing properties.

- Chemical evaluation studies have identified that red mud contains abundant amounts of silica, iron oxide, and alumina. In the case of calcined red mud at 600°C for 2 hours (600°C@2hr), it was found to contain 10.84% CaO, 21.92% SiO₂, and 22.62% alumina, making it more suitable as a cementing

material.

- Based on the XRD analysis, hematite remained stable throughout the calcination process. However, gibbsite in non-calcined red mud transformed into boehmite at RM1HR, and further calcination at 600 °C for 2 hours resulted in its conversion into alumina.
- The RM2HR calcined red mud replacement mixes exhibited high compressive strength and strength activity index values, specifically 46.27 MPa and 117.24%. It



was observed that this particular red mud contained a higher amount of silica (21.92%), a large specific surface area (2.2 m²/g), and a poorly crystalline structure. These factors played a positive role in the cementing activities.

- Finally, NALCO-produced red mud can be utilized as a cementing material in cement/concrete production after undergoing calcination at a temperature of 600 °C for 2 hours.

ETHICS

There are no ethical issues with the publication of this manuscript.

DATA AVAILABILITY STATEMENT

The authors confirm that the data that supports the findings of this study are available within the article. Raw data that support the finding of this study are available from the corresponding author, upon reasonable request.

CONFLICT OF INTEREST

The authors declare that they have no conflict of interest.

FINANCIAL DISCLOSURE

The authors declared that this study has received no financial support.

PEER-REVIEW

Externally peer-reviewed.

REFERENCES

- [1] Muraleedharan, M., & Nadir, Y. (2021). Factors affecting the mechanical properties and microstructure of geopolymers from red mud and granite waste powder: A review. *Ceram Int*, 47(10), 13257–13279. [CrossRef]
- [2] Çelikten, S., Atabey, İ. İ., & Bayer Öztürk, Z. (2022). Cleaner environment approach by the utilization of ceramic sanitaryware waste in Port land cement mortar at ambient and elevated temperatures. *Iranian J Sci Technol Trans Civ Eng*, 46(6), 4291–4301. [CrossRef]
- [3] Korkmaz, A. V., & Kayıran, H. F. (2022). Investigation of mechanical activation effect on high-volume natural pozzolanic cements. *Open Chem*, 20(1), 1029–1044. [CrossRef]
- [4] Gou, M., Hou, W., Zhou, L., Zhao, J., & Zhao, M. (2023). Preparation and properties of calcium aluminate cement with Bayer red mud. *Constr Build Mater*, 373, 130827. [CrossRef]
- [5] Venkatesh, C., Nerella, R., & Chand, M. S. R. (2020). Experimental investigation of strength, durability, and microstructure of red-mud concrete. *J Korean Ceram Soc*, 57(2), 167–174. [CrossRef]
- [6] Alam, S., Das, S. K., & Rao, B. H. (2019). Strength and durability characteristic of alkali-activated GGBS stabilized red mud as geo-material. *Constr Build Mater*, 211, 932–942. [CrossRef]
- [7] Mymrin, V., Alekseev, K., Fortini, O. M., Aibuldinov, Y. K., Pedroso, C. L., Nagalli, A., Winter, E. Jr., Catai, R. E. & Costa, E. B. C. (2017). Environmentally clean materials from hazardous red mud, ground cooled ferrous slag, and lime production waste. *J Clean Prod*, 161, 376–381. [CrossRef]
- [8] Ortega, J. M., Cabeza, M., Tenza-Abril, A. J., Real-Herraiz, T., Climent, M. Á., & Sánchez, I. (2019). Effects of red mud addition in the microstructure, durability, and mechanical performance of cement

mortars. *Appl Sci*, 9(5), 984. [CrossRef]

[9] Liu, Z., & Li, H. (2015). Metallurgical process for valuable elements recovery from red mud - A review. *Hydrometallurgy*, 155, 29–43. [CrossRef]

[10] Abdel-Raheem, M., Santana, L. G., Cordava, M. P., & Martínez, B. O. (2017). Uses of red mud as a construction material. In *AEI 2017* (pp. 388–399). [CrossRef]

[11] Patangia, J., Saravanan, T. J., Kabeer, K. S. A., & Bisht, K. (2023). Study on the utilization of red mud (bauxite waste) as a supplementary cementitious material: Pathway to attaining sustainable development goals. *Constr Build Mater*, 375, 131005. [CrossRef]

[12] Nikbin, I. M., Aliaghazadeh, M., Charkhtab, S. H., & Fathollahpour, A. (2018). Environmental impacts and mechanical properties of lightweight concrete containing bauxite residue (red mud). *J Clean Prod*, 172, 2683–2694. [CrossRef]

[13] Su, Z., & Li, X. (2021). Study on preparation and interfacial transition zone microstructure of red mud-yellow phosphorus slag-cement concrete. *Mater*, 14(11), 2768. [CrossRef]

[14] Yang, X., Zhao, J., Li, H., Zhao, P., & Chen, Q. (2017). Recycling red mud from the production of aluminium as a red cement-based mortar. *Waste Manag Res*, 35(5), 500–507. [CrossRef]

[15] Ghalehnovi, M., Shamsabadi, E. A., Khodabakhshian, A., Sourmeh, F., & De Brito, J. (2019). Self-compacting architectural concrete production using red mud. *Constr Build Mater*, 226, 418–427. [CrossRef]

[16] Venkatesh, C., Nerella, R., & Chand, M. S. R. (2020). Comparison of mechanical and durability properties of treated and untreated red mud concrete. *Mater Today: Proc*, 27, 284–287. [CrossRef]

[17] Raja, R. R., Pillai, E. P., & Santhakumar, A. R. (2013). Effective utilization of red mud bauxite waste as a replacement of cement in concrete for environmental conservation. *Ecol Environ Conserv*, 19(1), 247–255.

[18] Tang, W. C., Wang, Z., Liu, Y., & Cui, H. Z. (2018). Influence of red mud on fresh and hardened properties of self-compacting concrete. *Constr Build Mater*, 178, 288–300. [CrossRef]

[19] Li, Z., Zhang, J., Li, S., Gao, Y., Liu, C., & Qi, Y. (2020). Effect of different gypsums on the workability and mechanical properties of red mudslag based grouting materials. *J Clean Prod*, 245, 118759. [CrossRef]

[20] Liu, J., Li, X., Lu, Y., & Bai, X. (2020). Effects of Na/Al ratio on mechanical properties and microstructure of red mud-coal metakaolin geopolymer. *Constr Build Mater*, 263, 120653. [CrossRef]

[21] Raj, R. R., Pillai, E. P., & Santhakumar, A. R. (2012). Strength and corrosion properties of concrete incorporating metakaolin and red mud. *Eur J Sci Res*, 91(4), 569–579.

[22] Qaidi, S. M., Tayeh, B. A., Ahmed, H. U., & Emad, W. (2022). A review of the sustainable utilization of red mud and fly ash for the production of geopolymer composites. *Constr Build Mater*, 350, 128892. [CrossRef]

-
-
- [23] Zhao, Y., Zhang, B., He, F., Meng, F., Yang, S., Wang, Q., & Zhu, W. (2023). Effects of dosage and type of GGBS on the mechanical properties of a hybrid red-mud geopolymer. *J Mater Civ Eng*, 35(4), 04023008. [CrossRef]
- [24] Huang, X., Li, J. S., Jiang, W., Chen, Z., Wan, Y., Xue, Q., Liu, L. & Poon, C. S. (2022). Recycling of phosphogypsum and red mud in low carbon and green cementitious materials for vertical barrier. *Sci Total Environ*, 838, 155925. [CrossRef]
- [25] Ghalehnovi, M., Roshan, N., Hakak, E., Shamsabadi, E. A., & De Brito, J. (2019). Effect of red mud (bauxite residue) as cement replacement on the properties of self-compacting concrete incorporating various fillers. *J Clean Prod*, 240, 118213. [CrossRef]
- [26] Bajpai, R., Shrivastava, A., & Singh, M. (2020). Properties of fly ash geopolymer modified with red mud and silica fume: A comparative study. *SN Appl Sci*, 2, 1–16. [CrossRef]
- [27] Wang, S., Jin, H., Deng, Y., & Xiao, Y. (2021). Comprehensive utilization status of red mud in China: A critical review. *J Clean Prod*, 289, 125136. [CrossRef]
- [28] Zhao, R., Zhang, L., Guo, B., Chen, Y., Fan, G., Jin, Z., Guan, X., & Zhu, J. (2021). Unveiling substitution preference of chromium ions in sulphoaluminate cement clinker phases. *Compos B Eng*, 222, 109092. [CrossRef]
- [29] Luo, S., Liu, M., Yang, L., Chang, J., Yang, W., Yan, X., Yu, H., & Shen, Y. (2019). Utilization of waste from alumina industry to produce sustainable cement-based materials. *Constr Build Mater*, 229, 116795. [CrossRef]
- [30] Danner, T., & Justnes, H. (2020). Bauxite residue as supplementary cementitious material—efforts to reduce the amount of soluble sodium. *Nord Concr Res*, 62(1):1–20. [CrossRef]
- [31] Manfroï, E. P., Cheriaf, M., & Rocha, J. C. (2014). Microstructure, mineralogy and environmental evaluation of cementitious composites produced with red mud waste. *Constr Build Mater*, 67, 29–36. [CrossRef]
- [32] Liu, X., Zhang, N., Sun, H., Zhang, J., & Li, L. (2011). Structural investigation relating to the cementitious activity of bauxite residue – Red mud. *Cem Concr Res*, 41(8), 847–853. [CrossRef]
- [33] ASTM C150/C150M-16e1 (2016) Standard specification for Portland cement. ASTM International.
- [34] BIS, IS 383-2016 (2016) Specification for coarse and fine aggregates from natural sources for concrete. Bureau of Indian Standards.
- [35] Wu, C. S., & Liu, D. Y. (2012). Mineral phase and physical properties of red mud calcined at different temperatures. *Journal of Nanomaterials*, 2012, 1–6. [CrossRef]
- [36] ASTM C109/C109M. (2022). Standard Test Methods for Compressive Strength of Cement Mortar. ASTM International.
- [37] ASTM C31/C31M. (2019). Standard Practice for Making and Curing Concrete Test Specimens in

the Field. ASTM International.

[38] ASTM C311/C311M. (2022). *Standard Test Methods for Sampling and Testing Fly Ash or Natural Pozzolans for Use in Portland-Cement Concrete.* ASTM International.

[39] Nath, H., Sahoo, P., & Sahoo, A. (2015). *Characterization of red mud treated under high-temperature fluidization.* *Powder Technol*, 269, 233–239. [CrossRef]

[40] BIS (Bureau of Indian Standards) IS: 4031 (Part 11):1988. *Method of Physical Test for Hydraulic Cement (Determination of Density).* Bureau of Indian Standards.

[41] Zhang, Y. N., & Pan, Z. H. (2005). *Characterization of red mud thermally treated at different temperatures.* *J Jinan Uni Sci Technol*, 19(4), 293–297.

[42] Wang, P., & Liu, D. Y. (2012). *Physical and chemical properties of sintering red mud and Bayer red mud and the implications for beneficial utilization.* *Materials*, 5(10), 1800–1810. [CrossRef]

[43] Meher, S. N., & Padhi, B. (2014). *A novel method for the extraction of alumina from red mud by divalent alkaline earth metal oxide and soda ash sinter process.* *Int J Environ Waste Manag*, 13(3), 231–245. [CrossRef]

[44] Wang, Y., Burriss, L., Shearer, C. R., Hooton, D., & Suraneni, P. (2021). *Strength activity index and bulk resistivity index modifications that differentiate inert and reactive materials.* *Cem Concr Compos*, 124, 104240. [CrossRef]

[45] Kumar, K. S., Rao, M. S., Reddy, V. S., Shrihari, S., & Hugar, P. (2023). *Effect of particle size of colloidal nano-silica on the properties of the SCM based concrete.* *EDP Sciences.* [CrossRef]

[46] Madhavi, C., Reddy, V. S., Rao, M. S., Shrihari, S., Kadhim, S. I., & Sharma, S. (2023). *The effect of elevated temperature on self-compacting concrete: Physical and mechanical properties.* *EDP Sciences.* [CrossRef]

[47] Rossignolo, J. A. (2009). *Interfacial interactions in concretes with silica fume and SBR latex.* *Constr Build Mater*, 23(2), 817–821. [CrossRef]

[48] Chand, S. R. M., Kumar, R. P., Swamy, P. N. R. G., & Kumar, G. R. (2018). *Performance and microstructure characteristics of self-curing self-compacting concrete.* *Adv Cem Res*, 30(10), 451–468. [CrossRef]

[49] Venkatesh, C., Nerella, R., & Chand, M. S. R. (2021). *Role of red mud as a cementing material in concrete: A comprehensive study on durability behavior.* *Innov Infrastruct Solut*, 6(1), 13. [CrossRef]

Use of SCM in manufacturing the compressed brick for reducing embodied energy and carbon emission

Tejas M. JOSHI* , Hasan M. RANGWALA* , Apurv PRAJAPATI

Department of Civil Engineering, Nirma University Institute of Technology, Ahmedabad, Gujarat, India

ABSTRACT

Brick is one of the most used building materials in masonry construction. Conventionally burnt clay bricks are used. These bricks are manufactured from clay and burnt in a kiln at a higher temperature. This results in a very high amount of Co₂ emission and has high embodied energy, which highly affects the environment. Compressed bricks are one of the sustainable solutions to overcome these issues of high Co₂ emission and embodied energy. Adopting sustainable alternatives, such as compressed bricks incorporating supplementary cementitious materials or environmentally friendly brick manufacturing processes, can help mitigate these issues and promote more sustainable construction practices. In this study, attempts have been made to manufacture and test the bricks with different proportions of the soil, i.e., the mix of locally available soil with sand, cement as the cementitious materials, and SCMs like fly ash & GGBS. The research methodology involves the formulation of different mixtures with varying proportions of SCMs. The specimens were then prepared using a compression molding technique and cured under controlled conditions. This research paper aims to investigate the effects of incorporating supplementary cementitious materials (SCMs) on the properties of compressed bricks. The study focuses on evaluating the density, compressive strength, water absorption, and efflorescence, as well as calculating the embodied energy and carbon dioxide emissions associated with the production of these bricks. Furthermore, the paper comprehensively analyzes the embodied energy and Co₂ emissions associated with producing compressed bricks. These calculations consider the energy consumed and Co₂ emitted in manufacturing, including raw material extraction, transportation, and brick fabrication. The study's results demonstrate the influence of SCMs on the properties of the compressed bricks. The analysis of embodied energy and Co₂ emissions provided valuable insights into the environmental sustainability of the brick production process.

Cite this article as: Joshi, T. M., Rangwala, H. M., & Prajapati, A. (2023). Use of SCM in manufacturing the compressed brick for reducing embodied energy and carbon emission. *J Sustain Const Mater Technol*, 8(4), 260–268.

Key words: Co₂ emission, compressed brick, compressive strength, embodied energy, SCM

1. INTRODUCTION

"Brick" refers to a wide range of items made from clay mixed, prepared, and molded before being slowly dried and fired in an oven or kiln. Brick, the traditional material, is in rectangular shapes of baked clay and is used for many construction activities like building walls, pavements, canal lining, and many other masonry constructions. Brick is usually red or brown.

In India, the predominant construction method for buildings and houses involves cement blocks and

burnt clay bricks due to their availability, affordability, and familiarity. However, this approach comes with several disadvantages. One significant drawback is its environmental impact. The production of these materials requires the extraction and processing of raw materials, resulting in substantial carbon dioxide emissions and contributing to climate change.

Moreover, the depletion of natural resources poses environmental concerns—the high energy consumption associated with manufacturing cement blocks and burnt clay bricks. The kiln firing process for burnt clay bricks requires significant fuel, leading to increased energy demands and carbon emissions. However, exploring alternative construction materials that address these drawbacks can lead to greater sustainability in the long run.

In many nations experiencing significant economic growth, the requirement for brick clay is high, but it is valuable to farmers. It has become overly exploited, resulting in the devastation of agricultural areas. As a result, it is critical to identify alternate materials for replacing clay in bricks to minimize energy consumption caused by clay mining and the exploitation of non-renewable clay minerals. The construction sector has always been open to innovative research on materials [1, 2]. In brick manufacturing, research is being done on producing high-quality bricks using waste-based materials to replace clay as a viable strategy for developing environmentally friendly brick materials [3–6]. Concrete blocks, AAC blocks, and fly ash bricks have emerged as alternatives to traditional burnt clay bricks. But when compared to other construction materials, Compressed Stabilized Earth Blocks (CSEB) provide numerous benefits. It enhances the utilization of local resources, waste, and supplementary cementitious material (SCM), thereby reducing transportation costs. Additionally, constructing with local materials enables the employment of local individuals and fosters sustainability [7–9].

Embodied Energy is the total energy consumed by a product or system during its entire life cycle. The energy is considered comprised or 'embodied' in the product or system [10]. It includes all energy inputs necessary to extract, process, manufacture, transport, and dispose. By considering the energy used during the whole life cycle of a product or system, including the extraction of raw materials, manufacture, usage, and disposal, it offers a comprehensive view of the environmental effect of a given product or system. However, manufacturing bricks, mainly using conventional techniques, may significantly impact carbon dioxide (CO₂) emissions and contribute to environmental problems. The embodied energy of a fired clay brick is nearly 3.75–5.60 MJ/brick [7, 11] or 0.54–3.14 MJ/kg [12]. While the estimated CO₂ emissions for fired clay brick range from 97 - 526 gm/kg of fired brick [13, 14].

According to reports, global fly ash (FA) production is around 1.143 billion tons annually. It is typically utilized at an average rate of 60% [15], while in developing nations such as India, the utilization rate of approximately 50%–60% for fly ash (FA) has been reported [16]. According to reports, the yearly

global production of GGBS is around 530 million tonnes [17]. Currently, 65% of that amount is recycled [18]. Previous research has demonstrated that clay-based bricks incorporating FA can have desired properties equivalent to their traditional clay-based counterparts [19, 20]. A recent study on the behavior of clay based bricks containing GGBS showed that 60% of GGBS content can improve the mechanical and durability properties superior to clay-based bricks without GGBS [21]. A few authors also investigated the manufacturing of bricks by GGBS, which is waste from the iron and steel industry [22, 23]. A study discovered that the bricks produced from the mixture of slag, lime, and sand are of good quality and obtained good wet compressive strength in the range of 80-150 kg/cm² after 28 days at ambient temperature in humid curing conditions. The production of slag-based bricks utilizes less energy than traditional burnt bricks [22]. However, the replacement of clay with such SCM has been little investigated in clay-based bricks.

This study investigates the innovative concept of replacing clay with a mixture of GGBS and FA conventional clay-based bricks. This study evaluates the feasibility of developing SCM-based bricks using appropriate proportions of FA and GGBS. Various tests were performed on the brick samples to determine their water absorption, bulk density, and compressive strength. This study also presents a detailed account of embodied energy and CO₂ emissions to produce and deliver the bricks.

2. MATERIALS AND METHODS

The methodology for the present study, including procurement & properties of all the materials, mixing proportions, production, and curing, is discussed in this section.

2.1. Materials

2.1.1. Soil

A locally available soil sample collected from Chekhla Village of Sanand Taluka, Ahmedabad, Gujarat, India, was used for the study. The natural moisture content of the soil was found to be 22.05%, and the specific gravity was found to be 2.64. The soil contained 16.6% clay fraction, 48.2% silt content, and 35.2% sand as per IS 2720-part IV [24]. The soil used in this study had a 28% liquid limit and a 15% Plastic limit as per IS 2720-part V [25].

2.1.2. Sand

The sand was procured from Sabarmati River, Mahudi, Gandhinagar, Gujarat, India, which conforms to Grading zone II as per IS: 383:1970 [26] having a specific gravity of 2.68, fineness modulus of 2.4, and bulk density of 1610 kg/m³ was used.

2.1.3. Cement

The Ordinary Portland cement (OPC) used for this study was procured from Nuvoco Vistas Corp. Ltd., India. The specific gravity and surface area were 3.15 and 2410 cm²/gm, respectively [27].

2.1.4. Fly Ash

Fly ash used for this study was classified as Class F, which was procured from a fly ash pond, Torrent power, Pethapur, Gandhinagar, Gujarat, India. It has a light grey color and specific gravity of 2.3, conforming to IS 3812-2013 [28]. The chemical composition of fly ash provided by Torrent power is shown in Table 1.

Table 1. Chemical composition of fly ash

Sr. No.	Details	Test results	Requirement as per IS: 3812–2013 [28]
1	Specific surface area	416.4 m ² /kg	>200 m ² /kg
2	Loss of ignition	1.10%	<7.0% by mass
3	SiO ₂ +Al ₂ O ₃ +Fe ₂ O ₃	93.00%	>70.00% by mass
4	SiO ₂	61.40%	>35.00% by mass
5	Reactive silica	34.70%	>20.00% by mass
6	MgO	1.40%	<5.0% by mass
7	Na ₂ O	0.60%	<1.5% by mass
8	Retention on 45 μ sieve	21.10%	<50.0% by mass

Table 2. Chemical composition of GGBS

Sr. No.	Details	Test results	Requirement as per IS: 16714–2018 [29]
1	Specific surface area	364 m ² /kg	>275 m ² /kg
2	Loss of ignition	0.60%	<3.0% by mass
3	Magnesium oxide (MgO)	6.07%	<17.00%
4	Manganese oxide (MnO)	0.32%	<5.50%
5	Sulphide sulphur	0.57%	<2.0%
6	Sulphate (as SO ₃)	0.29%	<3.0%
7	Insoluble residue (IR)	0.21%	<3.0%
8	Chloride content (CI)	0.008%	<0.1%
9	Glass content	92.50%	>85.00%
10	Retention on 45 μ sieve	11.00%	--

2.1.5. GGBS

GGBS used for this study was collected from Suyog Elements India Pvt. Ltd., Bharuch, Gujarat, India. It was white and had a specific gravity of 2.89. The chemical composition of GGBS provided by the firm conforming to IS 16714 – 2018 [29] is shown in Table 2.

2.2. Mix Proportions

The mix adopted for manufacturing bricks was 3:3:1 (Sand: Clay: SCM), and SCM included FA, GGBS, and cement. The proportion of sand and clay used in the mix was taken as given in IS 1725: 2013, and it has been shown that the content of clay should be 5% to 18%, silt content should be 10% to 40%, and sand content should be 50% to 80%. The different SCM mixes considered for the present study are given in Table 3. In all mixtures, the total weight of SCM content was kept constant. The brick with mix label M0 is considered a reference mix to compare all other mixes. In mix label M0 (3:3:1), the amount of soil and sand was kept equal, i.e., 12kg, and instead of using fly ash and GGBS, only cement was used, which has a proportion of 4 kg.

2.3. Manufacturing of Bricks

In the present investigation, rectangular brick specimens of 230 mm x 105 mm cross-section with a height of 70 mm were produced using a hydraulic brick-making

Table 3. Proportions of dry mix

Mix label	Mix proportions (kg)				
	Soil	Sand	Fly ash	GGBS	Cement
M0	12	12	0	0	4
M1	12	12	3	0	1
SM2	12	12	0	3	1
M3	12	12	1.5	1.5	1
M4	12	12	1.75	1.75	0.5
M5	12	12	3.5	0	0.5
M6	12	12	0	3.5	0.5
M7	12	12	2	2	0

machine. The mix adopted for brick manufacturing was 3:3:1 (Sand: Soil: SCM) with SCM of different proportions, as shown in Table 3. A total of 8 different ratios were produced, and 15 bricks were manufactured for each proportion. Firstly, the soil and sand were mixed in the dry state in the mixer for 5 minutes. Then, FA, GGBS, and cement were added during mixing and continued for 5 minutes. One liter of water was added into the mix consisting of 12 kg of soil, 12 kg of sand, and 4 kg of cement or SCM. Subse

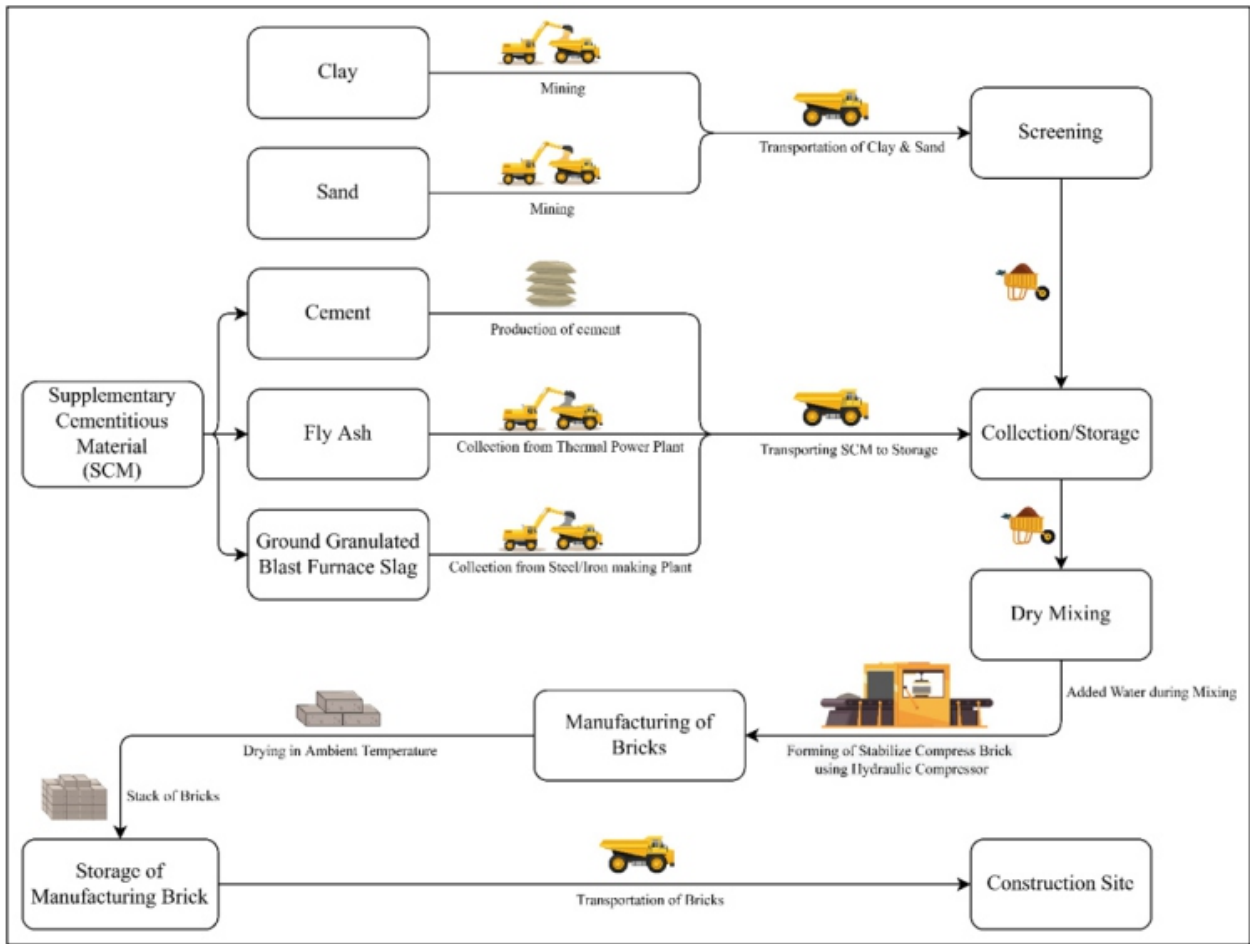


Figure 1. Flowchart for manufacturing of brick.

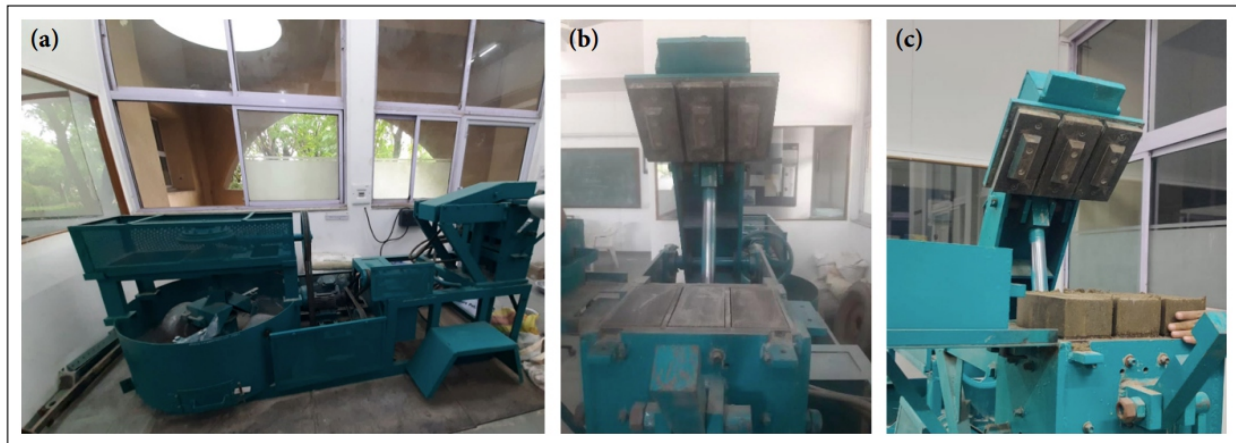


Figure 2. (a) Hydraulic brick-making machine. (a) Hydraulic compressor. (c) Production of brick.

quently, the mixing continued for another 5 minutes. Water was then added, and the blending was for another 5 minutes. The fresh mixture of all these materials was poured into the brick mold of a hydraulic brick-making machine. The freshly poured mixture was hydraulically stressed from above and below so that the height of the brick sample was obtained as required. After demoulding the brick samples, they were transferred for curing purposes. The whole process of manufacturing brick is illustrated in Figure

1. A hydraulic brick-making machine was used to produce brick, and the raw material and water were mixed and compressed in this machine, as shown in Figure 2a–c.

2.4. Curing

The consistency of water content remained uniform across all brick mixes. After demoulding, the brick

Table 4. Properties of bricks with different proportions

Name of test	Mix label							
	M0	M1	M2	M3	M4	M5	M6	M7
Density (kg/m ³)	1804	1775	1769	1769	1781	1757	1763	1727
Compressive strength (MPa) - B	4.23	3.57	3.50	3.60	4.21	3.61	3.56	3.77
Water absorption (%)	5.59	6.71	6.40	6.73	6.35	7.46	7.43	7.24
Efflorescence	No	No	No	No	No	No	No	No

Table 5. Dimension tolerance test results

Dimensions	Mix label								Limits as per IS 1725:2013	Remarks
	M0	M1	M2	M3	M4	M5	M6	M7		
Length	4599	4598	4600	4598	4601	4600	4599	4600	4520 mm to 4680 mm	Within the limit
Width	2098	2099	2100	2099	2099	2100	2098	2099	2160 mm to 2240 mm	Within the limit
Height	1403	1394	1402	1401	1400	1401	1396	1401	1360 mm to 1440 mm	Within the limit

samples were kept for drying at a controlled temperature of 27°C±1°C for one day. Then, the brick samples were cured at an ambient temperature of 22°C–24°C for 28 days.

3. RESULTS AND DISCUSSION

The comprehensive test outcomes are detailed in Table 4. It delineates the properties of the bricks, encompassing density, dimensional tolerance, compressive strength, water absorption, and efflorescence.

3.1. Density

Brick density is significant since it affects the material's durability and strength. It directly affects the structural stability and weight of a structure. While ensuring stability and efficiency in construction, the optimal brick density impacts significant parts of a building's operation. The details regarding the density of bricks are illustrated in Figure

3. Analysis of the test outcomes indicates a consistent density range between 1757–1781 kg/m³ for bricks incorporating FA, GGBS, and cement. Notably, this range exceeds the minimum density requirement of 1750 kg/m³ as outlined in the IS 1725: 2013 standard [30].

3.2. Dimensional Tolerance

Brick dimensional tolerance is essential for guaranteeing consistency and accuracy in building. It ensures that bricks follow prescribed size variations, making precise alignment and assembly easier while constructing. Accurate dimensional tolerance helps preserve structural integrity and aesthetic appearance by preventing wall thickness and alignment variations. Table 5 provides a comprehensive overview of the results of the dimensional tolerance of 20 bricks. However, every brick satisfies the requirements listed in IS 1725: 2013 [30].

3.3. Compressive Strength

The compressive strength of bricks is crucial as it signifies their ability to withstand significant loads without deformation or failure. It determines the capacity of brick to bear vertical loads, ensuring structural stability in buildings and other constructions. A higher compressive strength indicates resilience against external forces, ensuring durability and safety in various structures. The compressive strength test of brick was performed on a universal testing machine shown in Figure 4. The compressive strength of bricks for all eight mixes is shown in Figure 5. This assessment was conducted after a 28-day curing period. The reference mix, M0, exhibited a compressive strength of 4.23 MPa. Across all eight mixtures tested, the compressive strength ranged from 3.50 to 4.21 MPa. Notably, the compressive strength of all mixes surpasses the minimum requirement specified for Class 3.5, as outlined in IS 1725: 2013, ensuring compliance with these standards [30].

3.4. Water Absorption

The average value of water absorption for the individual mix is shown in Figure. 6. Notably, the reference mix, M0, demonstrated the lowest water absorption at 5.59%. In contrast, the remaining mixes exhibited a water absorption range between 6.35% and 7.46%. These values comply with the stipulated IS 1725: 2013 standard, which specifies that water absorption should not surpass 20% of the brick's weight. Additionally, it's worth noting that no efflorescence was observed on the surface of any of the bricks.

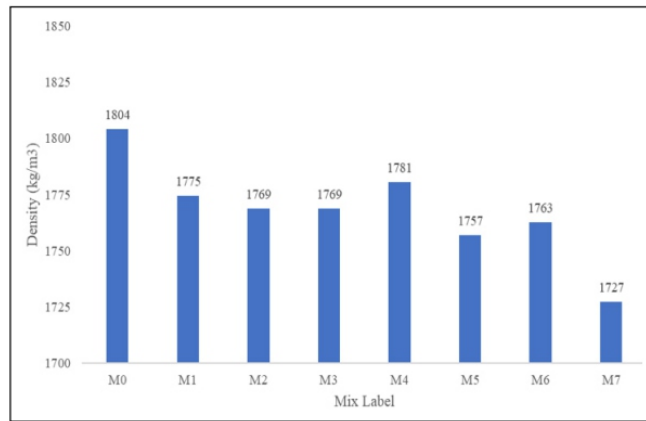


Figure 3. Density



Figure 4. Universal testing machine.

3.5. Embodied Energy

The energy used for excavation and transportation of raw materials is determined using the gathered field data. The field data of all raw materials, i.e., soil, sand, GGBS, fly ash, and cement, are assessed based on travel distance, time, capacity, and primary energy use. This work's sustainability aspects are limited to energy use and emissions. The calculation of energy use per unit amount of excavation and transportation demonstrates the influence of technological

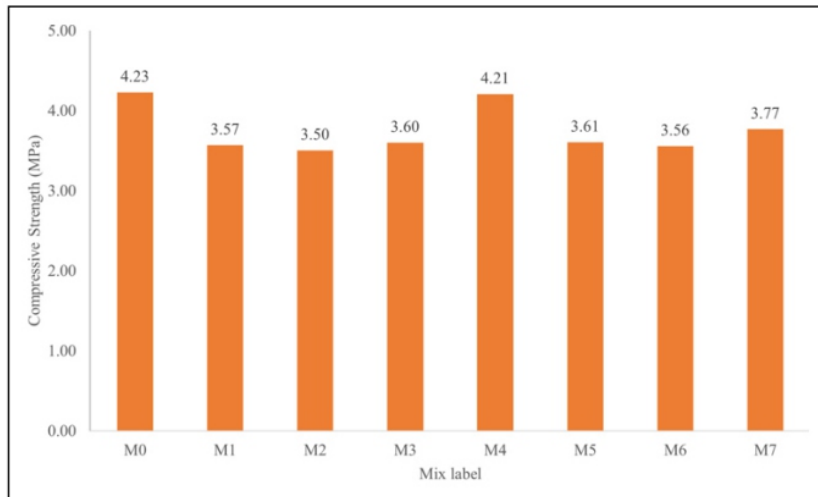


Figure 5. Compressive strength.

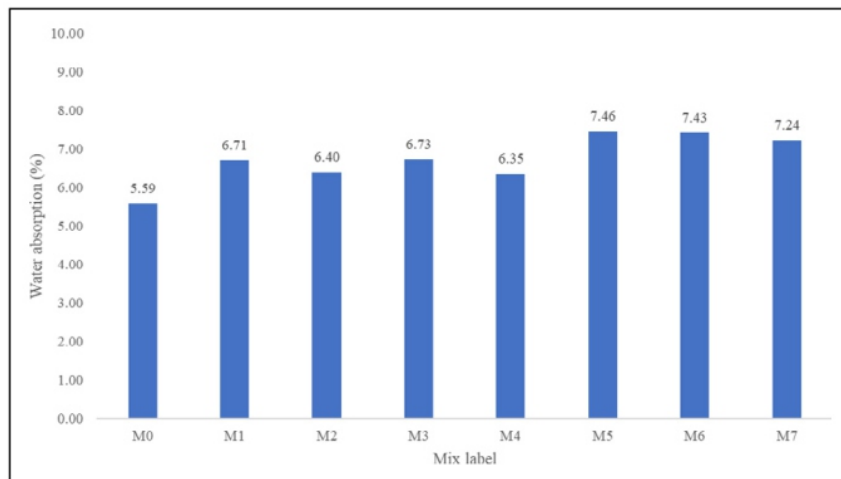


Figure 6. Water absorption.

and operational parameters. Several data have been considered for calculating embodied energy regarding the raw material, equipment, and transportation of brick.

The lorry transports a volume of 10 m³ in a single trip. The actual distance was considered for the transportation of the raw materials. The fuel consumption for the excavation of soil and sand was considered as per field data, which was about 0.35 litre per 1 m³ excavation [31]. The fuel consumption of a lorry for transporting materials was 5 km per 1 liter of fuel [31], and for energy calculation, both the trips (up trip and down trip) are considered. For all the activities of excavation and transportation, diesel was used as fuel, and it has an energy of 8.7 MJ per 1 liter of diesel [31]. The embodied energy is 3.6 MJ for 1 kg of cement production [31]. The brick-making machine was used to mix the raw materials and compress the brick; it consumes 7.5 kW. The capacity per day of the brick-making machine was 1000 bricks, for which working time was 10 hours per day. The amount of coal used is 0.7 kg for producing 1kWh of electricity, and coal has embodied energy of 20 MJ per 1 kg [31].

The calculated embodied energy for the production, excavation, and transportation of different raw

materials, brick-making equipment, and transportation of bricks are enlisted in Table 6.

3.6. Carbon Dioxide Emissions

The Co₂ emission during excavation and transportation of raw materials is determined. Moreover, Co₂emission during manufacturing and transporting bricks

Table 6. Calculated embodied energy for production and transportation

	Energy (MJ/Cu. m.)	
	Production	Transportation
Raw materials		
Soil	13.55	46.44
Sand	13.55	77.40
GGBS	-	928.80
Fly ash	-	46.44
Cement	5142.86	47.39
Manufacturing process		
Mixing & Compression	525	-
Transportation of bricks	-	77.40

Table 7. Calculated Co₂ emission for production and transportation

	CO ₂ Emission (kg/Cu. m.)	
	Production	Transportation
Raw materials		
Soil	0.89	3.05
Sand	0.89	5.08
GGBS	-	60.96
Fly ash	-	3.05
Cement	1142.86	3.11
Manufacturing process		
Mixing & Compression	51.45	-
Transportation of bricks		
Bricks	-	5.08

Table 8. Comparison of various properties of different mixes

Mix label	Compressive strength (MPa)	Water absorption (%)	Embodied energy (MJ/Cu. m.)	CO ₂ emission (kg/Cu. m.)
M0	4.23	5.59	806.15	167.96
M1	3.57	6.71	255.03	45.50
M2	3.50	6.40	283.22	47.35
M3	3.60	6.73	269.12	46.42
M4	4.21	6.35	179.62	26.17
M5	3.61	7.46	163.17	25.09
M6	3.56	7.43	196.07	27.25
M7	3.77	7.24	90.12	5.91

is also determined. The data for all raw materials, i.e., soil, sand, GGBS, fly ash, and cement, during the manufacturing transportation of brick, is assessed based on travel distance, time, and capacity.

As explained earlier, the data for Co₂ emission is the same as embodied energy. Some changed data is also considered; diesel produces 2.54 kg CO₂ per liter [31]. The Co₂ emission was 0.8 kg for 1 kg of cement production [31]. The coal has produced CO₂ of 1.96 kg per 1 kg coal [31]. The calculation of CO₂ emission for the output, excavation, and transportation of different raw materials, brick-making equipment, and transportation of bricks are enlisted in Table 7.

3.7. Comparison

Different mixes are employed in manufacturing bricks, each offering unique properties and characteristics. These mixes are carefully formulated to ensure optimal brick quality and performance. A comprehensive analysis of various brick mixes reveals a range of distinctive properties. The identified properties have been enlisted in Table 8, allowing for easy comparison and informed decision-making in brick manufacturing processes. The embodied energy and calculated Co₂ emission for different raw materials, processing, and transportation computed for the bricks manufactured for different mixes are tabulated in Table 8. The calculation for embodied energy and Co₂ emission is calculated for 1 Cu. m. which approximates 500 nos. of bricks.

These properties include compressive strength, water absorption, embodied energy, and Co₂ emission. After comparing all the data, mix M7 shows a reduction in embodied energy by 88.82% and a reduction in CO₂ emission by 96.48%. Also, it was found that the compressive strength of all mixes satisfies the minimum compressive strength specified for Class 3.5 designated as per IS 1725: 2013 [30]; hence, it can be used for structural members.

4. CONCLUSIONS

The investigation was conceived to adopt a sustainable alternative to the conventional bricks, attempting to reduce the Embodied energy and Co₂ emissions. Based on the experimental studies

conducted to evaluate the optimal mix for manufacturing bricks using fly ash (FA), ground granulated blast furnace slag (GGBS), and cement, the following significant conclusions have been drawn:

- All the stabilized compressed earth brick samples with different mixes meet the criteria for density, dimensional tolerance, compressive strength, and water absorption. This indicates that these mixes are suitable for brick production and exhibit satisfactory performance in essential properties.
- Mix M7 demonstrates the lowest embodied energy, measuring 90.12 MJ/m³ among the various tested mixes. This value is 88.82% lower than the reference mix (M0), with the highest embodied energy of 806.15 MJ/m³. The significantly lower embodied energy of Mix M7 signifies its superior sustainability in terms of energy consumption during the production process.
- Mix M7, which does not contain cement, exhibits the lowest Co₂ emissions of 5.91 kg/m³. This value is 96.48% lower than the reference mix (M0), with the highest CO₂ emissions of 167.96 kg/m³. The substantial reduction in Co₂ emissions achieved by Mix M7 highlights its superior environmental performance, contributing to lower carbon dioxide emissions during brick production.

In summary, the experimental study reveals that the stabilized compressed earth brick mixes, including the recommended Mix M7, i.e., without the use of cement and using only SCMs, meet the required standards for essential properties such as density, dimensional tolerance, compressive strength, and water absorption. Furthermore, Mix M7 stands out as a more sustainable option due to its significantly lower embodied energy and Co₂ emissions than the reference mix. These findings underscore the importance of alternative mixes using fly ash, ground granulated blast furnace slag, and reduced cement content to promote environmentally friendly and energy-efficient brick manufacturing practices.

Furthermore, with a comprehensive understanding of the environmental impact, future research should consider conducting a comparative analysis of additional parameters such as water usage, waste generation, and potential pollutants associated with different brick mixes.

ACKNOWLEDGEMENTS

The authors wish to acknowledge Nirma University, Ahmedabad, Gujarat, India, for providing production—and infrastructural support.

ETHICS

There are no ethical issues with the publication of this manuscript.

DATA AVAILABILITY STATEMENT

The authors confirm that the data that supports the findings of this study are available within the article. Raw data that support the finding of this study are available from the corresponding author, upon reasonable request.

CONFLICT OF INTEREST

The authors declare that they have no conflict of interest.

FINANCIAL DISCLOSURE

The authors declared that this study has received no financial support.

PEER-REVIEW

Externally peer-reviewed.

REFERENCES

1. Agarwal, S. K., & Gulati, D. (2007). Utilization of industrial wastes and unprocessed microfillers for making cost-effective mortars. *Constr Build Mater*, 20, 999–1004. [CrossRef]
2. Yazici, H. (2007). Utilization of coal combustion by-products in building blocks. *Fuel*, 86, 929–37. [CrossRef]
3. Domínguez, E. A., & Ullmann, R. (1996). "Ecological bricks" made with clays and steel dust pollutants. *Appl Clay Sci*, 11, 237–249. [CrossRef]
4. Wiebusch, B., & Seyfried, C. F. (1997). Utilization of sewage sludge ashes in the brick and tile industry. *Water Sci Technol*, 36, 251–258. [CrossRef]
5. Lin, K. L. (2006). Feasibility study of using brick made from municipal solid waste incinerator fly ash slag. *J Hazard Mater*, 137, 1810–1816. [CrossRef]
6. Yang, J., Liu, W., Zhang, L., & Xiao, B. (2008). Preparation of load-bearing building materials from autoclaved phosphogypsum. *Constr Build Mater*, 23, 687–693. [CrossRef]
7. Reddy, B. V. V., & Jagadish, K. S. (2003). Embodied energy of common and alternative building materials and technologies. *Energy Build*, 35, 129–137. [CrossRef]
8. Morel, J. C., Mesbah, A., Oggero, M., & Walker, P. (2001). Building houses with local material: Means to drastically reduce the environmental impact of construction. *Build Environ*, 36, 1119–1126. [CrossRef]
9. Reddy, B. V. V., & Kumar, P. P. (2009). Embodied energy in cement stabilized rammed earth walls. *Energy Build*, 42(3), 380–385. [CrossRef]
10. Deshmukh, R., & More, A. (2014). Low energy green materials by embodied energy analysis. *Int J Civ Struct Eng Res*, 2(1), 58–65.
11. Debnath, A., Singh, S. V., & Singh, Y. P. (1995). Comparative assessment of energy requirements for different types of residential buildings in India. *Energy Build*, 23, 141–146. [CrossRef]
12. Murmu, A. L., & Patel, A. (2018). Towards sustainable bricks production: An overview. *Constr Build Mater*, 165, 112–125. [CrossRef]

-
-
13. Kulkarni, N. G., & Rao, A. B. (2016). Carbon footprint of solid clay bricks fired in clamps of India. *J Clean Prod*, 135, 1396–1406. [CrossRef]
 14. Rajarathnam, U., Athalye, V., Ragavan, S., Maithel, S., Lalchandani, D., Kumar, S., Baum, E., Weyant, C., & Bond, T. (2014). Assessment of air pollutant emissions from brick kilns. *Atmos Environ*, 98, 549–553. [CrossRef]
 15. Yadav, V., Modi, T. Alyami, A. Y., Gacem, A., Choudhary, N., Yadav, K. K., Inwati, G. K., Wanale, S. G., Abbas, M., Ji, M. K., & Jeon, B. H. (2023). Emerging trends in the recovery of ferrospheres and plerospheres from coal fly ash waste and their emerging applications in environmental cleanup. *Front Earth Sci*, 11, 1160448. [CrossRef]
 16. Yadav, V. K., Gacem, A., Choudhary, N., Rai, A., Kumar, P., Yadav, K. K., Abbas, M., Khedher, N. B., Awwad, N. S., Barik, D., & Islam, S. (2022). Status of coal-based thermal power plants, coal fly ash production, utilization in India and their emerging applications. *Minerals*, 12, 1503. [CrossRef]
 17. Zhao, H., Sun, W., Wu, X., & Gao, B. (2015). The properties of the self-compacting concrete with fly ash and ground granulated blast furnace slag mineral admixtures. *J Clean Prod*, 95, 66–74. [CrossRef]
 18. Tsakiridis, P., Papadimitriou, G., Tsivilis, S., & Koroneos, C. (2008). Utilization of steel slag for Portland cement clinker production. *J Hazard Mater*, 152(2), 805–811. [CrossRef]
 19. Mohammadinia, A., Arulrajah, A., Horpibulsuk, S., & Chinkulkijniwat, A. (2017). Effect of fly ash on properties of crushed brick and reclaimed asphalt in pavement base/subbase applications. *J Hazard Mater*, 321, 547–556. [CrossRef]
 20. Eliche-Quesada, D., Sandalio-Pérez, J. A., MartínezMartínez, S., Pérez-Villarejo, L., & Sánchez-Soto, P. J. (2018). Investigation of use of coal fly ash in eco-friendly construction materials: Fired clay bricks and silica-calcareous non-fired bricks. *Ceram Int*, 44(4), 4400–4412. [CrossRef]
 21. Zawrah, M. F., Gado, R. A., Feltin, N., Ducourtieux, S., & Devoille, L. (2016). Recycling and utilization as assessment of waste fired clay bricks (Grog) with granulated blast-furnace slag for geopolymer production. *Process Saf Environ Prot*, 103, 237–251. [CrossRef]
 22. Malhotra, S. K., & Tehri, S. P. (1996). Development of bricks from granulated blast furnace slag. *Constr Build Mater*, 10(3), 191–193. [CrossRef]
 23. Mathew, B. J., Sudhakar, M., & Natarajan, C. (2013). Development of coal ash-GGBS based geopolymer bricks. *Eur Int J Sci Technol*, 2(3), 133–139.
 24. Soil Engineering Sectional Committee. (1983). IS 2720- part IV: Methods of test for soils: Grain size analysis. Bureau of Indian Standards.
 25. Bureau of Indian Standards. (1985). IS 2720- part V: Methods of test for soils: Determination of liquid and plastic limit. New Delhi, India: Author.
 26. Soil Engineering Sectional Committee. (1970). IS 383: Specifications for Coarse and Fine Aggregate from natural sources for concrete. Bureau of Indian Standards.
-
-

-
-
27. *BIS. (2015). IS 269: Ordinary Portland Cement - Specification. Bureau of Indian Standards.*
 28. *Cement and Concrete Sectional Committee. (2013). IS 3812 - part 1: Specification for Pulverized Fuel Ash - For Use as Pozzolana in Cement, Cement Mortar and Concrete. Bureau of Indian Standards.*
 29. *BIS. (2018). IS 16714: Ground granulated blast furnace slag for use in cement, mortar, and concrete - specification. Bureau of Indian Standards.*
 30. *BIS. (1982). IS 1725: Soil-based blocks used in general building construction. Bureau of Indian Standards.*
 31. *Jagadish, K. S. (2019). Sustainable building technologies. Government of India I.K. International Publishing House.*

Instructions for Authors

Essentials for Publishing in this Journal

- 1 Submitted articles should not have been previously published or be currently under consideration for publication elsewhere.
- 2 Conference papers may only be submitted if the paper has been completely re-written (taken to mean more than 50%) and the author has cleared any necessary permission with the copyright owner if it has been previously copyrighted.
- 3 All our articles are refereed through a double-blind process.
- 4 All authors must declare they have read and agreed to the content of the submitted article and must sign a declaration correspond to the originality of the article.

Submission Process

All articles for this journal must be submitted using our online submissions system. <http://enrichedpub.com/> . Please use the Submit Your Article link in the Author Service area.

Manuscript Guidelines

The instructions to authors about the article preparation for publication in the Manuscripts are submitted online, through the e-Ur (Electronic editing) system, developed by **Enriched Publications Pvt. Ltd.** The article should contain the abstract with keywords, introduction, body, conclusion, references and the summary in English language (without heading and subheading enumeration). The article length should not exceed 16 pages of A4 paper format.

Title

The title should be informative. It is in both Journal's and author's best interest to use terms suitable. For indexing and word search. If there are no such terms in the title, the author is strongly advised to add a subtitle. The title should be given in English as well. The titles precede the abstract and the summary in an appropriate language.

Letterhead Title

The letterhead title is given at a top of each page for easier identification of article copies in an Electronic form in particular. It contains the author's surname and first name initial, article title, journal title and collation (year, volume, and issue, first and last page). The journal and article titles can be given in a shortened form.

Author's Name

Full name(s) of author(s) should be used. It is advisable to give the middle initial. Names are given in their original form.

Contact Details

The postal address or the e-mail address of the author (usually of the first one if there are more Authors) is given in the footnote at the bottom of the first page.

Type of Articles

Classification of articles is a duty of the editorial staff and is of special importance. Referees and the members of the editorial staff, or section editors, can propose a category, but the editor-in-chief has the sole responsibility for their classification. Journal articles are classified as follows:

Scientific articles:

1. Original scientific paper (giving the previously unpublished results of the author's own research based on management methods).
2. Survey paper (giving an original, detailed and critical view of a research problem or an area to which the author has made a contribution visible through his self-citation);
3. Short or preliminary communication (original management paper of full format but of a smaller extent or of a preliminary character);
4. Scientific critique or forum (discussion on a particular scientific topic, based exclusively on management argumentation) and commentaries. Exceptionally, in particular areas, a scientific paper in the Journal can be in a form of a monograph or a critical edition of scientific data (historical, archival, lexicographic, bibliographic, data survey, etc.) which were unknown or hardly accessible for scientific research.

Professional articles:

1. Professional paper (contribution offering experience useful for improvement of professional practice but not necessarily based on scientific methods);
2. Informative contribution (editorial, commentary, etc.);
3. Review (of a book, software, case study, scientific event, etc.)

Language

The article should be in English. The grammar and style of the article should be of good quality. The systematized text should be without abbreviations (except standard ones). All measurements must be in SI units. The sequence of formulae is denoted in Arabic numerals in parentheses on the right-hand side.

Abstract and Summary

An abstract is a concise informative presentation of the article content for fast and accurate Evaluation of its relevance. It is both in the Editorial Office's and the author's best interest for an abstract to contain terms often used for indexing and article search. The abstract describes the purpose of the study and the methods, outlines the findings and state the conclusions. A 100- to 250-Word abstract should be placed between the title and the keywords with the body text to follow. Besides an abstract are advised to have a summary in English, at the end of the article, after the Reference list. The summary should be structured and long up to 1/10 of the article length (it is more extensive than the abstract).

Keywords

Keywords are terms or phrases showing adequately the article content for indexing and search purposes. They should be allocated heaving in mind widely accepted international sources (index, dictionary or thesaurus), such as the Web of Science keyword list for science in general. The higher their usage frequency is the better. Up to 10 keywords immediately follow the abstract and the summary, in respective languages.

Acknowledgements

The name and the number of the project or programmed within which the article was realized is given in a separate note at the bottom of the first page together with the name of the institution which financially supported the project or programmed.

Tables and Illustrations

All the captions should be in the original language as well as in English, together with the texts in illustrations if possible. Tables are typed in the same style as the text and are denoted by numerals at the top. Photographs and drawings, placed appropriately in the text, should be clear, precise and suitable for reproduction. Drawings should be created in Word or Corel.

Citation in the Text

Citation in the text must be uniform. When citing references in the text, use the reference number set in square brackets from the Reference list at the end of the article.

Footnotes

Footnotes are given at the bottom of the page with the text they refer to. They can contain less relevant details, additional explanations or used sources (e.g. scientific material, manuals). They cannot replace the cited literature.

The article should be accompanied with a cover letter with the information about the author(s): surname, middle initial, first name, and citizen personal number, rank, title, e-mail address, and affiliation address, home address including municipality, phone number in the office and at home (or a mobile phone number). The cover letter should state the type of the article and tell which illustrations are original and which are not.

